Structural Studies of Cytomegalovirus Entry Proteins

A Dissertation

submitted by

Heidi G Burke

In partial fulfillment of the requirements
for the degree of

Doctor of Philosophy

in

Molecular Microbiology

TUFTS UNIVERSITY

Sackler School of Graduate Biomedical Sciences

September 30th, 2016

Project Mentor: Ekaterina E Heldwein

Abstract

Human cytomegalovirus (HCMV), a dsDNA, enveloped virus, is a ubiquitous pathogen that establishes lifelong latent infections in 50-90% of the population. It causes disease in persons with compromised immune systems, e.g., organ transplant recipients or AIDS patients. HCMV is also a leading cause of congenital viral infections and developmental defects in newborns. Entry of HCMV into cells requires the conserved glycoprotein B (gB), thought to function as a fusogen and reported to bind signaling receptors. gB also elicits a strong immune response in humans and induces the production of neutralizing antibodies, although most anti-gB antibodies are non-neutralizing. The crystal structure of the HCMV gB ectodomain determined to 3.6-Å resolution presented in this work is the first atomic-level structure of any betaherpesvirus glycoprotein. The structure of HCMV gB resembles the postfusion structures of HSV-1 and EBV homologs, establishing it as a new member of the class III viral fusogens. Despite structural similarities, each gB has a unique domain arrangement, demonstrating structural plasticity of gB that may accommodate virus-specific functional requirements. The structure illustrates how extensive glycosylation of the gB ectodomain influences antibody recognition. Antigenic sites that elicit neutralizing antibodies are more heavily glycosylated than those that elicit non-neutralizing antibodies, which suggest that HCMV gB uses glycans to shield neutralizing epitopes while exposing non-neutralizing epitopes to act as an immune decoy. This glycosylation pattern may have evolved to direct the immune response towards the generation of non-neutralizing antibodies thus helping HCMV to avoid clearance. The structure provided the framework for understanding the antigenic regions (AD1-5) of the protein, however, clinical information was needed to know which region

would generate antibodies leading to protection in humans. By determining the level of antibodies against each antigenic region present in maternal sera from mothers of premature infants, we identified two trends affecting the ability of these antibodies to protect. The presence of antibodies against AD-5 correlated with protection from infection while the presence of antibodies against AD-1 interfered with protection. The latter was stronger and overcame the beneficial effects of anti-AD-5 antibodies. These trends await confirmation with larger sample sizes, yet they along with the HCMV gB structure offer valuable insights that may aid in the design of recombinant vaccines and monoclonal antibody therapies.

Acknowledgements:

Katya, your scientific excellence, and drive have never ceased to amaze me. Your ability to publish every finding in an expedient manner and the respect you command in the field are the perfect models to aspire to. However, what I appreciate about you most is what an incredibly caring mentor you are. You have the capacity and the will to help each of us become our best. From teaching us to be precise in our scientific language, ask relevant scientific questions, become great speakers, and improve our ability to write; you take the time to make each of us the best version of ourselves. You fight to ensure we publish, graduate, and get our dream positions; fully supporting us in whatever goal every step of the way. It has always been striking to me how much you care about our success, but also our well-being. From calibrations to lab outings to international conferences, you make sure we are happy as well as driven. Thank you for allowing me to spend four and a half amazing years in your lab and for molding me into a confident scientist. I am truly indebted to you.

I would like to thank my thesis committee, for years of support and guidance. Particularly, I would like to thank my chair, Ralph Isberg and my clinical mentor, Dr. David Snydman, for co-sponsoring and supporting my various applications. Additionally, I would like to express my appreciation to David for providing samples, helping to come up with interesting clinically relevant questions and to understand the results. David's willingness to give of his limited free time has always been appreciated. Moreover, Ralph for his vast knowledge and brilliant suggestions, Andrew Bohm for teaching me the theory of crystallography sharing his expertise and equipment, and Marta Gaglia providing valuable feedback, being an attentive committee member, and an excellent lab

neighbor. Finally, I would like to express my appreciation to the additional member of my examination committee, Sun Hur. I enjoyed our discussion.

I've been incredibly fortunate to have had a supportive, caring, and fun lab environment to conduct my thesis work. I've had the pleasure of being surrounded by some fantastic people day in and day out. Sapna Sharma, Tirumala Chowdary, Jessica Silverman, Elvira Vitu, Sam Stampfer, and Jared Pitts; you all made joining the lab the clear choice from the beginning. That amazing culture you established continued providing years of happiness. Henry Rogalin, Andrea Koenigsberg, Rebecca Cooper, Claire Metrick, Janna Bigalke, and Mike Freeman (our honorary lab mate); I've loved spending the last four and a half years getting to know each of you and sharing so much. Elizabeth Draganova, Ellen White, and Xuan Guo; you are clearly fantastic additions to this incredible lab culture that I will truly miss. I have to especially that Janna and Claire. Janna, the lab isn't the same without you. It was such a pleasure to be there through some of your important life moments, and I'm so grateful you let me share in them. I'll always think fondly of our trip to Brooklyn. Claire, we joined together and are lab twins in so many ways. Thank you for all the support, your friendship, and keeping the robot running. To all the past and current lab members, thank you for every amazing moment.

To the Molecular Microbiology Program and Department, every member has made this an incredible scientific environment. The collaborative, friendly atmosphere is unique and as made me excited to continue in science for life. To the Micro staff, Perry Riggle, Verna Manni, Rima Mycynek, Molly Kyle, Mike Healy, and Ann McKinney; you all do an amazing job making the place run, but you do so in a caring, friendly way making interacting with you all such a pleasure.

To my classmates, Claire Metrick, Mike Freeman, Kristin Kotewicz, John Yoon, Laurice Flowers, and Mimi Yen, It's been an honor to be on this journey with you. I have particularly adored my MERGE-ID cohort ever since bonding through clinical exposure. Jon, Laurice, and Mimi you've been a great support structure. Mimi, I will miss all of our coffee breaks.

To my family, Ruby Mason, Saundra Burke, Brian Burke, Matt Burke and Greg Burke, Holly Young, Jilly Tucker and all my adorable nieces and nephews; your unwavering support through the decades I've been in school has been crucial to my success. I love you all and am so grateful for your love in return.

Ben and Juliana, my oldest friends; you've been there through some of the hardest moments of my life, and your unwavering support has helped me through them. You've have shown me the world and open my mind through exposure to many different cultures and traditions. You have always been an advocate for my continued education and success. Thank you for always being there!

Tim, you were there for me during my rush to publish and helped me celebrate the accomplishment of my first scientific manuscript. You have been here for me know while I strive to obtain my greatest achievement. I could not imagine a more supportive partner and love you so much. To the Pitoniaks, particularly Claudia, thank you for making me a part of your family and for celebrating my achievements with me. Your inclusion in holidays and interest in my work means the world.

To my uncles, Dr. Richard Mason and Dr. Jeff Braman. Your hard work, dedication, and level of scientific excellence have always been an inspiration. Thank you for encouraging me to follow in your footsteps and earn a scientific Ph.D. Jeff, your

support and guidance throughout my many years of schooling have led me to this point. Your suggestion to pursue biochemistry for the best job prospects has been valuable. Your encouragement to achieve the highest level of education despite temporary market trends was wise. Finally, supporting my acceptance of a graduate position at Tufts to be in the heart of "the Hub" was great advice. I have enjoyed my time in graduate school immensely, and you were there to help me make the decisions that brought me here at every step of the way.

Finally, to my grandfather, Dr. Cassel Burke. You have always been an inspiration for academic excellence. Not only did you earn a doctorate in education at one of the best schools, UC Berkeley, you were also awarded an honorary doctorate for your continued excellence. Sadly, it was at your funeral that I made the decision to pursue my doctorate. I was deciding between a Ph.D. or an M.S., and Jeff convinced me to go for the Ph.D. I met with my good friend Ben afterward and told him of my new goal. His response was "Awesome; that means you will be Dr. Burke someday." My instant reaction was "no, that's my grandpa" and then realized what better way to honor your memory. I dedicate this achievement to you, Dr. Burke and hope to inspire new generations of doctors in our family to continue to honor your memory.

Table of Contents: **Page #**

List of Tables: **Page #**

List of Figures: **Page #**

List of Abbreviations:

°C	Degrees Celsius
Å	Ångstrom
AD-1-5	Antigenic regions 1-5
AD169	Laboratory adapted HCMV strain
Ab(s)	Antibody(s)
APBS	Adaptive Poisson-Boltzmann Solver
B-cell	Lymphocyte derived from the bone marrow that matures in lymphoid tissue
CD	Circular dichroism
CMV	Cytomegalovirus (human herpesvirus 5)
C term	Carboxy terminus
Cyto	Cytoplasmic domain
Cα	Alpha carbon (in amino acids)
Cβ	Beta carbon (in amino acids)
DNA	Deoxyribonucleic acid
DI-V	Domains I-V
EBV	Epstein-Barr virus (human herpesvirus 4)
EDTA	Ethylenediaminetetraacetic acid
EM	Electron microscopy
Fab	Fragment antigen-binding
Fc	Calculated amplitudes
FL	Cusion loop
Fo	Observed amplitudes
gB	Glycoprotein B (herpesvirus)
gB706	gB ectodomain, residues 25-706
gH	Glycoprotein H (herpesvirus)
gH/gL	Glycoprotein H/glycoprotein L heterodimer
gL	Glycoprotein L (herpesvirus)
gp42	Glycoprotein 42 (from EBV, forms a complex with gH/gL)
HA	Hemagglutinin (influenza virus)
HA2	Hemagglutinin fusion subunit
HCMV	Human cytomegalovirus (human herpesvirus 5)
HHV1-8	Human herpes virus 1-8
HIV	Human Immunodeficiency Virus
HN	Hemagglutinin-neuraminidase
hrs	Hours
HSV	Herpes Simplex Virus (includes both types)
HSV-1	Herpes simplex virus type 1
HSV-2	Herpes simplex virus type 2
HVEM	Herpesvirus entry mediator
Im	Imidazole
IMAC	Immobilized metal affinity chromatography
kDa	Kilodalton
KSCN	Potassium thiocyanate
KSHV	Kaposi's sarcoma-associated herpesvirus (human herpes virus 8)

LSQ	Least squares (method of superposition)
Luc	Luciferase
M	Molar
mg	Milligram
ml	Milliliter
mM	millimolar
MPR	Membrane-proximal region
NaCl	Sodium chloride
Ni-NTA	Nickel-nitriloacetic acid
nm	Nanometer
N terminus	Amino terminus
P1 virus	Passage 1 virus (first virus produced from bacmid transfection)
PCR	Polymerase chain reaction
PDB	Protein databank
PDB ID	Protein databank identification code
PEG	Polyethylene glycol
PI	Principal investigator
PMSF	Phenylmethylsulfonyl fluoride
PVDF	Polyvinylidene fluoride, a highly non-reactive polymer
qPCR	Quantitative polymerase chain reaction
r.m.s.	Root-mean squared
rmsd	Root-mean squared deviation
RNA	Ribonucleic acid
SDS	Sodium dodecyl sulfate
SF	Spodoptera frugiperda
SS	Signal sequence
S-S	Disulfide bond
SSM	Secondary-structure matching
T-cell	Lymphocyte that matures in the thymus
TCEP	Tris-(2-carboxyethyl) phosphine
TFF	Tangential flow filtration
TM	Transmembrane region
Tm	Melting temperature
TNE	20 mM tris pH 8.0, 150 mM sodium chloride, 1 mM EDTA
Tris	Trisaminomethane
UL	Unique long region (of HSV DNA)
VSV	Vesicular stomatitis virus
VZV	Varicella zoster virus (human herpesvirus 3)
wt	Wild-type
θ218	CD signal absorbance at 218 nm
µl	Microliter

Chapter One: Introduction

1.1 Human Cytomegalovirus

1.1.1. Herpesviruses

Viruses of the *Herpesvirales* order infect a notably wide range of hosts including fish, reptiles, birds, and mammals and are grouped into three families, *herpesviridae, alloherpesviridae, and malacoherpesviridae* [1]. There are eight members of the *Herpesviridae* family that infect humans. Based on the level of sequence identity, the eight human viruses along with non-human viruses are divided into three subfamilies, *alphaherpesviridae*, *betaherpesviridae*, and *gammaherpesviridae* [1]. All establish lifelong latent infections in their hosts, yet acute infection and reactivation present differently due to the unique cellular tropism of each species. Over 50% of the world's population is seropositive for six out of the eight herpesviruses [2-4].

There are three human-specific members of the *alphaherpesviridae* subfamily. Herpes simplex virus type I (HSV-1 or HHV-1) and herpes simplex virus type II (HSV-2 or HHV-2) are the causative agents of oral lesions often referred to as “cold sores” or “fever sores” and genital herpes, a sexually transmitted disease. Varicella-zoster virus (VZV or HHV-3) causes chicken pox and shingles upon initial infection and reactivation, respectively. All three human alphaherpesviruses are also capable of causing more serious conditions, ocular infection and encephalitis, although most commonly the causative agent of both is HSV-1 [5-8].

The betaherpesviruses include human cytomegalovirus (HCMV or HHV5), human herpes virus 6 (HHV6) and 7 (HHV7). The clinical implications of HMCV are described in detail below, in section 1.1.2 of the introduction. Briefly, acute infection may present with flu-like symptoms while serious disease can occur in the

immunocompromised and developing fetuses. In young children, HHV6 and HHV7 causes a fever and skin rash called roseola [9]. Additionally, HHV6 has been linked to infertility, cancer, and neurological issues [10-12].

The gammaherpesvirus Epstein-Barr virus (EBV or HHV4), causes infectious mononucleosis and several types of cancer such as nasopharyngeal carcinoma and B cell lymphoma [13]. Extreme fatigue is the most notable symptom of mononucleosis, but the condition also includes head and body aches, fever, rash, swollen lymph nodes, sore throat, and a swollen liver or spleen [14]. The other member of the gamma herpesviruses is Kaposi's sarcoma-associated herpesvirus (KSHV or HHV8). KSHV is the causative agent of Kaposi's sarcoma (KS), a tumor affecting AIDS patients that is otherwise rare. KS is a lymphatic or blood vessel cancer that leads to purple or brown tumors on the skin and mucosal surfaces [15].

1.1.2. Clinical HCMV

Human Cytomegalovirus (HCMV) is a ubiquitous virus infecting over 50% of adults in the US by the age of 40 [16]. Seroprevalence is higher in underprivileged areas and developing nations such as Brazil, South Africa, and India where greater than 90% of the population carries the virus [4]. Immunocompetent individuals often display no apparent symptoms after initial HCMV infection. When symptoms are apparent, they are present as an acute mononucleosis or flu-like symptoms, consisting of fever, fatigue, enlarged lymph nodes, sore throat, rashes, malaise, muscle aches, and loss of appetite [17, 18]. After initial infection, HCMV establishes latency in myeloid progenitor cells, and infection persists throughout life [19]. The virus elicits a robust immune response,

allowing competent immune systems to keep the virus in check although asymptomatic reactivations continue to occur [20, 21]. By contrast, HCMV is an important pathogen in the immunocompromised including AIDS, cancer, and transplant patients.

HIV and HCMV coinfection is common and when CD4 counts drop low enough to categorize the HIV infection as AIDS, the loss of cell-mediated immunity allows HCMV to reactivate [22]. HCMV viremia in HIV-positive persons can eventually lead to diarrhea, severe vision problems including blindness, infections of the stomach and intestines, and even death. HCMV was a leading cause of AIDS-related deaths in the early days of the HIV epidemic, with up to 50% resulting from multiple types of HCMV end-organ diseases [23, 24]. With the successful implementation of HIV antiretroviral treatment (ART), the level of HCMV mortality in AIDS patients has dropped dramatically, and HCMV retinitis now occurs in less than 1% of HIV patients [25]. Nevertheless, HCMV remains the leading cause of AIDS-related vision loss when ART is not available.

HCMV has been implicated in many types of cancer. HCMV DNA and proteins have been found in most types of tumors, while not in surrounding tissue [26-29]. It is unclear if HCMV plays a role in tumor biology. HCMV antivirals have been shown to reduce tumor growth in animal models and have improved outcomes when added on to cancer treatment in humans [26, 30-32]. Differentiation of latently infected monocytes causes reactivation of HCMV [33, 34]. Therefore, it could be that the virus is causing a lytic infection in immune cells responding to tumor growth to the detriment of the immune response and treating HCMV addresses this by treating the immune cells

allowing them to attack the tumor. Additional studies of the pathology of HCMV in tumors are needed to clarify this and test viable treatment options.

HCMV is a major complication in transplantation, leading to an estimated 20-30% increase in mortality. Hematopoietic stem cell and lung transplant patients have the highest occurrence of HCMV disease [35]. Common symptoms in transplant patients include digestive track pain, fever, and malaise. Diarrhea, respiratory issues, pancreatitis, meningoencephalitis, myocarditis, and hepatitis are rare but indicative of severe disease [36]. HCMV plays a significant role in graft-vs.-host disease. The risk of HCMV disease is higher when the graft comes from a seropositive donor, and the recipient is seronegative. Serological matching of donors and recipients improves HCMV related outcomes. Extensive prophylaxis with HCMV-antivirals has decreased the prevalence of disease and improved outcomes dramatically [37].

1.1.3. Congenital HCMV

If a developing fetus is congenitally infected with HCMV, it can cause hearing loss, blindness, mental disabilities, and death, particularly if infection occurs during the first or second trimester [38-40]. The first report of HCMV congenital disease was described by Dr. Carl Weigert in 1898. Since then, the prevalence of HCMV related birth defects has been slow to gain appreciation. HCMV is estimated to infect 27,000 seronegative pregnant women in the US a year and 0.5-1% of all infants worldwide are born with HCMV [41, 42]. Yet, only a third of the population has ever heard of the virus or its danger to fetuses while awareness of other less common causes of birth defects such Down syndrome are high [40]. Globally, roughly 11% of infants born with HCMV

are born with abnormalities resulting from the infection [42]. In the US, it is estimated that of the ~40,000 infected babies a year, 8000 have disabilities and 400 will die [40]. Pregnant women who are infected during pregnancy (primary infection) have a much higher risk of transmitting the virus to their fetus than recurrent HCMV infection (32.3% compared to 1.4% respectively) [42]. Increased awareness and knowledge of the need for good hygiene while pregnant may help decrease the incidence of infection during pregnancy [40]. Although, treatment options are sorely needed for this high-risk population when prevention fails.

1.1.4. Treatment and challenges

HCMV treatments need to prevent disease due to lytic reactivation in the immunocompromised as well as provide prophylaxis in transplant patients and pregnant women. Ganciclovir and the prodrug version, valganciclovir, are the most effective antivirals available against HCMV. They have associated renal toxicity, however, and cannot be given to pregnant women or renal transplant patients [43]. Ganciclovir is a nucleoside, inhibiting viral DNA replication after being converted into ganciclovir-5'-triphosphate [44]. A clinically prevalent, established mechanism of resistance exists, conferred by mutations in UL97, a viral phosphotransferase, and UL54, the viral DNA polymerase [43, 45]. Another nucleoside, foscarnet, has activity against HCMV and HIV, thus is useful in the treatment of HCMV retinitis, although it is also toxic [46]. Other antivirals such as lefluenomide, artesunate, and maribavir, have shown efficacy in some types of transplant patients but failed in others [47-51]. Other antivirals are being examined for treatment such as CMX001 and letermovir with pending results [52, 53].

Immunoglobulin from HCMV seropositive individuals (CMVIG) or hyperimmunoglobulin (HCMVIG) from high titer IgG HCMV donors has been used as passive immunity treatment in transplant patients with some efficacy [54, 55]. However, the available antivirals are more effective thus remain the standard of care unless toxicity or resistance are of concern [56]. There have been trials conducted to test HCMVIG in pregnant women and premature infants [39, 57]. However, there are concerns regarding the safety of using a human blood derived treatment in these cohorts. There are many efforts underway aimed at producing a potent monoclonal antibody therapeutic in hopes of improving safety and efficacy, though none are currently approved [58, 59].

Infectious HCMV particles are secreted in bodily fluids such as sperm, urine, and saliva. Therefore, preventative measures include good hand washing, not sharing utensils with toddlers (who shed high levels of virus), and condom usage while pregnant. Another approach to prevention is the dissemination of a vaccine and developing one against HCMV has been designated the highest priority level by the National Vaccine Advisory Committee [60]. A gB vaccine with an MF59 adjuvant decreased viremia in phase II clinical trials with transplant patients [61], and reduced congenital and maternal HCMV infection rates [62]. Efficacy of the vaccine was not sufficient to make it to the market. A phase I study is underway, testing the safety and dosage of a vector/pp65/gB based vaccine (Hookipa Biotech, HB-101) and many other vaccine efforts are still ongoing.

1.2. Herpesvirus Biology

1.2.1. Herpesvirus Virion Structure

All herpesviruses have a linear double-stranded DNA (dsDNA) genome (Fig.

1.1). Most herpesviral genomes range between 124 and 170 kilobases (kb) in length [63-69]. The HCMV genome, however, is considerably larger at over 235 kb, with approximately 192 unique open reading frames (ORFs) [70, 71]. It consists of a long unique (UL) region flanked by a terminal repeat long (TRL) at the 5' end and an internal repeat long (IRL) at the 3' end (Fig 1.1). This is followed by an internal repeat short (IRS) and terminal repeat short flanking a unique short (US) region [70]. The names of herpesviral proteins are based on the region in which they are found and then numbered sequentially. For instance, UL85 is the 85th ORF encoded in the long unique region and US12 is the 12th ORF encoded in the unique short region.

Figure 1.1. The structure of the HCMV Linear dsDNA Genome. The unique long (UL) region of the HCMV genome, containing genes UL1-151, is flanked by two repeats. The terminal repeat long region (TRL), encoding genes TRL1-14, is located at the 5' end of the genome, upstream of the UL region. The internal repeat long (IRL) encoding genes IRL14-1, is located downstream of the UL region. The unique short (US) region, containing genes US1-36, is flanked by two additional repeats, the internal repeat short (IRS) and terminal repeat short (TRS). Both encode 1 gene, IRS1 and TRS1.

The herpesviral genome is packaged into an icosahedral capsid. The HCMV capsid is composed of a minor and major capsid protein (mCP and MCP, genes UL85 and UL86 respectively) [72], a mCP binding protein (mC-BP, gene UL46) [73], and a small capsid protein (SCP, gene UL48.5) [74] (Fig. 1.2). The capsid is surrounded by the tegument layer, which consists of multiple proteins. These function during post-entry events, immune evasion, gene expression, genome replication, assembly and egress.

Finally, the virion is surrounded by an envelope, a lipid bilayer derived from the *trans*-Golgi network (TGN) or endosomes [75]. The surface of the envelope is studded with viral glycosylated proteins, referred to as glycoproteins. In HCMV, these include gB and complexes formed by gM/gN, gH/gL/gO and gH/gL/UL128/UL130/UL131 (Fig. 1.2). the glycoproteins have been shown to be important in attachment and entry [76].

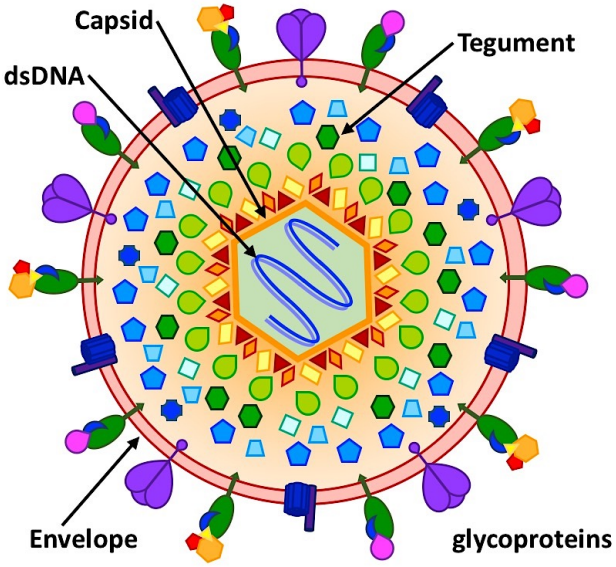

Figure 1.2. The structure of the Herpes Virion. A schematic representation of the herpes structure of a herpes virion. dsDNA (blue lines) in the viral capsid (orange line), surrounded by capsid associated tegument (red, orange, and yellow shapes) with other tegument surrounding that (blue and green shapes). The tegument surrounded capsid is encased in a viral envelope (red lines) studded with glycoproteins (outer shapes).

1.2.2. Herpesvirus Replication Cycle

Alpha and betaherpesviruses generally cause lytic, actively replicating infection in one cell type while establishing a quiescent, latent infection in another. HCMV can lytically infect many cell types including fibroblasts, macrophages, endothelial, epithelial, and dendritic cells [77-79]. The virus establishes latency in myeloid progenitor cells, and differentiation is thought to cause reactivation [33, 80]. HCMV enters susceptible cells by fusion at the plasma membrane or through endocytosis, depending on the cell type, losing its envelope in the process (to be discussed in greater detail) [81]

(Fig. 1.3). Then, the capsid travels to the nucleus along microtubules with the aid of viral tegument proteins (reviewed in [82]). The dsDNA genome is injected into the nucleus though a nuclear pore.

During lytic infection, immediate-early genes activate the transcription of early genes that are capable of DNA replication such as the viral DNA polymerase [83]. Late genes are then transcribed which encode the capsid structural proteins among other things [84]. Capsids are assembled and packaged with the viral dsDNA in the nucleus (Fig. 1.3). Capsids undergo nuclear egress with the aid of the nuclear egress complex (NEC), formed by UL50 and UL53 in HCMV [85]. The NEC causes capsid budding at the nuclear membrane into the perinuclear space creating enveloped perinuclear virions. The newly acquired membrane envelope then fuses with the outer nuclear membrane, releasing the capsid into the cytosol, de-enveloping in the process. In the case of HCMV, the capsid acquires tegument proteins while trafficking to the viral assembly compartment (AC), a juxtanuclear body created by HCMV by rearranging cellular components. This cellular rearrangement increases the size of the cell, in particular, the nucleus, and gives cytomegalovirus, or "big cell virus" its name. Histopathologically, HCMV infected cells are referred to as owl eyes due to this rearrangement (Fig. 1.4). The capsid acquires an envelope derived from TNG in the AC by budding into intracellular vesicles [86]. The virions are released from the cell by exocytosis [87]. Virions can either be released into the extracellular space or spread to neighboring cells by utilizing cell junctions, which allows the virions to avoid the immune system [82].

In myeloid progenitor cells, after the virus dsDNA genome is injected into the nucleus, latency-associated genes are transcribed rather than immediate early genes.

Latency-associated genes do not lead to the secretion of infectious virions [88]. The viral genome does not insert itself into the cellular genome but persists in the nucleus of latently infected cells. Again, reactivation is triggered when the infected myeloid progenitor cells differentiate into macrophages and dendritic cells, immediate early genes are transcribed, and the virus returns to its lytic cycle [19].

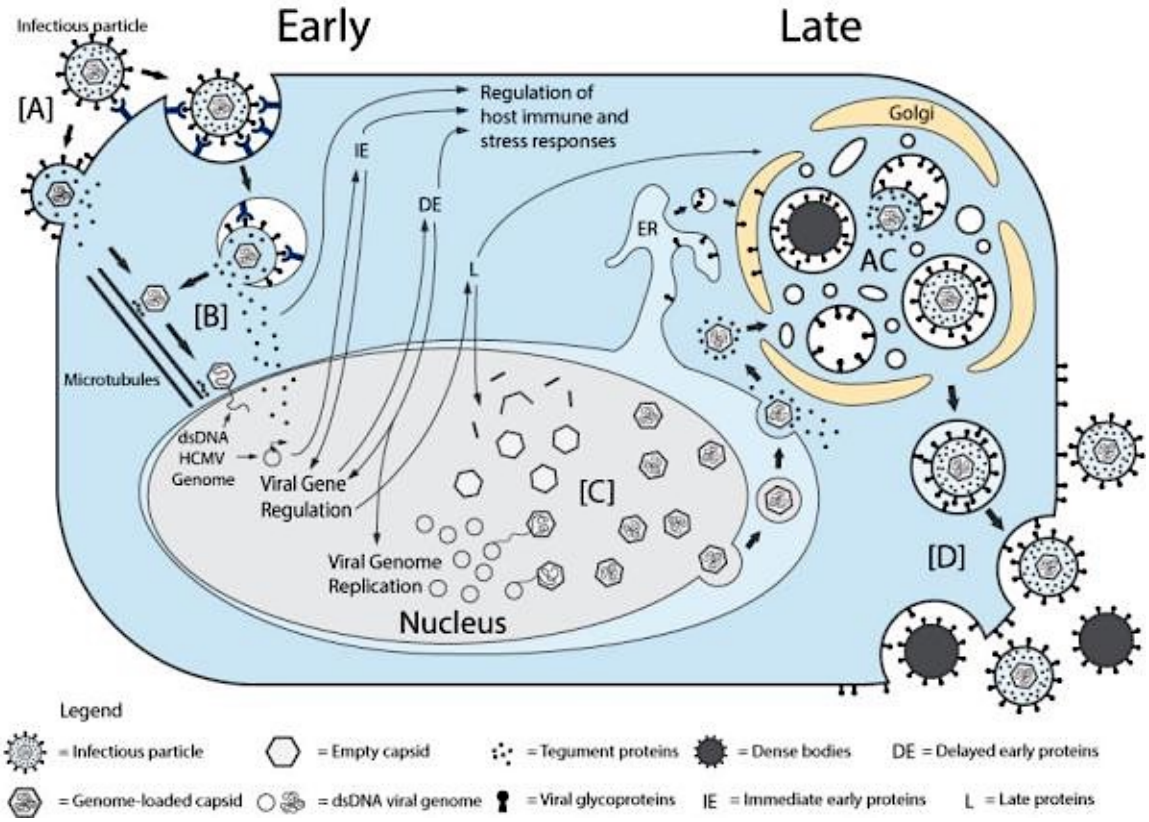

Figure 1.3. The HCMV Replication Cycle. (A) Viral particles attach to the cellular surface, fuse their viral envelope with the cell membrane, transferring their capsid and tegument into the cytosol. (B) The capsid travels along microtubules to the nucleus where dsDNA genome is inserted through nuclear pores. Tegument proteins initiate the expression of viral immediate early (IE) genes, followed by early (DE) genes, which initiate viral genome replication, and late (L) genes. (C) Late genes encode capsid proteins. Assembly of the capsid and insertion of the viral genome occurs in the nucleus. Then the capsid undergoes nuclear egress to the cytosol. Capsids

traffic to the viral assembly compartment (AC), acquiring tegument proteins as they do. The AC contains components of the endoplasmic reticulum (ER), Golgi apparatus and endosomal machinery. The capsids bud into AC intracellular vesicles, providing the viral envelope. (D) Enveloped viral particles exocytose along with non-infectious dense bodies. Figure kindly provided by [82].

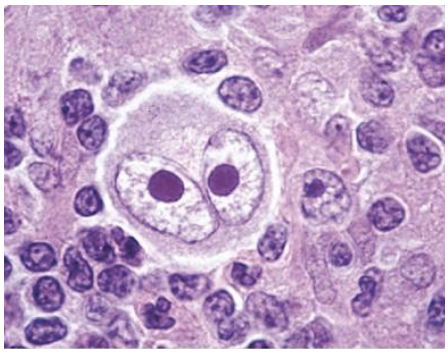

Figure 1.4. HCMV "Owl Eyes". Histological section of HCMV infected tissue demonstrating the characteristic "owl eyes" formed by nuclear inclusion bodies [89].

1.2.3. Entry of Herpesviruses into host cells

Entry of herpesviruses occurs in four steps: attachment, receptor binding, membrane fusion, and capsid release into the cytosol. The molecular mechanisms of HSV and EBV entry have been studied in detail and are the most understood of the herpesviruses. Viral cell surface attachment proteins and cellular receptor pairs are species and cell type specific. In HSV, glycoproteins C and B (gC and gB) interact with Heparan sulfate proteoglycans (HSPGs) [90, 91]. After attachment, a cell surface receptor is bound by the HSV receptor-binding protein, glycoprotein D (gD). The cell surface receptors gD binds are nectin-1, HVEM, or 3-O-sulfated heparin sulfate which determine cellular tropism [92, 93]. gD/receptor interaction is next thought to trigger the conserved heterodimer made up of glycoproteins H and L (gH/gL) [94]. gH/gL then likely triggers the viral fusogen, glycoprotein B (gB) [95-97]. There is evidence that the cytodomain of gH/gL, the domain located in the cytoplasm of the cell, may act as an activator while the

cytodomain of gB acts as an inhibitor of fusion [98-100]. When gH/gL is triggered, its cytodomain may disrupt the gB cytodomain, allowing the gB ectodomain to catalyze the membrane fusion reaction, releasing the capsid to enter the cell [101-103].

EBV entry begins with attachment of glycoprotein p350/220 (gp350/220) to the complement receptor type 2 (CR2) on B cells while attachment to epithelial cells remains unclear as CR2 is expressed at low levels if at all [53-55]. EBV gH/gL binds to integrins αvβ6 or αvβ8 on the surface of epithelial cells [56]. By contrast, entry into B cells requires an additional binding partner, gp42, which forms a ternary gp42/gH/gL complex and interacts with a B-cell receptor HLA-DR, an MHC class II molecule [53, 57, 58]. The binding site for gp42 within gH/gL overlaps the integrin-binding site making the two complexes mutually exclusive [59]. Thus, binding of gp42 to gH/gL blocks epithelial cell entry, while permitting entry into B cells. In turn, MHC class II molecules sequester gp42 produced in B cells. This leads to less gp42 on the surface of virions produced in B cells, which are then optimal for entry into epithelial cells [60]. Interaction of gH/gL and gH/gL/gp42 with their respective receptors is thought to trigger fusion mediated by the fusogen, gB [53].

1.2.4. HCMV Entry

HCMV is noteworthy in that almost all cell types are both susceptible and permissive to the virus giving it broad human cellular tropism, while latency is established in bone marrow-derived myeloid progenitor cells [53]. HCMV attachment is mediated by binding of gM or gB to HSPG [54, 55]. Binding of gB to cellular integrins or PDGFR has been proposed to initiate cellular signaling cascades thought to prepare the

cell for viral entry [104, 105]. As with all herpesviruses, HCMV gB and gH/gL are essential for fusion and entry into all cell types. Additionally, HCMV gH/gL requires cell-type-specific binding partners for entry. gH/gL forms a pentameric complex with UL128, UL130, and UL131. This pentamer is necessary for entry into monocytes, endothelial and epithelial cells, which occurs through endocytosis in a pH-dependent manner [56-58]. The pentamer is thought to bind an as yet unidentified receptor on these cells [106-108]. gH/gL also forms a trimeric complex with glycoprotein O (gO), which is required for entry into fibroblasts, occurring by fusion at the plasma membrane [58][106]. Expression of the pentamer in epithelial cells prevented 90% of HCMV entry into epithelial cells while not interfering with viral surface attachment [109]. By contrast, pentamer expression in fibroblasts did not block HCMV entry into fibroblasts whereas expression of gH/gL blocked HCMV entry by 40%. Expression of receptor binding proteins causes interference with entry by obstructing or sequestering the cellular receptor. Passaging through fibroblasts produces a strong selective pressure against UL128-131. Loss of function mutations in UL128, UL130, and UL131 can arise in clinical strains in as few as 5 passages in fibroblasts [110]. The laboratory strains, including AD169, have been highly propagated in fibroblasts, and all have mutations or deletions in these genes. This renders them incapable of infecting endothelial and epithelial cells, highlighting the requirement of functional UL128-131 for entry into these cells. “Clinical” strains such as TR and Merlin, with limited propagation in fibroblasts, do retain their ability to infect endothelial and epithelial cells [106]. Taken together, these data suggest that the trimer and the pentamer are cell-type specific receptor-binding complexes, which is reminiscent of the mutually exclusive EBV gH/gL and gH/gL/gp42

complexes. PDGFR has recently been established as the fibroblast receptor of gH/gL/gO while the pentamer cellular receptor has yet to be identified [111].

1.3. gH/gL complexes

1.3.1 gH/gL

gH/gL is a conserved heterodimer present in all herpesviruses that has been shown to be required for entry and is thought to activate the fusogen, gB. The structures of gH/gL from HSV-2 and EBV have been determined revealing HSV-2 gH/gL is boot shaped and EBV gH/gL is cylindrical [95, 112]. While the orientations of the domains are different, the C-terminal H2 and H3 domains are conserved between HSV-2, EBV, and HCMV. However, the H1 and overall sequence identity of gH as well as that of gL is low (HCMV gH – 29.6%, gL - 19% with EBV and HCMV gH – 27.4%, gL – 22.3% with HSV-2) (Fig. 1.5) [95, 112, 113]. This may indicate H2 and H3 mediate a conserved viral function, e.g., interaction with the highly conserved gB, while the poorly conserved H1 and gL are less conserved to be able to bind virus-specific cell surface receptors. Unlike HSV and EBV, gH/gL of HCMV is present on the viral surface in complex with UL128/UL130/UL131 or gO and is rarely found alone [114]. HCMV gH/gL is also unusual because gL of HSV-1 and EBV have chemokine-like structure while HCMV gH/gL does not [115]. Additionally, the HCMV gH/gL complex was suggested to be covalently linked by disulfide bonds [116]. This was confirmed by mass spectrometry indicating gH-C95 and gL-C47 form the covalent linkage [117]. This makes HCMV gH/gL the only disulfide-bonded heterodimer of the three which may indicate that unlike their HSV and EBV counterparts, HCMV gH and gL do not interact extensively, thus

requiring the disulfide bond for stability. These species-specific differences suggest that gH/gL plays an adapter role between the specific needs for entry into various target cell types and the activation of the conserved fusogen, gB [118].

gH has six predicted glycans, is 743 amino acids (AA) long, migrating at ~90 kDa, and consists of an ectodomain, transmembrane domain, and a short cytosolic tail five residues in length. HCMV gL has one predicted glycosylation sites, is 278 AA-long, migrating at ~33 kDa and is disulfide bonded to gH. Therefore, both proteins migrate at ~123 kDa under non-reducing conditions [116].

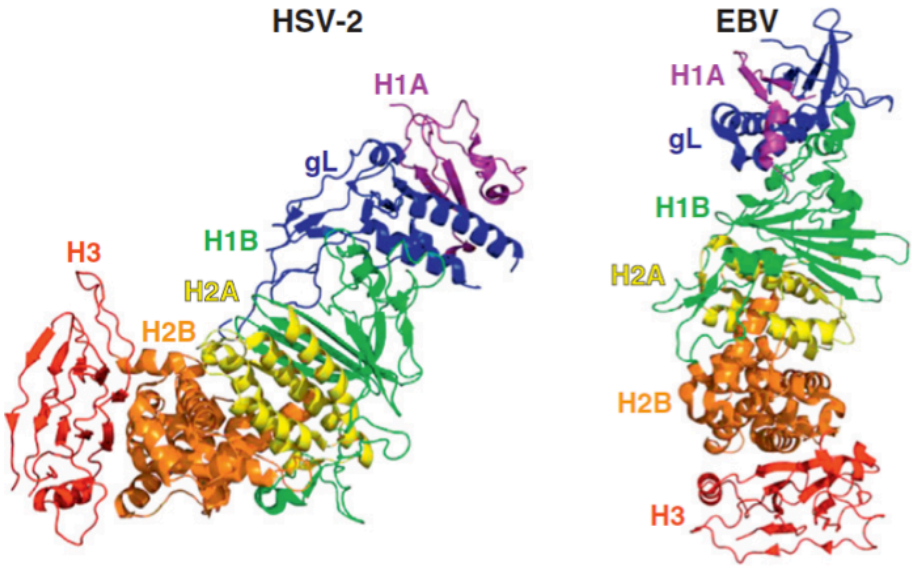

Figure 1.5. HSV-2 and EBV gH/gL Structures. The HSV-2 and EBV gH/gL with conserved domains, yet drastically different orientation. gL is colored in blue, H1A in purple, H1B in green, H2A in yellow, H2B in orange, and H3 in red. Conservation decreases down the rainbow with H3 being the most conserved and H1A/gL the least. Image courtesy of [118].

1.3.2. gH/gL/gO

The gH/gL/gO complex is important for entry into fibroblasts, though gO was initially reported to be a protein chaperone for gH/gL [119]. Further experiments revealed that gO has many isoforms and is associated with gH/gL on the viral envelope. The ratio of gH/gL/gO to pentamer on the viral surface appears to be strain specific as well as dependent on which type of cell the virions were replicated in [114, 120]. Mass spectrometry (MS) analysis indicated that gO is covalently bonded to gH/gL through a disulfide bond formed between gL-C144 and gO-C351 forming a 1:1:1 heterotrimer (Fig. 1.6) [121]. A low-resolution structure of the heterotrimer was recently published indicating that gH/gL has a boot-like shape similar to that of HSV-2 gH/gL and gO sits at the top of the boot where gL-C144 is located [95, 117]. gH is the only complex protomer with a transmembrane domain, thus it tethers the other two protomers to the viral envelope. gO has 11 predicted glycosylation sites, which is impressive for the size of the protein (472 amino acids long) [117].

Figure 1.6. The gH/gL/gO and Pentamer Complexes. Low-resolution EM structures of the HCMV gH/gL heterodimer bound to either gO or UL128/UL130/UL131 in a mutually exclusive manner via the same gL-C144. Figure courtesy of [117].

1.2.3. gH/gL/UL128/UL130/UL131

The pentameric complex formed by gH/gL/UL128/UL130/UL131 is important for entry into endothelial, epithelial, and monocytes and is thought to be the receptor binding complex for these cells. The 214 AA-long UL130 and 110 AA-long UL131 proteins

migrate as a ~35 kDa and ~18 kDa bands, respectively, under reducing conditions but as a single ~50-kDa band under non-reducing condition, indicating they are disulfide bonded [116]. UL128 is 145 AA-long and 17 kDa in size, with no predicted glycosylation sites. Interestingly, UL128 has a conserved pattern of cysteines characteristic of CC chemokines and has been shown to exhibit chemokine activity, recruiting peripheral blood mononuclear cells (PBMCs) [refs]. UL128 also increases expression of interleukin-6 (IL-6) and tumor necrosis factor-a (TNF-a) 2-3 fold over a UL128 knockout [122]. UL130 has been shown to have three glycosylation sites has been suggested to also have chemokine sequence homology [123, 124]. UL131, with one predicted glycosylation site, has no additional functions proposed beyond epithelial/endothelial cell entry.

UL131 was thought to non-covalently bind the gH/gL heterodimer, tethering UL130 to the complex as well [116]. This was shown to be incorrect by a low-resolution EM structure recently published alongside the gH/gL/gO EM structure. The EM structure of the pentamer indicated that UL128, in fact, was bound to gL through UL128-C162 and the same gL cysteine bound by gO, C144 (Fig. 1.7) [117]. UL130 is bound to UL128 which tethers UL131 to the complex. As with gH/gL/gO, the pentameric complex is tethered to the viral envelope via the transmembrane domain of gH.

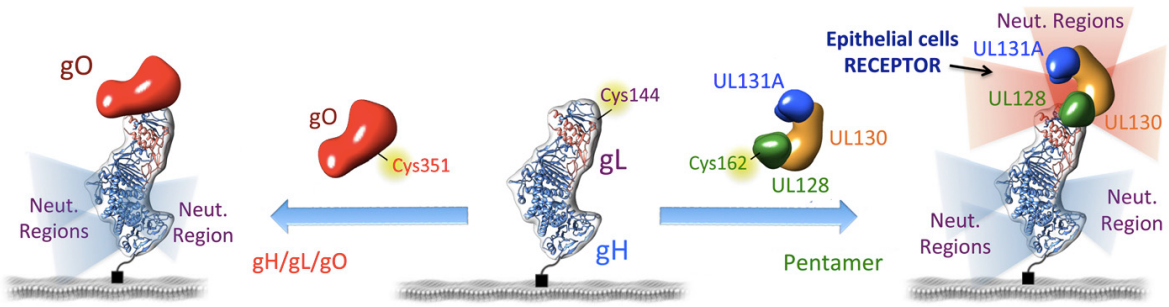

Figure 1.6. The gH/gL/gO and Pentamer Complexes. Low resolution EM structures of the HCMV gH/gL heterodimer bound to either gO or UL128/UL130/UL131 in a mutually exclusive

manner via the same gL-C144. Figure courtesy of [117].

1.2.3. gH/gL/UL128/UL130/UL131

The pentameric complex formed by gH/gL/UL128/UL130/UL131 is important for entry into endothelial, epithelial, and monocytes and is thought to be the receptor binding complex for these cells. The 214 AA-long UL130 and 110 AA-long UL131 proteins migrate as a ~35 kDa and ~18 kDa bands, respectively, under reducing conditions but as a single ~50-kDa band under non-reducing condition, indicating they are disulfide bonded [116]. UL128 is 145 AA-long and 17 kDa in size, with no predicted glycosylation sites. Interestingly, UL128 has a conserved pattern of cysteines characteristic of CC chemokines and has been shown to exhibit chemokine activity, recruiting peripheral blood mononuclear cells (PBMCs) [refs]. UL128 also increases expression of interleukin-6 (IL-6) and tumor necrosis factor-a (TNF-a) 2-3 fold over a UL128 knockout [122]. UL130 has been shown to have three glycosylation sites has been suggested to also have chemokine sequence homology [123, 124]. UL131, with one predicted glycosylation site has no additional functions proposed beyond epithelial/endothelial cell entry.

UL131 was thought to non-covalently bind the gH/gL heterodimer, tethering UL130 to the complex as well [116]. This was shown to be incorrect by a low resolution EM structure recently published alongside the gH/gL/gO EM structure. The EM structure of the pentamer indicated that UL128, in fact, was bound to gL through UL128-C162 and the same gL cysteine bound by gO, C144 (Fig. 1.7) [117]. UL130 is bound to UL128 which tethers UL131 to the complex. As with gH/gL/gO, the pentameric complex is tethered to the viral envelope via the transmembrane domain of gH.

1.4 Herpes viral Fusogen, gB

1.4.1. Fusion Mechanism

All enveloped viruses must fuse their viral envelope with the cellular membrane to enter cells and replicate. Membranes repel each other, thus this is an energetically unfavorable event and requires something to drive fusion. Fusogens are proteins that undergo extensive refolding to drive fusion of the viral envelope with the target cell membrane (reviewed in [125]). The exact mechanism is not known for any of the 8 herpesviruses. However, it can be inferred from what is known of other viral fusogens (Fig. 1.8). The proteins begin in a compact, metastable, prefusion state. Once triggered by binding of a cell surface receptor, they extend, inserting their fusion loops, also called fusion peptides, into the cellular membrane [126, 127]. The unstable, extended intermediate conformation folds back onto itself, pulling the two membranes into close proximity until they begin to merge. This results in a hemifusion state in which only the outer leaflets of the viral envelope and cell membranes have merged [127]. Once the inner leaflets also merge, a pore is formed, which expands until large enough for the viral capsid to be released into the cytoplasm. The fusogen is left in a stable, postfusion conformation. The energy released in the transition from the metastable prefusion state to the stable postfusion state is thought to drive membrane fusion [125]. The conformational pathway has not yet been mapped for any of gB homologs and may have unique features due to the reliance on additional viral proteins for function [128, 129].

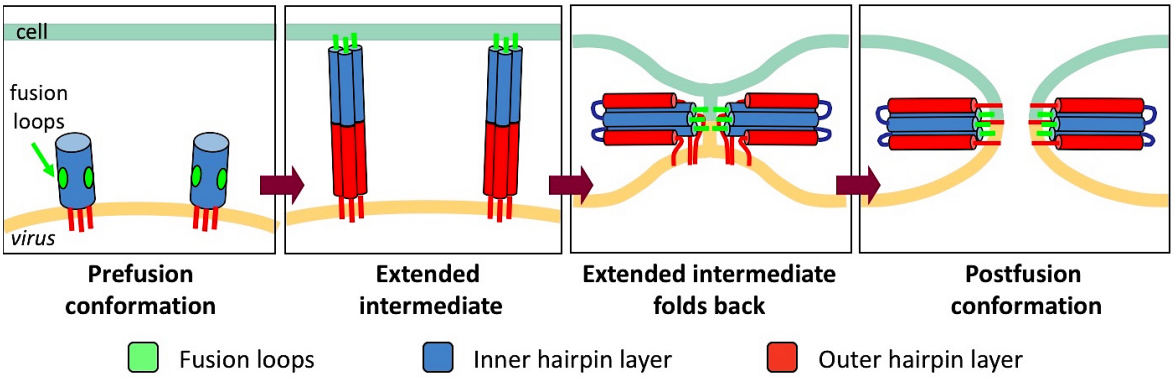

Figure 1.7. Mechanism of Viral Fusogens. A schematic representation of what is known about the basic mechanism of viral fusogens. The four stages of fusion are illustrated. Fusion loops, or fusion peptides, are shown in green, the outer layer of the hairpin formed by the postfusion conformation is colored blue and the inner layer is colored red. The figure was kindly provided by Cooper and Heldwein [129].

1.4.2. Classes of Viral Fusogens

There are three classes of viral fusogens (class I-III), designated based on structure. Class I fusogens have a long core made of an alpha helical coiled-coil and are trimeric in both their pre and postfusion states [130-134]. The core forms a 6-helix bundle with the C-terminus in the postfusion conformation (Fig. 1.8A) [132, 135]. Class I fusogens must undergo proteolytic cleavage to free the internal fusion peptide which is used to anchor the fusogen in the cell membrane [136-140]. The fusion peptide is located near the membrane in the postfusion state (Fig. 7A). Members of this class include HIV Env, influenza hemagglutinin, and paramyxovirus F [130, 132, 133, 141].

The alphavirus E and flavivirus E make up the class II fusogens [142-144]. Activation of this type of fusogen does not involve proteolytic cleavage of the fusogen itself. Rather cleavage of the fusogen's partner is necessary resulting in a mechanism to prevent premature activation [145, 146]. Prefusion conformations include homodimers or

heterodimers that dissociate at low pH, depending on the species [142, 145, 147]. However, the postfusion conformation of class II fusogens is trimeric like other viral fusogen classes (Fig. 1.8B). Class II viral fusogens typically have one hydrophobic fusion loop at the bend of a beta hairpin [143, 144, 148].

Class III is the most recently discovered class of viral fusogens. Its members include G of vesicular Stomatitis virus (VSV), gp64 of baculovirus and gB of HSV-1 and EBV [127, 149]. The postfusion conformations have been determined for each (Fig. 1.8), but the prefusion conformation is only available for VSV G [102, 113, 150-152]. All of the known structures are trimeric, including VSV G prefusion. Similar to class I, a coiled-coil makes up the core of the postfusion structures. Conversely, like class II, class III typically have hydrophobic fusion loops at the bend of a beta-hairpin, although there are two fusion loops in class III. While proteolysis does occur in some class III fusogens, it has not been shown to be important for fusogenic activity [153]. Thus, class III shares some characteristics with both of the originally defined classes, with additional class-specific features.

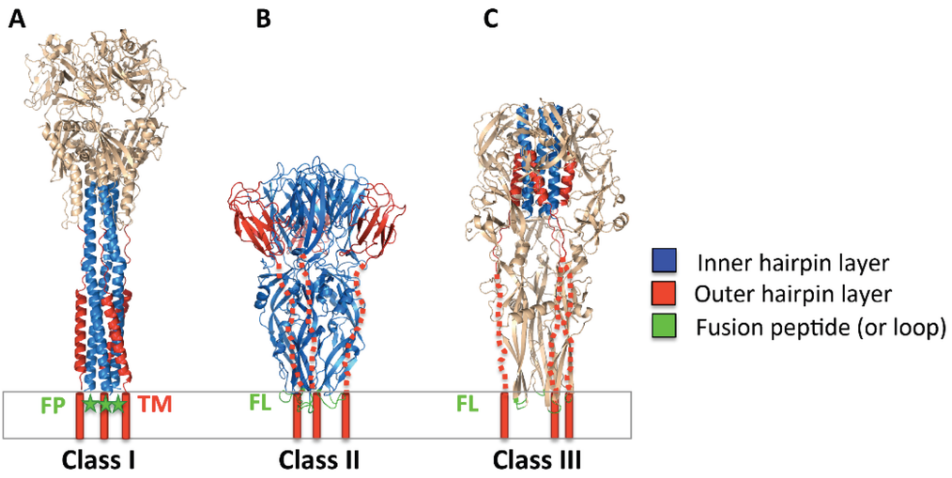

Figure 1.8. The Three Classes of Viral Fusogens. Examples of Class I, II, and III viral fusogens in their postfusion conformation. Paramyxovirus F (1ZTM) representing class I, Dengue E

(1OK8) representing class II, and vesicular Stomatitis virus G (2CMZ) representing class III. The membrane (white box), transmembrane domains (red cylinders), and unresolved extended segments (red dashes) are modeled as are the unresolved F fusion peptides (green stars). The structure of the outer layer of the hairpin is colored blue and the inner layer is colored red. Figure courtesy of Cooper and Heldwein [129].

1.4.3. Structure of the Viral Fusogen, gB

The available crystal structures of gB ectodomains from HSV and EBV show their postfusion forms [102, 113], while their perfusion conformations have not yet been characterized (Fig. 1.8B). The postfusion structures of HSV and EBV gB share a structural similarity with vesicular stomatitis virus (VSV) glycoprotein G (Fig.1.7) and baculovirus gp64 [152, 154]. gB is about 900 amino-acid long (HCMV: 906 aa; HSV-1: 904 aa; EBV: 857 aa) and contains a large ectodomain, a hydrophobic membrane-proximal region (MPR), a transmembrane domain (TM), and the intraviral (or cytoplasmic) domain (cytodomain) (Fig. 1.8A). HCMV gB shares 24.2% and 30.2% identity with its HSV-1 and EBV homologs, respectively, within its ectodomain. Despite the relatively low sequence identity, the crystal structures of HSV-1 and EBV gB ectodomains are very similar. Both are spike-like trimers in which each protomer consists of 5 domains (DI-V) with a disordered N-terminal region [102, 113]. DI, or fusion domain (FD), is composed of a pleckstrin homology domain (PHD) module and finger-like beta-sheet protrusions containing fusion loops at their tips. DII consists of another PHD. DIII, or core domain (CD), harbors the long helix that forms a central triple coiled-coil within gB trimer. DIV or crown domain (CRD) forms ear-like protrusions at the end of the spike distal from the fusion loops. Finally, DV is an extended polypeptide that

spans nearly the entire length of the gB spike and fits into a long groove formed by DIII and DI of the two neighboring protomers.

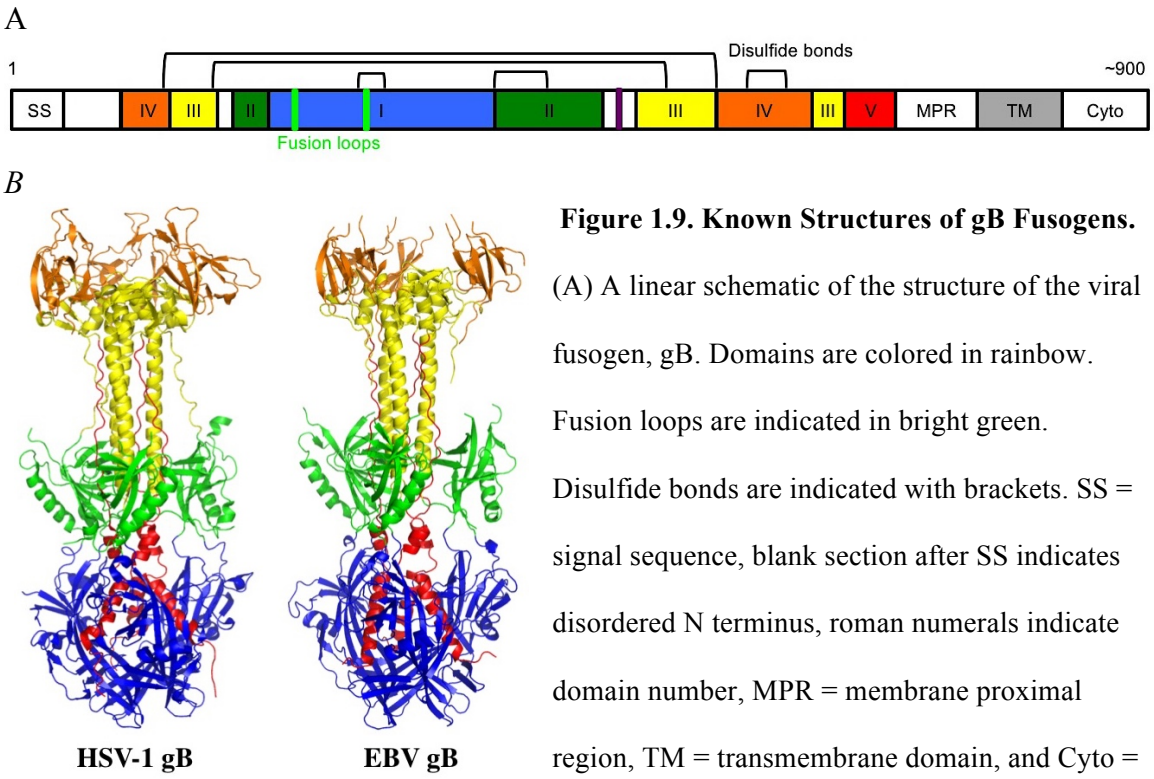

Figure 1.9. Known Structures of gB Fusogens. (A) A linear schematic of the structure of the viral fusogen, gB. Domains are colored in rainbow. Fusion loops are indicated in bright green. Disulfide bonds are indicated with brackets. SS = signal sequence, blank section after SS indicates disordered N terminus, roman numerals indicate domain number, MPR = membrane proximal region, TM = transmembrane domain, and Cyto = cytoplasmic domain. (B) The ectodomain of HSV-1 (2GUM) and EBV is shown in their postfusion form and colored according to A to indicate domains. Figure created in Pymol (http://www.pymol.org).

1.4.4. HCMV gB

HCMV gB is thought to function as a fusogen by analogy with its homologs from other herpesviruses, such as HSV and EBV [76]. gB is conserved among herpesviruses, and like all gB homologs, HCMV gB is essential for entry into all cell types [76]. Antibodies against gB prevent entry, but not attachment, neutralizing at a post absorption step [155], supporting the idea that gB is the viral fusogen.

Sharma, et al. characterized many structural aspects of HCMV gB. They found that gB is cleaved by furin proteases in mammalian cells, though not homogeneously with a portion remaining uncleaved. Cleavage results in a ~70 kDa N-terminal fragment and a ~35 kDa C-terminal fragment held together by disulfide bonds [156]. There are 11 conserved cysteines present in gB which form 5 disulfide bonds with one unbonded cysteine. MALDI-TOF mass spectrometry indicated that gB is 101.3 kDa and yet it migrates at around 120 kDa in SDS-PAGE gels. Both are much higher than calculated (78.4 kDa) likely due to extensive glycosylation or the protein. HMCV gB has eighteen predicted glycosylation sites, which is much higher than the five of HSV-1 gB and nine of EBV gB. The ectodomain of HCMV gB was shown to be a trimer by multiangle light scattering (MALS). Finally, Like many class II viral fusogens, the fusion loops of HCMV gB are highly hydrophobic, a trait shown to be required for HCMV entry [156].

In addition to being the predicted HCMV fusogen, HCMV gB has several other putative functions. Binding of gB to cellular integrins or PDGFR has been proposed to initiate cellular signaling cascades necessary for viral internalization [104, 105]. A stretch of HCMV gB sequence from R92-C111 has been identified as being characteristic of a disintegrin-like motif ($RX_{5-7}DLXXF/L$) which is present in the disintegrin domain some members of the A disintegrin and metalloproteinase (ADAM) family [104, 157]. ADAMs are phylogenetically related to snake venom metalloproteases (SVMPs), both of which are transmembrane glycoprotein proteases that bind integrins [158]. This disintegrin-like motif (DL motif), is a consensus sequence found in all but 2 of the more than 30 members of the ADAMs family and has been shown to bind integrins [157]. The C-terminus of gB contains a DL motif which has been suggested to allow HCMV gB to

bind β1 integrin. Consistent with this observation, the virus cannot enter β1 integrin-deficient cells [104]. Moreover, a fragment of gB consisting of residues 57 to 146 containing the putative DL motif immunoprecipitated β1 integrin [159] and a peptide derived from this motif (RVCSMAQGTDLIRFERNIIC) inhibited HCMV entry into fibroblasts [104].

1.5 Antibody Response to Herpesviral Fusogens

1.5.1 Immunogenicity of HSV gB

Many HSV gB antibodies have been isolated and characterized using mutational and peptide mapping, showing recognition of epitopes in DI, DII, DIV and DV [102, 160, 161]. Two antibodies, SS106 and SS144, bind the C terminus of DV at residues S697-A725 and R715-A725 respectively [162]. DIV of HSV gB is free of glycans in HSV which leaves it open for binding. A large epitope of the neutralizing antibody, SS10 (residues Y640-F670), has been mapped to the side of the crown DIV forms. Residue G594, located at the top of the crown, has been shown to be important for binding of two antibodies, B2 and B5. HSV-1 DII has four predicted glycans and two proximal to the domain. Three antibodies that recognize DII have been characterized, C226, H1781, and H1838. The epitope of H1838 consists of residues A390-G410, while H1781 recognizes P454-S473, and C226 binds D419. In DI, three distinct regions are bound by seven HSV antibodies H233 (residues A315, R328), H126 (Y303), H1375 (R304), B4 (E305), and SS55 (D199, A203) in the domain [163]. This domain is predicted to be glycosylation-free, corresponding with its high immunogenicity. Interestingly, the binding affinity of

several HSV antibodies (H126, SS55, SS106, and SS144) were decreased at low pH due to conformational changes of HSV-1 gB [162].

1.5.2 Immunogenicity of HCMV gB

gB and the pentamer elicit a strong immune response with a large portion of the anti-HCMV antibodies having specificity for these proteins [164-166]. Many antibodies that recognize viral surface proteins are capable of preventing viral entry in cell culture through various methods, a property referred to as neutralizing capacity. The appreciation of the pentamer as a major neutralizing immunogen neutralizing is relatively new while the neutralizing immunogenicity of gB has been long established and well-characterized. Additionally, gB is necessary for entry into all cell types while pentamer is dispensable for fibroblast entry [76, 108]. Furthermore, anti-gB IgG could protect human trophoblast progenitor cells (TBPCs), the precursors to placental cells, while anti-pentamer IgG could not [167]. For these reasons, the human anti-gB antibody repertoire has been studied more extensively. Five antigenic regions, historically referred to as antigenic domains AD-1 through AD-5, have been identified thus far [155]. AD-1, located in DIV, was the first to be characterized followed by AD-2, located in the region of the N terminus predicted to be disordered (Fig. 1.10). AD-3 is a linear peptide spanning the cytoplasmic domain ($_{798}$VTSGSTKD$_{805}$) [168, 169]. Consistent with this, isolated human antibodies are not neutralizing, thus AD-3 is not relevant and will not be discussed further. More recently, AD-4 and AD-5 have been discovered and are located in DII and DI, respectively. These antigenic regions are described in more detail in the following sections.

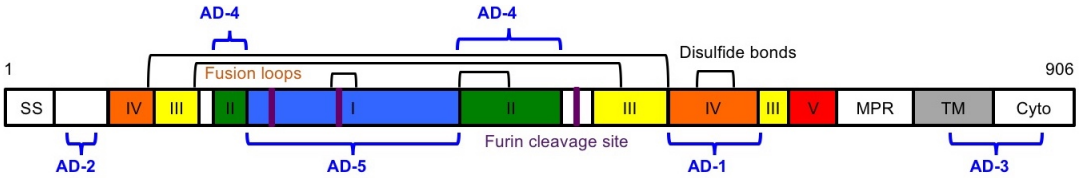

Figure 1.10. Antigenic Regions. A linear schematic of the structure of the viral fusogen, gB with the location of 5 known antigenic regions (AD-1-5) indicated in blue brackets. Domains are colored in rainbow. Fusion loops are indicated in bright green. Disulfide bonds are indicated with brackets. SS = signal sequence, roman numerals indicate domain number, MPR = membrane proximal region, TM = transmembrane domain, and Cyto = cytoplasmic domain.

1.5.3 AD-1

AD-1, which localizes to domain DIV, residues 484-650 (Fig. 1.10), is the most immunogenic region with 100% of HCMV-positive sera containing antibodies against it [169-173]. Furthermore, 38-50% of the anti-gB antibodies within each serum sample bind AD-1 [155, 174]. AD-1 elicits antibodies with varying levels of neutralizing capacity. Most anti-AD-1 antibodies (>90%) are nonneutralizing and these can interfere with the neutralizing activity of the few anti-AD-1 antibodies that do neutralize [155, 175]. An in-depth study aimed at identifying residues important for binding of anti-AD-1 antibodies was conducted to identify neutralizing versus non-neutralizing determinants [176]. Speckner, et al. generated 600 random single point mutations in a DIV *E. coli* expression construct (residues 484-650). After screening for proper AD-1 expression, Western blot was used test for a decrease in binding of a panel of anti-AD-1 monoclonal antibodies (mAbs), seven neutralizing and four non-neutralizing. They identified fifteen mutations that reduced or abolished binding of one or more tested antibodies (R562C, P577L, S587L, Y588C, G592S, G595D, L601P/H605N, C610Y, L612F, P613Y, Y625C,

Y627C, F632L, and K633T). The binding of each antibody was reduced by a subset of mutations, with extensive overlap of neutralizing and non-neutralizing sets (Fig. 1.7). Thus, this study failed to identify the determinants of neutralization.

	Human mAb						Murine mAb					
	Neutralizing				Non-		Neutralizing			Non-		
AD-1 mutation	89-104	ITC52	ITC48	ITC63B	ITC33	ITC39	7-17	9-3	27-287	27-156	27-11	Human serum
AD-1	+++	+++	+++	+++	+++	+++	+++	+++	+++	+++	+++	+++
R562C	++	++	++	++	+	-	-	++	-	+	++	++
P577L	-	+	-	+	(+)	-	-	-	(+)	+	-	(+)
S587L	++	++	++	+++	++	++	++	+	++	++	(+)	++
Y558C	+++	+++	+++	+++	+++	+++	+++	+++	+++	+++	-	+++
G592S	(+)	++	++	++	++	+	++	+	++	+++	(+)	++
G595D	+++	+++	++	+++	+++	+++	++	+	+++	+++	++	+++
LHL601/ 5/12/PNF	-	+++	++++	++	-	-	-	-	+	+++	-	-/+
LH601 /5PN	ND	+++	-	++	-	ND	-	-	-	+++	-	(+)
C610Y	-	-	-	-	-	-	-	-	-	-	-	-
P613Y	++	++	-	++	+	++	++	-	+++	+++	++	++
Y625C	+++	++	+	++	+	+	+	(+)	(+)	+	+	(+)
Y627C	-	-	-	-	-	(+)	-	-	+	(+)	+	(+)
F632L	+++	+++	+++	+++	+++	+++	-	+++	(+)	+++	+++	ND
K633T	ND	-	(+)	-	-	-	-	+	-	-	++	ND

Table 1.1. AD-1 antibody Binding Residues. Eleven anti-AD-1 gB antibodies were tested for loss of binding to AD-1 with 15 random mutations by Western blot. Neutralizing antibodies are designated with crosses. Level of reactivity compared to AD-1 is categorized as: - no reactivity, (+) barely detectable, + decreased, ++ slightly decreased, +++ equal, ++++ enhanced, and ND for not determined. Figure courtesy of [177].

1.5.4 AD-2

AD-2 is located in the N terminus, which is predicted to be disordered based on the structure of the gB homologs in HSMV-1 and EBV (Fig. 1.10) [156]. Correspondingly, epitopes identified in this region are linear [178, 179]. antibodies against AD-2 are rare being found in only 25-50% of HCMV-seropositive patients and even then only contributing 1-2% of the total anti-gB antibodies [155, 178, 180]. AD-2

contains two sub-antigenic binding sites: site I consisting of residues 68-77 and site II consisting of residues 50-54 [58, 178, 179]. antibodies against site II do not neutralize viral entry in cell culture and are strain-specific [178]. By contrast, all antibodies against site I that have been isolated are broadly neutralizing [58, 179, 181] . Additionally, non-neutralizing anti-site II antibodies do not inhibit binding of anti-site I antibodies, which suggests that site I and site II are antigenically distinct [178]. This is not the case with non-neutralizing anti-AD-1 antibodies making AD-2, site I a more interesting antigenic target for mAb therapeutics than AD-1 [175].

1.5.5 AD-4

The recently identified antigenic region, AD-4, elicits exclusively neutralizing Abs. More than 90% of HCMV-seropositive individuals produce antibodies against the regions [155, 163]. AD-4 is located within the discontinuous DII (residues 121-132 and 344-438) (Fig. 1.10). This domain contains a putative PH domain [182] and a disordered loop containing a furin cleavage site. A set of antibodies recognizing AD-4 were isolated from the same individual (SM5 Abs) representing different maturation states [155]. Every member of this set was shown to be capable of neutralizing viral entry into endothelial cells, epithelial cells, dendritic cells, and fibroblasts. The structure of a representative from this set (SM5-1) was determined in complex with DII expressed in *E. coli*. (Fig. 1.11) [182]. The structure established that the SM5-1 epitope includes residues 359-362 and 379-383 and the structure of DII confirmed the predicted PH domain.

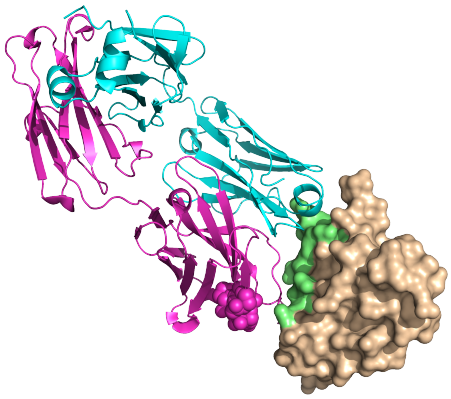

Figure 1.11. The DII/SM5-1 Fab structure. DII (AD-4) in complex with the Fab of a human neutralizing Ab, SM5-1 (4OT1). The heavy chain of SM5-1 is colored in magenta, the light chain is in slate, ADII surface representation in wheat, and AD-4 epitope is in lime. Figure reproduced from [182].

1.5.6 AD-5

The antigenic region AD-5 was also recently identified alongside AD-4 [155]. AD-5 also exclusively elicits neutralizing antibodies and is immunogenic. It was initially reported that 50% of HCMV-seropositive individuals had anti-AD-5 antibodies [155]. However, further examination with improved AD-5 constructs found that level to be closer to 90% [163]. AD-5 localizes to DI (residues 133-343) (Fig. 1.10), which contains also contains a predicted PH domain [182] and the two fusion loops. Three anti-AD-5 antibodies were isolated and characterized from different individuals (1G2, 2C2, and SM10). Each neutralized endothelial cells, epithelial cells, and fibroblasts. Additionally, no reduction in binding or neutralization was detected due to the presence of non-neutralizing, AD-1 or AD-2, site II antibodies for AD-5 or AD-4 antibodies [155]. Mutating residues N284 and Y280 were shown to decrease binding of 1G2 while mutating N293, D295, and Y280 reduced binding of both 2C2 and SM10 [163]. This suggests the antibodies bind different, yet overlapping epitopes. Interestingly, 1G2 and 2C2 displayed a ~3-fold increase in neutralization when N286 was mutated, although an increase in gB binding was not observed. N286 is predicted to be glycosylated which

may hint to a mechanism for this decrease while supporting the prediction. The structure of gB in complex with an anti- AD-5 antibody is needed to confirm these observations.

1.6. Unanswered Questions of HCMV Entry and Immunogenicity

The mechanism of herpesviral entry has been studied extensively in HSV and EBV, yet less so in HCMV. Entry proteins for which the homologs of the three viruses are highly conserved may act in similar manners allowing us to infer some mechanistic details from the more studied herpesviruses. The sequence identities of gB and gH/gL are low between HSV, EBV, and HCMV. However, there may still be structural similarities. To confirm this possibility, the structure of gB and the gH/gL trimeric and pentameric complexes are needed. Such structures may also highlight species specific details. Furthermore, gB and the gH/gL complexes are strong immunogens capable of eliciting neutralizing antibodies. The immunogenicity of gB has been studied, but a structural framework is needed to understand the determinants of antibody recognition. If an epitope is not linear, a structure of the antibody in complex with the antigen is needed to ensure mutational studies are correct when identifying the exact epitope as is the case with AD-1, AD-4, and AD-5. If a neutralizing epitope is unstructured and linear, as is the case with AD-2, a structure of the antibody/antigenic protein complex is still necessary to understand the method of neutralization.

Finally, gB elicits antibodies with a wide range of neutralizing capacity. Since neutralization is an in vitro assay, it may not correlate with protection from HCMV infection. Determining which antigenic region elicits the most protective antibodies in humans would improve the likelihood that appropriately designed recombinant gB vaccines and monoclonal antibody therapies have great enough efficacy to be

administered to patients. Due to resistance and toxicity of available antivirals, these two methods of prevention and treatment are sorely needed. Therefore, the aim of this thesis is to characterize and determine the structure of the HCMV entry proteins as well as the complexes gB forms with human neutralizing antibodies. Additionally, the protective capacity of such antibodies will be examined.

Chapter two: Materials and Methods

2.1. Cloning/Mutagenesis

2.1.1. gB constructs and mutagenesis

Constructs used to express the gB ectodomain and various mutants of it were all derived from the laboratory adapted strain, AD169 (Table 2.1). gB was truncated at residue 706 for expression of only the ectodomain and not the hydrophobic membrane proximal region, transmembrane, or cytodomains of the C-terminus. The endogenous signal sequence at the N-terminus was also truncated and replaced with the Honey Bee Melittin secretion signal sequence present in the pFastBac1 plasmid backbone (Invitrogen) [156].

Previously, the ectodomain of gB (strain AD169), residues 25-706 (gB706), was cloned into pFastBac1 plasmid for insect cell expression using PCR with primers and 4 hydrophobic residues in the predicted fusion loops were mutated to their non-hydrophobic HSV-1 and EBV counterparts (Y155G/I156H/Y157R/W240A) [156]. Three additional residues were also mutated (Y206H/L241T/Y242H) using splicing by overlap extension (SOE) PCR with primers (forward flanking: 5'-CGGTCTAGAACCATGAAATTCTT-3', Y206H mutation: forward 5'-CATAGGGACAGTCATGAAAACAAAACC-3'; reverse 5'-GGTTTTGTTTTCATGACTGTCCCTATG-3'; L241T and Y242H mutations: forward 5'-GGCAGCACCGCGACCCATCGT-3'; reverse 5'-ACGATGGGTCGCGGTGCTGCC-3', reverse flanking: 5'-CGCGCATATGTTTGATTGTAT-3') and cloning into the pFastBac1::gB706-4M plasmid (pSS2) using the restriction enzymes XbaI and NdeI, generating the construct pFastBac1::gB706-7M (pSS9).

The N-terminus of gB706-7M was truncated before amino acid 78 (gB78-706-7M) using primers (forward flanking HB27, Δ5' reverse HB28, Δ3' forward HB29, and reverse flanking HB30 in Table 3.2). Cloning was accomplished using plasmid's restriction site SacI and endogenous restriction site NdeI, generating construct pFastBac1::gB78-706-7M (pHB14).

The endogenous furin cleavage site was replaced with an enterokinase cleavage site (DDDDK) using primers (forward flanking HB31, enterokinase 5' reverse HB32, enterokinase 3' forward HB33; reverse flanking HB34) generating the construct pFastBac1::gB78-706-7M-E (pHB15 - gB78-706-7M-). Endogenous internal NdeI and HindIII restriction sites were utilized for cloning into gB78-706-7M.

The endogenous furin cleavage site was also mutated four serines in the construct with the N-terminus still intact (pSS9 - gB706-7M → gB706-7M-FM for furin mutant) using primers (forward flanking HB31, FM 5' reverse HB37, FM 3' forward HB38; reverse flanking HB34) containing the four serines, generating construct pFastBac1::gB706-7M-FM (pHB17). Once again, endogenous internal NdeI and HindIII restriction sites were utilized for cloning into gB706-7M.

The N-terminus of gB706-7M-FM was truncated before amino acid 51 (gB51-706-7M-FM) using primers (forward flanking HB31, Δ51 5' reverse HB39, Δ51 3' forward HB40; reverse flanking HB34) generating construct pFastBac1::gB706-7M-FM (pHB17). Endogenous internal NdeI and HindIII restriction sites were utilized for cloning into gB706-7M-FM. All clones were sequenced and verified to contain the correct reading frame and appropriate sequences. Due to the cloning strategy, all mature gB proteins contain two extra residues (DP) at the N terminus.

2.1.2. gH/gL constructs and mutagenesis

Sequences used for generating gH and gL constructs were from the "clinical" strain TR which was minimally passaged in fibroblasts. A two-protein expression variant of pFastBac1, pFastBacDual (Invitrogen), was used to co-express gH/gL in SF9 cells. (Table 2.1). TR gH tagged with eight C-terminal histidines and gL were cloned into the pFastBacDual backbone using primers (forward 5' HB1 and reverse 3' HB2) (Table 2.2) generating construct pFastBacDual::gH-His8/gL (pHB1). NotI and BglII restriction sites were utilized for cloning into the backbone.

The plasmid backbone, pMT/BiP/V5-His A (Invitrogen) was used to stably co-transfect gH and gL in *Drosophila* S2 cells. TR gH tagged with eight C-terminal histidines was cloned into the pMT/BiP/V5-His A backbone using primers (forward 5' HB16 and reverse 3' HB17) generating construct pMT/BiP/V5-His::gH-His8 (pHB12). TR gL was also cloned into the pMT/BiP/V5-His A backbone using primers (forward 5' HB18 and reverse 3' HB19) generating construct pMT/BiP/V5-His::gL (pHB13). EcoRI and BglII restriction sites were utilized for cloning into the backbone. The sequence of all three clones was verified to contain the correct reading frame and appropriate sequences by sequencing.

2.1.3. UL128/UL130/UL131 constructs and mutagenesis

UL128, UL130, and UL131 sequences were also derived from TR and had intact, un-mutated sequences of the three genes allowing the strain to maintain the ability to enter endothelial and epithelial cells. The pET24b *E. coli* expression vector with a N-terminal Hisx6 tag, a SUMO solubility tag, and a PreScission protease site cloned in

(pJP4) and a GST tag expression vector, pGEX-6P-1 (GE Healthcare Life Sciences), were used for expression of UL128, UL130, and UL131 in T7 Express (NEB) or Origami *E. coli*. (EMD Millipore) (Table 2.1). Each UL gene was cloned into both backbones to provide constructs with 2 different tags (His6-SUMO-PP and GST) for each. Primers pairs for each gene and each backbone are listed in Table 2.2. pFastBacDual backbone using primers (forward 5' HB1 and reverse 3' HB2) generating construct pFastBacDual::gH-His8/gL (pHB1). BamHI and NotI restriction sites were used for cloning into pGEX-6P-1 and BamHI and HindIII restriction sites were used for cloning into pJP4. Sequences were confirmed by sequencing.

Protein	Name	Backbone	Insert
AD169 HCMV gB	pSS9	pFastBac1	gB706-7M
	pHB14	pFastBac1	gB78-706-7M
	pHB15	pFastBac1	gB78-706-7M-E
	pHB17	pFastBac1	gB706-7M-FM
	pHB18	pFastBac1	gB51-706-7M-FM
TR gH/gL	pHB1	pFastBacDual	gH-His8/gL (SF9 expression)
TR gH	pHB12	pMT/BiP/V5-His A	gH-PP-His8 (S2 expression)
TR gL	pHB13	pMT/BiP/V5-His A	gL (S2 expression)
TR UL130	pHB5	pGEX-6P-1	GST- UL128-28 (CO)
	pHB6	pET24b-His-SUMO-PP (pJP4)	His6-SUMO-UL128-28 (CO)
TR UL128	pHB3	pGEX-6P-1	GST- UL130-26 (CO)
	pHB4	pJP4	His6-SUMO-UL130-26 (CO)
TR UL131	pHB7	pGEX-6P-1	GST- UL131-19 CO
	pHB8	pJP4	His6-SUMO-UL131-19 CO

Table 2.1. Plasmids created for this work. Numbers indicate residues the protein is truncated to. Abbreviations include: seven fusion loop mutations (7M), PreScission Protease cleavage site (PP), Enterokinase cleavage site (E), Histidine tag X Histidine long (HisX), solubility tag (SUMO), Glutathione S-transferase (GST), and codon optimized (CO).

Plasmid	Name	Sequence	Descript.
pSS9		CGGTCTAGAACCATGAAATTCTT	F5’ flank
	Y206H	CATAGGGACAGTCATGAAAACAAAACC	5’ FOR
	Y206H	GGTTTTGTTTTCATGACTGTCCCTATG	3’ REV
L241T/Y242H		GGCAGCACCGCGACCCATCGT	5’ FOR
L241T/Y242H		ACGATGGGTCGCGGTGCTGCC	3’ REV
		CGCGCATATGTTTGATTGTAT	R3’ flank
pHB14	HB27	TAC TAC GGA GCA AGT TCC CGA	F5’ flank
	HB28	ACTCCCACCACATCTCCGTACGCTAGCGCATAGATGTAAGAAATG	R5’ flank
	HB29	CATTTCTTACATCTATGCGCTAGCGTACGGAGATGTGGTGGGAGT	F3’ flank
	HB30	TGGTTTCGAAGACGGACACGTT	R3’ flank
pHB15	HB31	ATCGCAATGCCAGCTACTTTG	F5’ flank
	HB32	CTTATCATCATCATCATGAGTGATATTCAGACTGGATC	R5’ flank
	HB33	GATGATGATGATAAGAGTACGAGTGACAATAATACAACT	F3’ flank
	HB34	CTACAAATGTGGTATGGCTGATT	R3’ flank
pHB17	HB31	ATCGCAATGCCAGCTACTTTG	F5’ flank
	HB37	GGAGGAGGAGGAATGAGTGATATTCAGACTGGATC	R5’ flank
	HB38	TCCTCCTCCTCCAGTACGAGTGACAATAATACAACT	F3’ flank
	HB34	CTACAAATGTGGTATGGCTGATT	F5’ flank
pHB18	HB31	ATCGCAATGCCAGCTACTTTG	R5’ flank
	HB39	AGACGTTACGTGTTGAGAATAGACTGACGGATCCGCATAGATGTAAGA AATG	F3’ flank
	HB40	CATTTCTTACATCTATGCGGATCCGTCAGTCTATTCTCAACACGTAACG TCT	R3’ flank
	HB34	CTACAAATGTGGTATGGCTGATT	5’ FOR
pHB1	HB1	AATTTAGTCGACATGCGTCCCGGCCT	5’ FOR
	HB2	GGTGAAAGCTGTTACGTA	3’ REV
pHB12	HB16	ATCATACTAATCCCATGGGCAGACGCCGCATCCGAAGC	5’ FOR
	HB17	ATCATACTAATCGAATTCTTATTAATGGTGATGGTGATGGTGATGGT GTTGAAAGAGGACTTCGAGGTCGGTGGCGTCCACGACAA	3’ REV
pHB13	HB18	ATCATACTAATC AGATCT ATGTGCCGCCGCCCGGATT	5’ FOR
	HB19	ATCATACTAATC GAATTC TTAGCGAGCATCCACTGCTTGA	3’ REV
pHB5	HB4	ATAATAATA **GGATCC** AGCAGCTGGTCAACCCTGA	5’ FOR
	HB5	ATAATAATA **GCGGCCGC** TTATTACACGATCAGGTTCGG	3’ REV
pHB6	HB4	ATAATAATA **GGATCC** AGCAGCTGGTCAACCCTGA	5’ FOR
	HB6	ATAATAATA **AAGCTT** TTATTACACGATCAGGTTCGG	3’ REV
pHB3	HB7	ATAATAATA GGATCC GAAGAATGTTGTGAATTTATCAAT	5’ FOR
	HB8	ATAATAATA **GCGGCCGC** TTATTACTGCAGCATATAACCC	3’ REV
pHB4	HB7	ATAATAATA GGATCC GAAGAATGTTGTGAATTTATCAAT	5’ FOR
	HB9	ATAATAATA **AAGCTT** TTATTACTGCAGCATATAACCC	3’ REV
pHB7	HB10	ATAATAATA **GGATCC** CAGTGTCAGCGTGAAACCG	5’ FOR
	HB11	ATAATAATA **GCGGCCGC** TTATTAGTTGGCAAACAGACGA	3’ REV
pHB8	HB10	ATAATAATA **GGATCC** CAGTGTCAGCGTGAAACCG	5’ FOR
	HB12	ATAATAATA **AAGCTT** TTATTAGTTGGCAAACAGACGA	3’ REV

Table 2.2. Primers designed for cloning plasmids. Primers were given arbitrary names in the format HBXX for organization. Red lettering indicates restriction enzyme site used for digestion and ligation into the plasmid backbone. Primers all read 5’ to 3’, left to right. 5’ forward or 3’

reverse is indicated. For deletions and replacements, F5' flank and R5' flank indicates the forward and reverse primers for the 5' flanking fragment and F3' flank and R3' flank indicates the forward and reverse primers for the 3' flanking fragment to be joined by SOE PCR.

2.2. Protein Expression and Purification

2.2.1. Transient, glycosylated, secreted expression of gB and gH/gL

Spodoptera frugiperda (Sf9) cells were grown in SF-900 II SFM (Invitrogen) in suspension at 27ºC. Recombinant baculoviruses of all HCMV gB ectodomain constructs were generated using Bac-to-Bac system (Invitrogen). After two rounds of amplification, passage 3 (P3) stocks of baculoviruses were harvested and stored at 4ºC in the dark and in the presence of 2% Fetal Bovine Serum (FBS, Invitrogen).

Expression and purification of HCMV gB ectodomain from supernatants of Sf9 cells infected with recombinant baculovirus have been previously described [156]. Briefly, ~7.5 mL of viral stocks were added to 1.5 L of SF9 cells at $2x10^6$ cells/mL. The supernatant was harvested at 68-72 hours post infection by pelleting cells at 3750 rpm at 4ºC for 1 hour. The supernatant was filtered (0.45 μm filter), then concentrated by Tangential Flow Filtration with a 20-KDa PLTK cartridge (Millipore). To decrease media components, the buffer was exchanged once with phosphate-buffered saline (PBS) and 0.1 mM PMSF was added as a protease inhibitor.

2.2.2. Stable, glycosylated, secreted expression of gH/gL

S2 cells were stably transfected with the pMT/BiP/V5-His plasmids and copper sulfate (CuSO4) was used induction of protein production. S2 cells were conditioned for several 3weeks in SF9 media prior to transfection. Then varying ratios of the two

plasmids (pHB12 – gH-His6 and pHB13 - gL) were added to cells in the presence of Blasticidin. Once cells reached a large enough volume to occupy a large spinner flask (~1.5 L), expression was induced using 500 -750 μM CuSO4, allowed to continue for 5-9 days. The cells were harvested and pelleted at 3750 g for 30 minutes at 4°C. A 0.22 μm filter was used to remove remaining cells and the protease inhibitor PMSF was added to the supernatant. No ratio of gH to gL plasmid tried generated gH expression while gL was only in present in the insoluble fraction. Thus, purification of gH/gL was not performed from S2 cell supernatant.

2.2.3. Bacterial expression of UL128, UL130, UL131

Expression of UL128, UL130, and UL130 each with a GST or His6-SUMO tag was tested in T7 Express and Origami (containing a Kan^R cytoplasm reducing) *E. coli* strains. Expression temperature (18^oC or $37\ ^oC$ overnight) was also tested for each protein/*E. coli* pair. Bacteria were lysed via freeze/thaw and centrifuged to separate the insoluble material from the soluble. Fractions were run on a 12% gel and stained with coomassie.

2.2.4. Antibody purification of gB

gB was purified from the concentrated supernatant via immunoaffinity chromatography, with mAb 27-39 coupled to CNBr-activated Sepharose 4B (GE Healthcare). The column was washed with 10 mM Tris (pH 8.0), 500 mM NaCl and gB was eluted with 3 M potassium thiocyanate (KSCN) in wash buffer. The eluate was concentrated using Millipore Amicon Ultra-15 with 50 kDa molecular weight cutoff, and

run over size exclusion chromatography (SEC) on a Superdex 200 10/300 GL column with a 24 ml bed volume (GE Healthcare) to further purify gB. The gel filtration buffer used was 20 mM Tris pH 8.0, 150 mM NaCl. 1 mM EDTA was added to the buffer if purification was not followed by trypsin or furin cleavage.

2.2.5. Purification of gH/gL Using Nickel Sepharose

The C-terminal His6 tag attached to gH was purified used to gH/gL generated in SF9 cells via batch-binding to Nickel Excel beads (GE Life Sciences 17-3712-01). Imidazole was added to concentrated gH/gL supernatant to a final concentration of 20 mM. 3 ml of nickel sepharose was then added and batch binding was allowed to proceed overnight at 4°C with gentle stirring (~75 rpm). The nickel sepharose beads were transferred to a disposable chromatography column (Bio-Rad poly prep chromatography column, Catalog #731-1550). and washed with 10-bed volumes of 20 mM imidazole, 20 mM Tris pH 8.0, and 150 mM NaCl. A second wash was done with 20-bed volumes of 40 mM imidazole in the same buffer followed by elution of gH/gL with 10-bed volumes of 140 mM imidazole in buffer. PMSF was added to the eluate to a final concentration of 0.1 mM. A Millipore Amicon Ultra-15 with 50 kDa molecular weight cutoff was used to concentrate the eluted complex which was then run over size exclusion chromatography (SEC) on a Superdex 200 10/300 GL column with a 24 ml bed volume (GE Healthcare) to further purify gB with 20 mM Tris pH 8.0, 150 mM NaCl, 1 mM EDTA.

2.2.6. Affinity tag purification of UL128, UL130, and UL131

Refolding of insoluble UL128 was attempted with Ni-NTA purified His-SUMO-UL128. The insoluble protein was solubilized with 6 M Gdn-HCl and was then dialyzed to 2 M Gdn-HCl, 1 M, 0.75 M, and 0.5 M Gdn-HCl stepwise. The protein began to precipitate at 0.75 M Gdn-HCl, and ¾ precipitated at 0.5 M Gdn-HCl. Samples were taken, then the tag was cleaved with PreScission Protease (PP) to test the activity of PP under various Gdn-HCl concentrations. Again, samples were run on a 12% gel and stained with Coomassie.

2.2.7. Antibodies

Hybridoma cell lines expressing anti-HCMV gB monoclonal antibody 27-39, 27-156, and 7-17 were a gift from William J. Britt (University of Alabama) [175, 183]. The monoclonal antibodies were purified at the GRASP facility at Tufts Medical Center. 27-39 is a conformational mAb that recognizes the oligomeric form of HCMV gB ectodomain [184]. Purified TRL345 was provided without compensation, for academic use, by Larry Kauvar at Trellis Bioscience, Menlo Park, CA [58]. Purified 1G2 and SM5-1 IgG, biotinylated IgG, and Fab and were gifted by Michael Mach (Institut für Klinische und Molekulare Virologie, Friedrich-Alexander Universität Erlangen-Nürnberg, Erlangen, Germany) [155]. The mouse monoclonal anti-gH antibody, AP86, was obtained from David C. Johnson (Oregon Health Sciences University) [106, 116, 185], although it was originally isolated by Bill Britt (University of Alabama) [185]. R683, a rabbit polyclonal anti-HCMV IE86 antibody was also provided by David Johnson [106].

2.2.8. Formation of Antibody/gB Complexes

1G2 and TRL345 Fabs were added to various gB constructs at a molar ratio of 1 gB protomer to 1.3 Fab molecules to ensure gB saturation. Mixtures were incubated at room temperature for 1 hour. The mixtures were then spun down at 13,000 x g for 10 minutes to pellet any aggregated protein. Next, they were run over an Agarose/dextran S200 SEC column to separate the complex from excess Fab. Various samples were taken at each stage and run on an SDS page gel stained with Coomassie to confirm complex formation.

2.3. Proteolysis and Biochemical Assays

2.3.1. *Trypsin and Furin*

Limited trypsin proteolysis was conducted on various gB constructs to cleave the endogenous furin cleavage site to completion by incubating with trypsin (Sigma) at room temperature at protease to substrate ratios of 1:100 for 2 hours. Trypsin was removed with Benzamidine Sepharose beads (GE Healthcare Life Sciences). Furin proteolysis was conducted on various gB constructs by incubating with furin (NEB) at room temperature or 30°C with protease to substrate ratios of 1:10, 1:100 and 1:200 for 2-14 hours in 0.1 M Tris pH 7.5, 0.5% Triton X-100, 1 mM $CaCl_2$, 1 mM 2-mercaptoethanol, Furin was inhibited using HALT protease inhibitor cocktail and was removed by Agarose/dextran SEC as described. To monitor proteolysis, samples were taken at various stages and run on Coomassie-stained gels (below).

2.3.2. Papain for Fab generation

TRL345 Fab was generated by cleavage into Fc and Fab fragments with immobilized papain (Thermo Fisher - product #20341) according to the recommended protocol with few modifications (marked by *). Briefly, papain beads were washed with 16-bed volumes of sample buffer (20mM sodium phosphate, 10mM EDTA; pH 7.0) containing freshly added cysteine•HCl at a final concentration of 20 mM and pH of 6.5* in a disposable chromatography column (Bio-Rad poly prep chromatography column, Catalog #731-1550). Then, the beads were resuspended in one volume of buffer. TRL345 at 10.6 mg/ml was digested with vary ratios* of IgG to papain beads to optimize digestion. TRL345 IgG was provided in PBS pH 7.4. To lower the pH to the active range of papain (pH 6.0-7.0), the pH of the sample buffer lowered to pH 6.5. This was crucial for digestion. 1 ml of buffer was added to the protein mixture to obtain the correct pH for papain activity (6.0-7.0). A Immobilized Protein A column (Thermo Fisher - product #20356). PBS, pH 7.2 was used as the protein A column binding buffer, washing the column with it three times with 2 ml PBS, then spinning at 100 g for 1 minute per wash. The volume of the papain digest was brought to 2.5 ml and added to the column and incubated rotating for 10 minutes at room temperature. Then flow-through containing Fab (and in this case, uncleaved IgG) was eluted by gravity flow. 2.5 ml 0.1 M glycine, pH 2.5 was used to elute Fc (and TLR345 IgG and Fab) which was neutralized with 0.25 ml of 1M Tris pH 8.5. Due to incomplete separation of Fab from Fc and IgG fractions, Agarose/dextran SEC Superdex 200 10/300 GL column with a 24 ml bed volume (GE Healthcare) was used to separate IgG from Fab/Fc and gB to separate Fab from Fc, generating the gB/TRL345 Fab complexes.

2.3.3. N-terminal sequencing

For N-terminal sequencing, protein samples were resolved on a 4-15% SDS-PAGE gel and then transferred to a PVDF membrane. The membrane was stained with Coomassie R-250. The protein bands of interest were cut out and submitted for sequencing by Edman degradation at the Tufts University Core Facility.

2.3.4. SDS-PAGE and Western blot

Three conditions were used in preparation of samples for SDS-PAGE: reducing denaturing (1% SDS, reducing agent, boiling), non-reducing denaturing (1% SDS, no reducing agent, boiling), and mildly denaturing (0.1% SDS, no reducing agent and no boiling). For Coomassie staining, gels were stained with GelCode BlueSafe Protein Stain (Thermo Fisher, product #24594) for an hour. Then, gels were destained in water for at least an hour.

For Western blotting, after separation of proteins, gels were transferred onto nitrocellulose membranes. The membranes were blocked with 5% skimmed milk in Tris-buffered saline containing 0.05% Tween-20 and probed with primary mAb (usually 27-156 for gB) at mAb appropriate dilutions. Following incubation with secondary antibody, conjugated to horseradish peroxidase, blots were developed using HRP substrate chemiluminescence kit (Bio-Rad).

2.4. X-ray crystallography

2.4.1. Crystal screening of gB and antibody complexes

Purified, uncleaved gB706-7M failed to crystallize, but both trypsin-cleaved

gB706-7M and gB78-706-7M formed crystals in the presence of polyethylene glycol (PEG) 8000 as precipitant. Crystals were grown by vapor diffusion in hanging drops using 1 μL protein at ~5 mg/ml and 1 μL crystallization solution (10-14% PEG 8000, 0.1 M Tris, pH 7.5-8.5, 0.15 M $Mg(NO_3)_2$) at room temperature.

2.4.2. Cryoprotection and freezing of crystals

Crystals were flash frozen in solution identical to the well solution (8-15% PEG 8000, 0.1 M Tris, pH 7.5-8.5, 0.15 M 0.15 M $Mg(NO_3)_2$) plus 20% glycerol for data collection. Glycerol was found to be optimal for all crystals from all complexes tested after screening various cryoprotectants (i.e. MPD, Sucrose, PEG 400, etc.).

2.4.3. Data processing of gB and gB/Ab datasets

X-ray diffraction data were collected at 100 K on NE-CAT beamlines 24IDC and 24IDE at the Advanced Photon Source, Argonne National Laboratory, and processed using XDS [186] as implemented in RAPD (https://rapd.nec.aps.anl.gov/rapd). All gB crystals adopted the orthorhombic space group and had cell dimensions consistent with 3 gB molecules (one trimer) per asymmetric unit. Data were processed in P222 space group. Many gB78-706-7M (trypsin and furin-cleaved) crystals were tested to identify ones that diffracted to medium resolution, 3.6-Å, but these crystals were prone to radiation damage, and the collected data sets had low completeness. The crystals of uncleaved gB78-706-7M-E diffracted better on average and provided a complete 3.6-Å dataset used for structure determination. An 8.8-Å data set was obtained from one gB78-706-7M-E/1G2 Fab crystal grown in PEG 8000, 0.1 M Tris, pH 7 frozen in 20% glycerol.

2.4.4. Molecular replacement for structural determination of gB

Molecular replacement as implemented in *Phaser-MR* [187] yielded a clear solution with correct packing only when using the $P2_12_12_1$ space group and the structure of trimeric EBV gB ectodomain (PDB ID 3FVC) [113] as a search model. The structure of trimeric HSV-1 gB ectodomain (PDB ID 2GUM) [102] did not yield a clear solution. However, the resulting maps were streaky, likely due to low data completeness. The first interpretable maps were obtained when molecular replacement was carried out with gB78-706-7M-E dataset and the EBV gB ectodomain as a search model. Density modification including 3-fold averaging, solvent flattening, and histogram matching, as implemented in *Autosol* [187] resulted in good-quality maps. *Autobuild* [187] was used to trace ~30% of the model; the rest was built manually in *Coot* [188] using density-modified maps generated by *Autobuild*. Domain II of HCMV gB (PDB ID 4OT1) [182] and domains I and IV of HSV-1 gB (PDB ID 2GUM) [102] were manually positioned into the density and rebuilt in *Coot*. Extensive rebuilding was necessary because neither HSV-1 nor EBV structures fit well into the experimental density. Prior to refinement, 5% of reflections set aside as a reference. The model was refined using gradient minimization and thermal parameter refinement as implemented in *phenix.refine* [187]. NCS and secondary structure were restrained initially. Several rounds of alternating refinement and rebuilding decreased R to 29.0% and R_{free} to 31.8%. At this point, secondary structure restraints were released, and the model underwent several additional rounds of refinement and rebuilding. The final R_{work} is 24.82% and R_{free} is 27.45%. Relevant crystallographic statistics are in Table 1. The final model has residues 87-696 in chain A (unresolved 78-86, 117-120, 409-410, 435-475), residues 86-697 in chain B (unresolved 78-85, 116-121,

439-474), and residues 83-695 in chain C (unresolved 78-82, 117-118, 441-475), one calcium ion located at the three-fold symmetry axis, and two water molecules.

2.4.5. Molecular replacement gB/1G2 Fab low-resolution data set

Again, *Phaser-MR* [187] was implemented on an 8.8-Å data set obtained from gB78-706-7M-E/1G2 Fab crystals. A clear solution with correct packing was obtained when the R3 space group and the structure of HCMV gB ectodomain (PDB ID 5XCF) as a search model. No density was observed for the Fab, but crystal packing allowed ample space for 3 Fabs to fit.

2.5. ELISA

Sera samples were stored at -20^{o}C since the conclusion of the study and were recently obtained from Dr. Snydman and the Massachusetts State Laboratory for our use.

2.5.1. Sera anti-gB levels ELISA

The gB ectodomain with the seven furin loop mutations and an intact N terminus intact (gB706-7M) was used for all ELISA experiments to provide soluble protein with minimal alterations. The wells of 96-well polystyrene plates (Costar, product #3370) were washed with 200 µl of phosphate buffer saline (PBS) three times. Next, 200 µl of 1 µg/ml gB706-7M (in PBS) was added to each well to allow binding and to coat the surface with gB. The plates were incubated at 4°C for four hours. The plates were moved to room temperature and incubated for an additional hour, rocking. Wells were washed with 200 µl of PBS with 0.05% Tween 20 (PBS-T) three times. Plates were blocked with

200 µl 2% Bovine Serum Albumin (BSA) (Fisher BioReagents, product #BP1600) in PBS-T at 4°C overnight. Plates were warmed to room temperature, rocking (15 minutes) and wells were washed with 200 µl PBS-T three times. Maternal sera samples were serially diluted from 1:10 to $1:1x10^6$ in steps of 1:10 in 1% BSA, PBS-T. 50 µl of each dilution was added to wells in triplicate. Serum from a seronegative mother was used as a negative control HCMVIG was used as a positive control on each plate. Plates were incubated with the sera samples for 2 hours at room temperature, rocking. Wells were washed with 200 µl PBS-T three times. A goat anti-human IgG-HRP conjugate (Bio-Rad Laboratories, catalog #172-1050) was used as a secondary antibody to detect levels of sera antibodies bound to gB. Plates were incubated, rocking for 1 hour at room temperature. Wells were washed with 200 µl PBS-T three times. 50 µl of 1-Step Ultra TMB-ELISA (Thermo Scientific, product #34028) was added to each well and plates were incubated for 15 minutes, rocking, at room temperature in the dark. To halt the reaction, 50 µl of 1 N sulfuric acid (Sigma-Aldrich, product #320501) was added to wells and the absorbance was read at 450 nm with a microplate reader (BioTek Synergy HT, Gen5 2.03). Prism 7 (GraphPad Software, for Mac OS X, 7.0a) was used to plot the absorbance against serum dilution and to calculate the concentration at which half the gB sites are occupied (Kd).

2.5.2. Blocking ELISA

Again, the soluble, complete gB ectodomain (gB706-7M) was used for all blocking ELISAs experiments so that all 4 antigenic regions (AD-1-4) were preserved. The wells of 96-well polystyrene plates were washed with 200 µl of PBS three times.

Next, wells were coated with gB by adding 200 µl of 1 µg/ml gB706-7M (in PBS) to each and the plates were incubated at 4°C for 4 hours. The plates were moved to room temperature and incubated for an additional hour, rocking. Wells were washed with 200 µl PBS-T three times. Plates were blocked with 200 µl 2% BSA in PBS-T at 4°C overnight. Plates were warmed to room temperature, rocking (15 minutes) and wells were washed with 200 µl PBS-T three times. Maternal sera samples were diluted 1:10 in 1% BSA, PBS-T and 50 µl was added to 18 wells each (to test six mAb dilutions in triplicate). 18 wells had only 50 µl of 1% BSA, PBS-T added for blocking comparison. HCMVIG was used as a positive blocking control on each plate. Plates were incubated with the sera samples for 2 hours at room temperature, rocking. Wells were washed with 200 µl PBS-T three times. Six serial dilutions of the mAb being tested for blocking were made, ranging from 10 µg/ml to 0.1 ng/ml, diluted in steps of 1:10. Each mAb dilution was tested with 50 µl in triplicate for each sera sample. Plates were incubated with biotinylated mAb for 2 hours at room temperature, rocking. Biotinylation was carried out when needed using the EZ-Link™ Sulfo-NHS-Biotinylation Kit (Thermo Fisher Scientific product #21425) as instructed. Wells were washed with 200 µl PBS-T three times. 50 µl of streptavidin HRP (Thermo Fisher Scientific, product #SNN2004) was added to each well and plates were incubated at room temperature for 30 minutes, rocking. Wells were washed with 200 µl PBS-T three times. 50 µl of 1-Step Ultra TMB-ELISA was added to each well and plates were incubated for 15 minutes, rocking, at room temperature in the dark. To halt the reaction, 50 µl of 1 N sulfuric acid was added to wells and the absorbance was read at 450 nm. Prism was used to plot the absorbance against mAb dilution and to calculate the mAb concentration at which half the gB sites

are occupied (Kd). The percent inhibition was calculated using the Kd of the curves without sera (Kd buffer) and the Kd of the sera samples (Kd serum) in the equation:

$$\% \text{ inhibition} = (1 - \text{Kd buffer} / \text{Kd serum}) \times 100\%$$

If the sera blocked too extensively and saturation was not achieved, ELISAs were repeated with a mAb dilution range of 100 μg/ml to 1 ng/ml.

Chapter Three: The Structure of HCMV gB

3.1 The Crystal Structure of HCMV gB

3.1.1 Previously known aspects of HCMV gB

gB is the putative HCMV fusogen based on homology to HSV and EBV gB, but it shares low sequence identity with them (24.2% and 30.3% respectively). Like HSV and EBV gB, HCMV gB has a large ectodomain, membrane proximal region (MPR), transmembrane domain (TM), and cytoplasmic domain and has five disulfide bonds important for proper folding (Fig. 3.1) [102, 113, 156]. The structure of DII of HCMV gB was determined in complex with a human neutralizing Ab, SM5-1 [182]. Beyond this, little structural information was available for HCMV gB at the onset of this study. Functionally, gB has been shown to be required for entry into all cell types. gB has also been implicated in cell surface attachment, possibly binding cellular integrins with a putative DL motif [104, 159]. Additionally, HCMV gB is a major viral immunogen with four antigenic domains (AD1-5) with varying levels of antibody neutralizing susceptibility [155]. To confirm that gB is, in fact, the HCMV fusogen and to map species-specific functional, areas of conservation, and antigenic regions, the crystal structure of HCMV gB is needed.

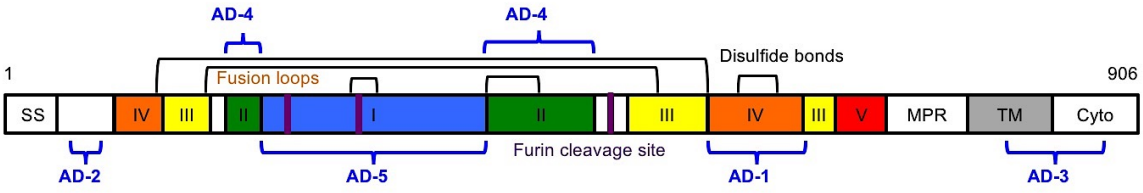

Figure 3.1. HCMV gB ectodomain structure. Schematic representation of the full-length HCMV gB. Disulfide bonds are represented as black brackets, antigenic domains (AD-1-5) are indicated in blue brackets, and mutations are shown using red bars. Structural domains, are colored as follows: domain I = blue, II = green, III = yellow, IV = orange, V = red, as in [102,

113]. SS=signal sequence, MPR=membrane proximal region, TM=transmembrane domain, and Cyto=cytoplasmic domain. Numbers denote the amino acid length of the entire protein.

3.1.2. Construct design, crystallization and structure determination.

Previously, we showed that the purified ectodomain of HCMV gB formed rosette-like aggregates, in which gB molecules associated through their exposed fusion loops [156]. To eliminate aggregation, we had replaced four exposed hydrophobic residues within the fusion loops, Y155, I156, Y157, and W240, with their more hydrophilic HSV-1 counterparts. Although these four mutations reduced aggregation [156], they did not abolish it. Analysis of an HSV-1 gB-based HCMV gB homology model, described previously [156], suggested that the remaining hydrophobic residues L241 and Y242 within the second fusion loop and the nearby residue Y206 could be responsible for the residual aggregation (Fig. 3.2). To completely abolish aggregation, residues Y206 and Y242 were replaced with their HSV-1 counterparts, while residue L241 was replaced with its EBV counterpart because HSV-1 has a hydrophobic residue, phenylalanine, at this position (Fig. 3.2). The resulting septuple mutant Y155G/I156H/Y157R/Y206H/W240A/L241T/Y242H (gB706-7M) was monodisperse (Fig. 3.3) and used for all subsequent work.

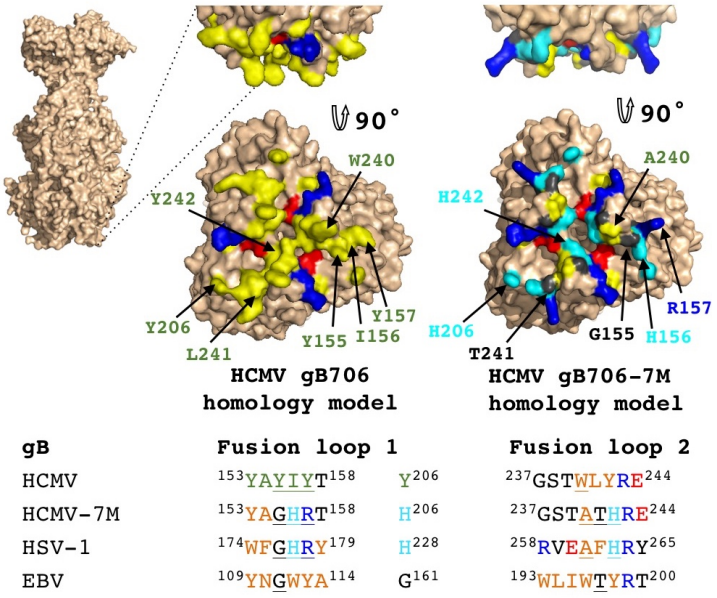

Figure 3.2. Mutations in the putative fusion loops. Mutated residues in the putative fusion loops are shown using an HCMV gB homology model generated using the structure of HSV-1 gB. Residues are colored as follows: hydrophobic (yellow), positively charged (blue), negatively charged (red), uncharged (grey), and histidines (cyan). Side chains of mutated residues in HCMV gB706 and gB706-7M mutant are labeled (in only one protomer, for simplicity). Figures were generated using PyMol (/www.pymol.org). A sequence alignment of the HCMV gB706, HCMV gB706-7M, HSV-1 gB and EBV gB fusion loops shows which mutations were introduced to generate the gB706-7M mutant (color scheme maintained). The figure is modified from [156].

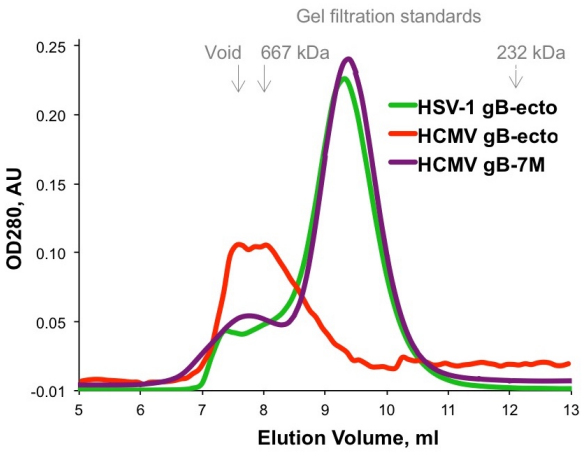

Figure 3.3. SEC of HSV-1 gB730, HCMV gB706, and HCMV gB706-7M. Agarose/dextran size exclusion chromatograms (SEC) of HSV-1 gB ectodomain (gB730, green), HCMV gB ectodomain (gB706, red), and HCMV gB ectodomain with the putative 7 hydrophobic fusion loop residues mutated (gB706-7M,

purple) are overlaid. Elution volumes of the size-exclusion standards and the void volume are labeled with arrows.

HCMV gB contains a furin cleavage site (residues 456-459) within the unstructured loop in DII that is partially cleaved during expression in mammalian cells [189, 190] (Fig. 3.1). Insect cells express furin-like proteases [191], and the gB706-7M mutant was partially cleaved during expression in Sf9 cells (Fig. 3.4). gB706-7M did not crystallize. To obtain crystals, we cleaved gB706-7M with low amounts of trypsin, a strategy that was successful in obtaining diffraction-quality crystals of HSV-1 gB ectodomain [102]. Although trypsin-cleaved gB706-7M crystallized, crystals clustered and diffracted poorly. N-terminal sequencing revealed that trypsin treatment, in addition to cleaving the unstructured loop in DII, generated heterogeneity at the N terminus with gB starting at residues S51, A67, or Y78. To eliminate heterogeneity within the N terminus, we generated a construct that started at residue Y78 (gB78-706-7M). This construct crystallized with or without trypsin treatment. Although trypsin treatment improved the diffraction, residual trypsin (present despite its removal post-cleavage) resulted in further cleavage during sample storage and crystallization (Fig. 3.4), which caused crystal degradation. To obviate complications due to non-specific trypsin cleavage, recombinant furin was used instead but proved inefficient at cleaving gB (Fig. 3.4). Finally, the furin cleavage site was replaced with an enterokinase site (gB78-706-7M-E), which prevented cleavage during expression. Uncleaved gB78-706-7M-E (Fig. 3.5A) was stable during storage (Fig. 3.4) and yielded crystals with the strongest diffraction, which suggested that both the removal of the N terminus of gB and the elimination of heterogeneous cleavage in the unstructured DII loop was beneficial for crystallization.

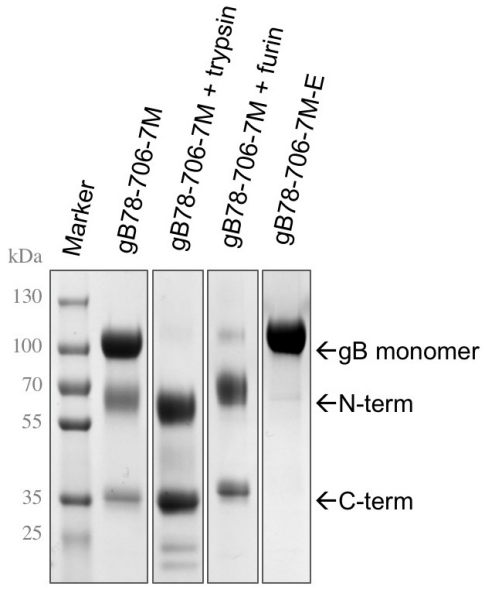

Figure 3.4. Cleavage patterns of various HCMV gB constructs. gB78-706-7M (partial cleavage during expression), trypsin cleaved gB78-706-7M (non-specific cleavage), furin-cleaved gB78-706-7M (incomplete cleavage), and gB78-706-7M-E (uncleaved) constructs were expressed and purified in SF9 cells and analyzed by SDS-PAGE and Coomassie staining. Arrows indicated uncleaved gB monomers and the cleavage products, ~70 kDa N-terminus and ~35 kDa C terminus.

A 3.6-Å resolution data set collected on a crystal of uncleaved gB78-706-7M-E was used to determine the structure of HCMV gB by molecular replacement. Both HSV-1 gB and EBV gB were tested as search models, but only EBV gB yielded a clear solution. There is one gB ectodomain trimer in the asymmetric unit. The use of 3-fold averaging, *de novo* model tracing, and extensive manual rebuilding using density-modified maps ensured that the resulting structure was minimally biased by the search model.

3.1.3. The structure of the postfusion conformation of HCMV gB ectodomain.

HCMV gB is an elongated trimer resembling a spike; each protomer consists of 5 domains (Fig. 3.5B, Fig. 3.6) assigned based on the structure of the HSV-1 gB homolog [102]. Chain A contains residues 87-696 (unresolved 78-86, 117-120, 409-410, 435-475), chain B contains residues 86-697 (unresolved 78-85, 116-121, 439-474), and chain C contains residues 83-695 (unresolved 78-82, 117-118, 441-475). HCMV gB ectodomain contains eleven cysteines, ten of which are conserved. In the structure, these conserved

cysteines form five disulfides leaving the nonconserved cysteine C246 unpaired. Previously, C246 was proposed to form a disulfide with a neighboring conserved cysteine C250 [192]. In the structure, C250 forms a disulfide bond with cysteine C185. Both C246 and C250 are located in strand β12 within the elongated fusion subdomain of DI and are unlikely to move into proximity.

Table 3.1. Data collection and refinement statistics

	gB78-706-7M-E
Data collection[a]	
Space group	$P2_12_12_1$
Cell dimensions	
a, *b*, *c* (Å)	92.15, 134.10, 295.56
α, β, γ (°)	90, 90, 90
Resolution (Å)	147.7-3.6 (3.75-3.6)
R_{sym} or R_{merge}	0.167 (0.961)
$I/\sigma I$	9.0 (1.6)
Completeness (%)	99.4 (99.9)
Redundancy	4.1 (4.1)
Wilson B	88.37
Refinement	
Resolution (Å)	57.63-3.60
No. reflections (free)	42515 (1891)
R_{work}/R_{free}[b]	0.2482/0.2745
No. atoms	14380
Protein	14377
Ca	1
Solvent	2
B-factors	115.5
Protein	115.5
Ca	85.7
Solvent	83.1
RMS[c] deviations	
Bond lengths (Å)	0.005
Bond angles (°)	1.024
Ramachandran plot[d]	
Favored (%)	97.04
Allowed (%)	2.78
Outliers (%)	0.18
All-atom clash score[d]	12.81

[a]Values in parentheses are for the highest-resolution shell.

[b]R_{work} and R_{free} are defined as $\sum||F_{obs}|-|F_{calc}||/\sum|F_{obs}|$ for the reflections in the working or

the test set, respectively.

[c]RMS, root mean square.

[d]As determined using Molprobity (molprobity.biochem.duke.edu) [193].

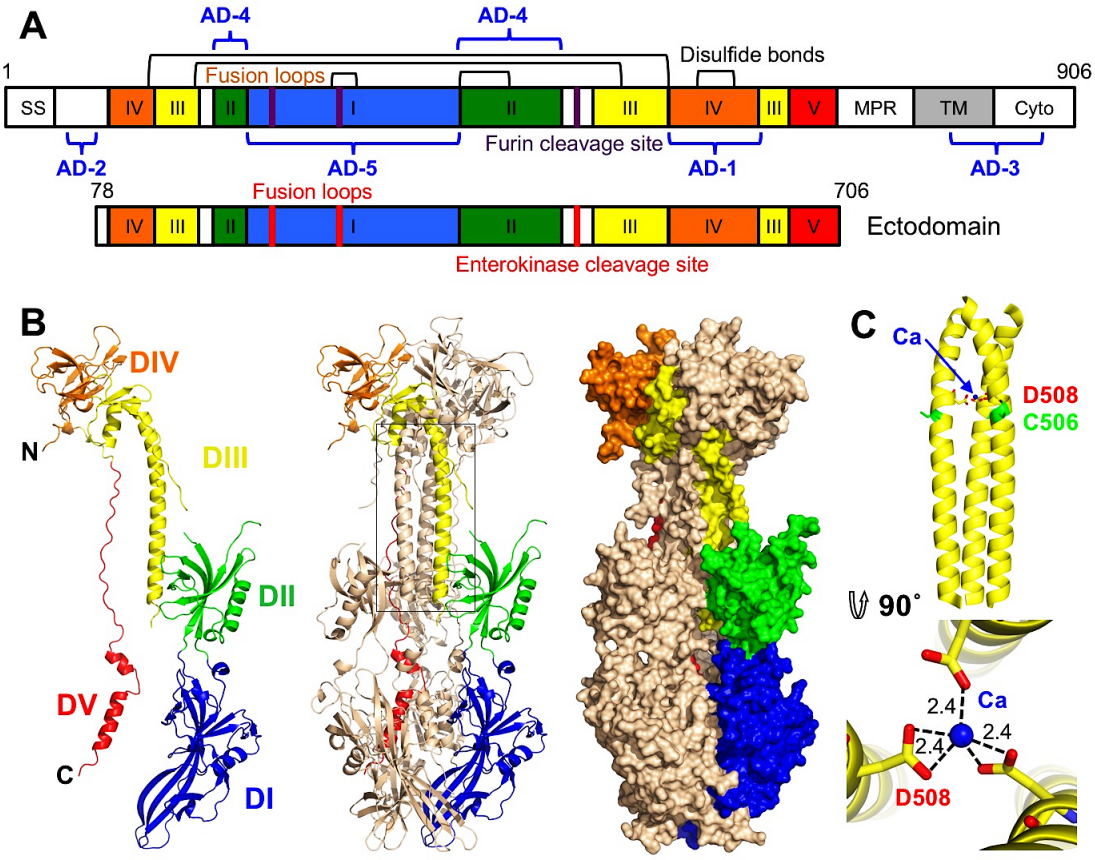

Figure 3.5. HCMV gB ectodomain structure. (A) The full-length HCMV gB (top) (again for clarity) and the crystallized construct, gB78-706-7M-E (bottom). Disulfide bonds are represented as black brackets, antigenic domains (AD-1-5) are indicated in blue brackets, and mutations are shown using red bars. Structural domains, are colored as follows: domain I = blue, II = green, III = yellow, IV = orange, V = red, as in [102, 113]. SS=signal sequence, MPR=membrane proximal region, TM=transmembrane domain, and Cyto=cytoplasmic domain. Numbers denote construct boundaries. (B) The crystal structure of the HCMV gB ectodomain is shown as a protomer and a trimer in cartoon representation as well as a trimer in surface representation. Chain B is colored by domain as in (A). (C) Side and top down view of the coiled coil in DIII with a coordinated

calcium ion (CA) (blue sphere). Side chains of D_{508} (yellow) with carboxyl oxygens (red) and C_{506} (green) are also shown. Dashed lines indicate distances between the carboxyl oxygens in D_{508} and the calcium ion. All structure figures were made in Pymol (http://www.pymol.org).

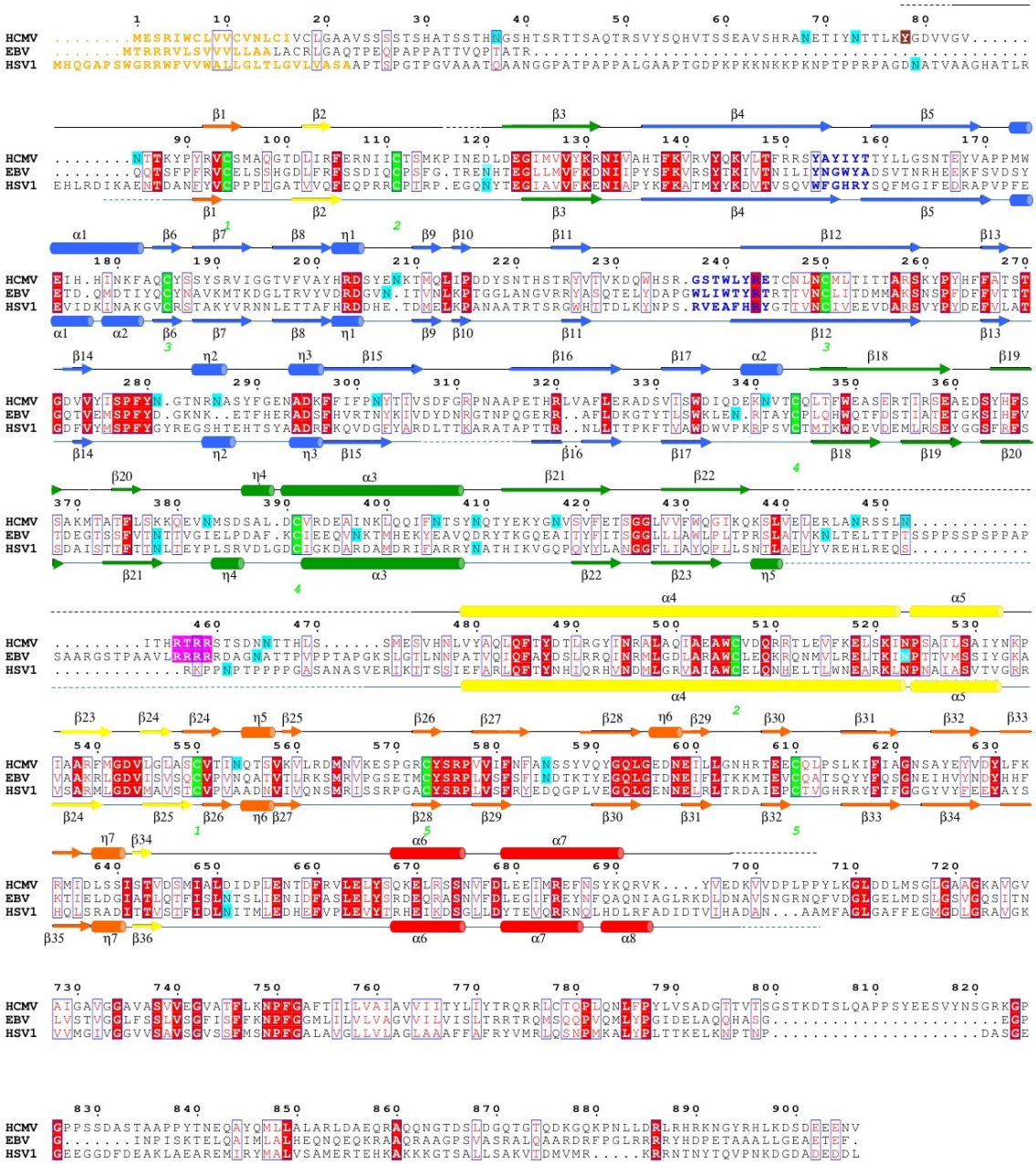

Figure 3.6. Multiple sequence alignment of gB homologs. Protein sequence alignment of HCMV (strain AD169), EBV (strain B958), and HSV-1 (strain KOS) (UniProtKB accession numbers P06473, Q777B0, P06437, respectively) was generated and analyzed using ClustalW2

[194] and ESPript 3.x [195]. The secondary structure of HCMV is displayed above the alignment, and the secondary structure of HSV-1 (2GUM) [102] is displayed below the alignment. Secondary structure elements are colored by domain, as in Figure 3.5. Unresolved residues are denoted with dashed lines, signal sequences as orange letters and residues in fusion loops as blue letters. Cysteines participating in disulfide bonds are highlighted in green, furin cleavage sites in pink, and glycosylation sites in cyan. The first residue in the crystallized HCMV gB construct, Y78 is highlighted in brown. Identical residues are shown as white text on red background, and similar residues are shown as red text.

A strong density found within the core of the central coiled coil, at the three-fold symmetry axis, was modeled as a Ca^{2+} ion, which is coordinated by the side chains of D508 from the three gB protomers (Fig. 3.5C). Residue D508 is located C-terminally to C506, which forms a disulfide with C111 from an extended region in the N terminus. This portion of the coiled coil is not expected to be unfolded in the prefusion form [196], by analogy with VSV G [197], which means that the Ca^{2+} ion is unlikely to be involved in the conformational transition from the prefusion to the postfusion form. The Ca^{2+} ion could potentially contribute to the stability of the coiled coil. Interestingly, the coordinating residue D508 is conserved among all CMV strains shown in Fig. 3S1.

The regions missing from the structure are likely conformationally flexible. The N terminus of each chain is unresolved, similarly to HSV-1 and EBV gB structures (Fig. 3.6). Residues 441-473 make up the disordered loop in domain II that contains the furin cleavage site in the WT gB and the enterokinase cleavage site in the crystallized construct. Although this loop was left uncleaved in the crystallized construct, it remained flexible and unresolved in the structure.

HCMV has a high level of variability among strains thus is beginning to be appreciated as quasi-species [198, 199]. We aligned gB sequences from 60 clinical and laboratory isolates (Fig. S1) and mapped conservation patterns onto the structure (Fig. 3.7). Conservation scores of the analyzed strains ranged from 88.16 to 99.89%. The regions with the greatest diversity lie within the unstructured N terminus and the disordered DII loop, which are truncated or unresolved in the postfusion structure, respectively. Although the exact sequence of the furin cleavage site varies (RTRR, RTKR, or RAKR), and R468 was reported to be under positive selection [199], the furin cleavage site itself is completely conserved across all compared sequences. Although proteolytic processing of gB is dispensable for viral growth in culture [200], the conservation of the furin site implies that it is beneficial to the virus for an as yet unknown reason. The least conserved region within the resolved structure is located within the pleckstrin homology sub-domain of DI. The variable residues create a patch on the right face of this subdomain (Fig. 3.7). The next most variable region is nestled in the crown of DIV (Fig. 3.7).

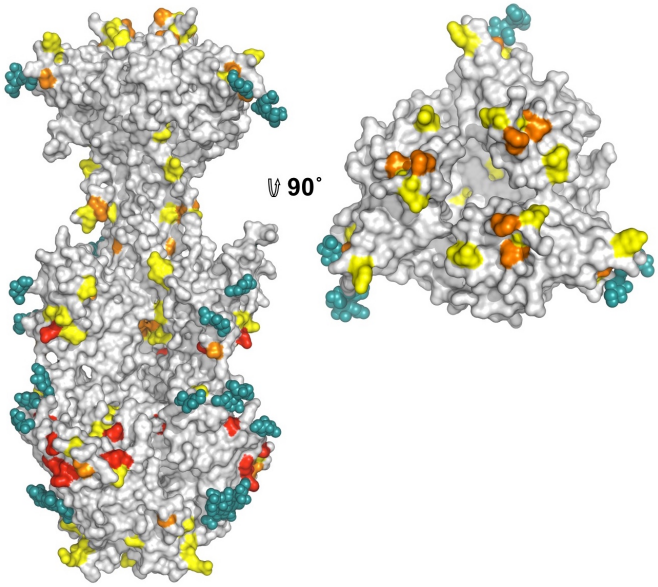

Figure 3.7. Mapping of poorly conserved residues within HCMV gB. Surface representation of gB with non-conserved residues displayed in red, semi-conserved residues in orange, conserved residues in yellow, and completely conserved residues in grey. Glycans (teal) are shown in space-filled representation. Side and top views are shown.

3.1.4. HCMV gB shares similar fold with HSV-1 and EBV homologs but has a distinct domain arrangement.

As anticipated from the 25-30% of sequence identity, the overall structure of the HCMV gB resembles the postfusion structures of HSV-1 and EBV gB ectodomains (Fig. 3.8A-B). This similarity confirms that the HCMV gB structure represents its postfusion conformation and places HCMV gB among class III fusogens. Each of the 5 domains can be superimposed onto its counterpart (Fig. 3.9, Table 3.2). Among the 5 domains, DII and DIII are the most similar (Fig. 3.9B,C). DIV are also similar even though a number of loops in DIV of EBV gB are unresolved precluding detailed comparisons (Fig. 3.9A). The fold of DI is also conserved with the exception of the β hairpin β7-β8 (residues 188-201 in HCMV gB), which adopts similar orientations in HCMV and EBV gB that differ from its orientation in HSV-1 (Fig. 3.9E). Within the DV, helices α6 and α7 of HCMV gB DV differ from their counterparts in length and orientation (Fig. 3.9D). Thus, in terms of the fold, domains that are closest to the (fused) membrane display the highest structural divergence.

Despite these local differences, the overall domain folds are very similar. By contrast, relative domain orientations are different between HCMV, HSV-1, and EBV gB structures (Fig. 3.8). The most obvious difference is the hinge between DIII and DIV and the linker between DIV and DV, which positions DIV noticeably differently from that in HSV-1 and EBV relative to the gB "core", DIII/DV (Fig. 3.8C). Additional differences are found within the hinges linking DII and DIII, as well as DI and DII (Fig. 3.8D). As the result, each gB protomer appears "twisted" in a unique way, which is apparent when the three structures are superposed on the conserved DII (Fig. 3.8C-D). This architectural

variation suggests structural plasticity that could have evolved to fine-tune gB to carry out virus-specific functions while preserving its conserved fusogenic role.

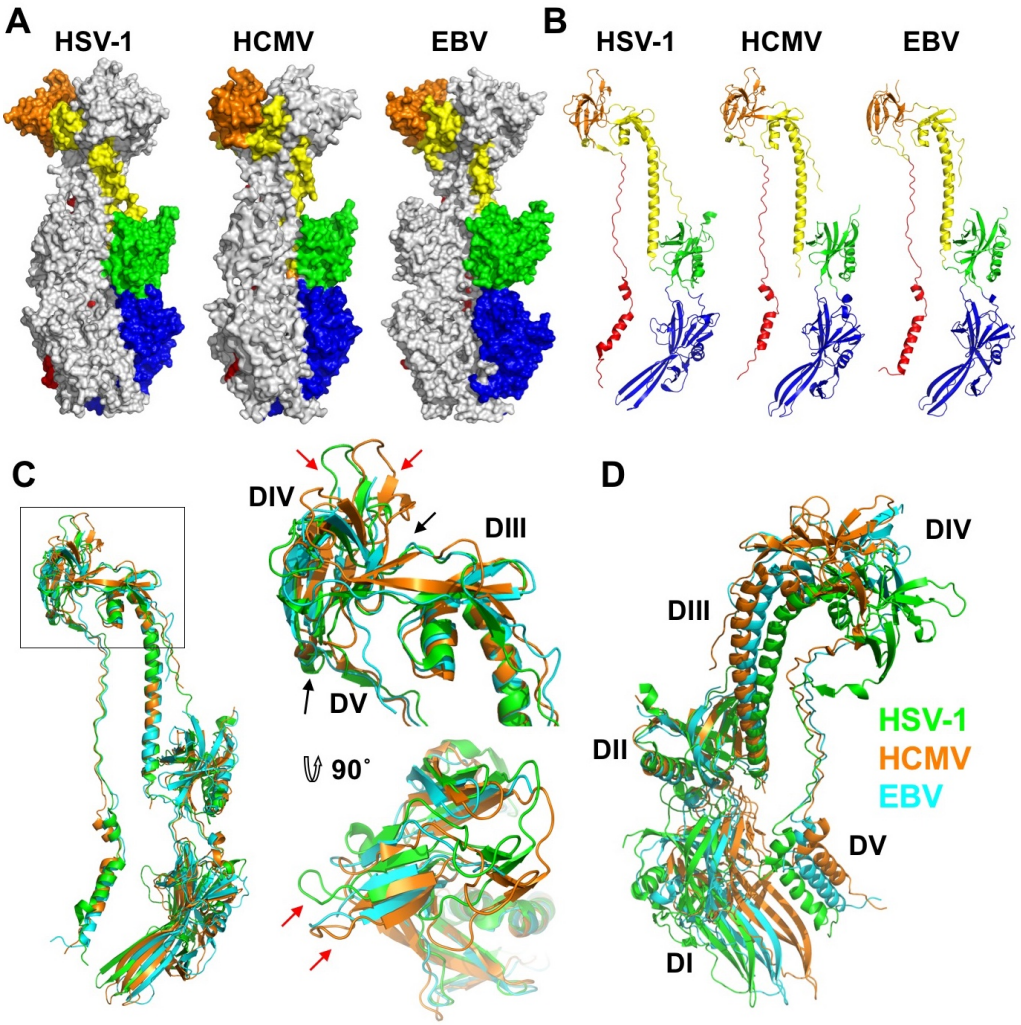

Figure 3.8. Structures of HCMV, HSV-1, and EBV gB ectodomains. The structures of HSV-1 (2GUM), HCMV (5CXF), and EBV (3FVC) gB ectodomains are aligned on the central trimeric helices and are displayed side-by-side as (A) trimers in surface and (B) protomers in cartoon representations. The domains I-V of each homolog are colored as in [102, 113]. (C) Single protomers (chain B in HSV-1 and HCMV) are aligned on the core helix α4. DIV and DIII are enlarged and shown from the side and top down. Red arrows indicate differences in the domain placement of the homologues, while black arrows indicate the hinge between domains. HSV-1 gB

is colored in green, HCMV gB is colored in orange, and EBV gB is colored in cyan. (D) Single protomers (chain B in HSV-1 and HCMV) are aligned on DII, demonstrating the species-specific twist of each, using the same color scheme as in C.

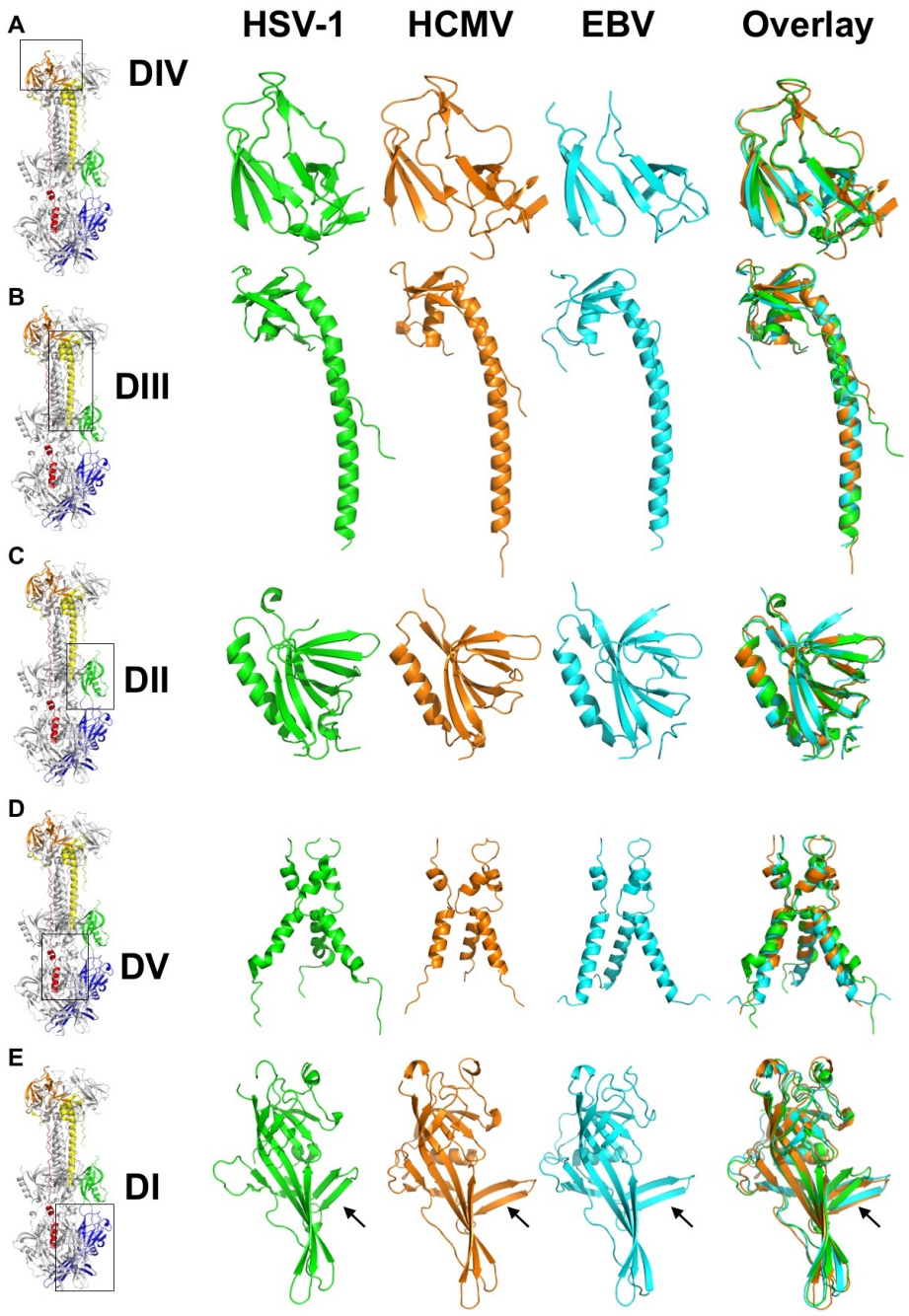

Figure 3.9. Alignment of individual gB domains. Individually aligned domains IV, III, and II of HSV-1 (2GUM) (green), HCMV (orange), and EBV (3FVC) (cyan) are shown side by side and

as an overlay. Residues used in alignments and RMSDs are listed in Table S1. Boxes indicate the location of the aligned region within the HCMV gB structure.

Domain		HSV-1	HCMV	EBV
DI	Chain B			
	Residues	154-363	133-343	89-294
	RMSD	2.002		1.587
DII	Chain B			
	Residues	142-153, 364-476	121-132, 344-438	7-88, 295-390
	RMSD	0.833		0.991
DIII	Chain B			
	Residues	117-133, 500-669	121-131, 346-437	52-68, 455-624
	RMSD	1.396		1.015
DIV	Chain B			
	Residues	111-116, 573-660	87-95, 549-637	42-51, 528-616
	RMSD	1.354		0.985
DV	Trimer			
	Residues	670-725	647-698	625-679
	RMSD	3.286		2.334

Table 3.2. RMSD values from domain alignments of HSV-1, HCMV, and EBV gB. Residues used in aligning individual domains of the three homologs are listed. RMSDs between HSV-1 and HCMV gB domains are listed under HSV-1. RMSDs between EBV and HCMV gB domains are listed under EBV. Pymol (http://www.pymol.org) was used to calculate RMSDs.

3.1.5. Locations of motifs of potential functional importance.

Several motifs of potential functional importance have been identified in HCMV gB. A peptide corresponding to residues 678-694 inhibited cell entry of several HCMV strains [201]. The structure helps explain this inhibitory activity because residues 678-694 form helix α7 in the extended DV, which forms the outer layer of the trimeric postfusion hairpin (Fig. 3.5B). Analogous peptides derived from the outer layer of the postfusion hairpin in other viral fusogens block fusion by binding to the extended intermediate and preventing its refolding into a trimeric hairpin (reviewed in [202, 203]).

The HCMV peptide 678-694 may similarly inhibit fusion by blocking the formation of the postfusion form.

HCMV cannot enter fibroblasts deficient in the β1 integrins $\alpha_2\beta_1$, $\alpha_6\beta_1$, and $\alpha_v\beta_3$ [104], which suggests that HCMV binding to β1 integrins is necessary for entry into fibroblasts. It has been proposed that β1 integrin binding is mediated by a disintegrin-like motif (DL motif) within the crown of HCMV gB [104]. Furthermore, a peptide derived from this motif inhibited HCMV entry into fibroblasts [104] while a larger gB fragment immunoprecipitated β1 integrin [159]. The DL motif ($RX_{5-7}DLXXF/L$) was first identified in several ADAMs (a disintegrin and metalloproteinase) family members [157] and is distinct from the classic integrin-binding RGD/KGD motif found in most of the related integrin binding, snake venom metalloproteases (SVMPs) [158]. The DL motif is found in the integrin-binding domain of ADAMs has been demonstrated to bind $\alpha_9\beta_1$ integrins while the RGD motif binds $\alpha_v\beta_3$ integrins [204]. In the HCMV gB structure, the proposed DL motif does not form a domain but maps instead to the extended polypeptide that belongs to DIII and DIV. Residues identified as important for $\alpha_9\beta_1$ integrin binding in ADAMs, except for D101, are buried (Fig. 3.10). Although we cannot exclude the possibility that these residues are exposed in the prefusion structure, how the proposed disintegrin-like motif in HCMV gB participates in binding to β1 integrins is currently unclear. Unfortunately, what the disintegrin-like motif in ADAMs look like is unknown because the only available crystal structure of a disintegrin domain is that of ADAM10, one of the two ADAMs which lacks this motif [157].

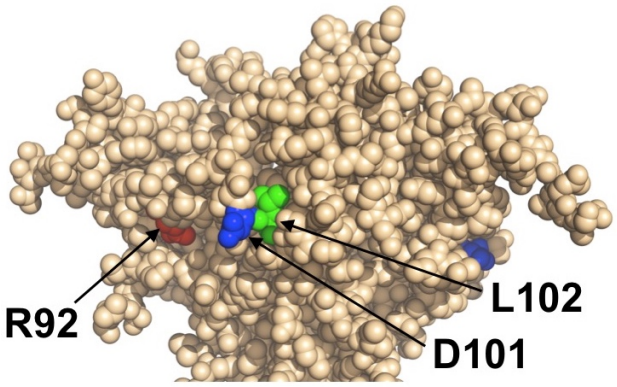

Figure 3.10. Putative disintegrin-like motif (DL motif) is largely buried. Residues in the putative DL motif require for integrin binding, R92 (red), D101 (blue), L102 (green) are highlighted on the structure of HCMV gB. F105 is completely buried. The figure was made in Pymol (http://www.pymol.org).

3.1.6. HCMV gB is extensively glycosylated.

Unlike HSV-1 and EBV, HCMV gB ectodomain is extensively glycosylated, with eighteen predicted N-linked glycosylation sites in strain AD169 [156]. Within gB78-706, fifteen asparagines are predicted to be glycosylated. Of these, four are located within the unresolved regions of the polypeptide (N85, N447, N542, and N465) but all of the remaining eleven sites contain glycans in the structure (even though at some sites, the glycans are not ordered in all three polypeptides). Most glycans, with one exception, are unresolved beyond the first two NAG moieties due to their flexibility. Only the glycan at residue N208 is well ordered with clear density for the mannose moieties beyond the branching point ((Man4-GlcNAc2-N-Asn)) (Fig. 3.11A). This glycan packs against the protein, with the second NAG stacking against the side chain of W174, which explains why it is well ordered in the crystal. Sequence alignment of HCMV gB sequences from 60 strains revealed that seventeen out of eighteen N-linked glycosylation sites are completely conserved (Fig. S1). The glycosylation site at N37 in AD169 is not

conserved, while strains Towne, Merlin, and related clinical isolates contain a potential glycosylation site at N456, which is absent from AD169 strain.

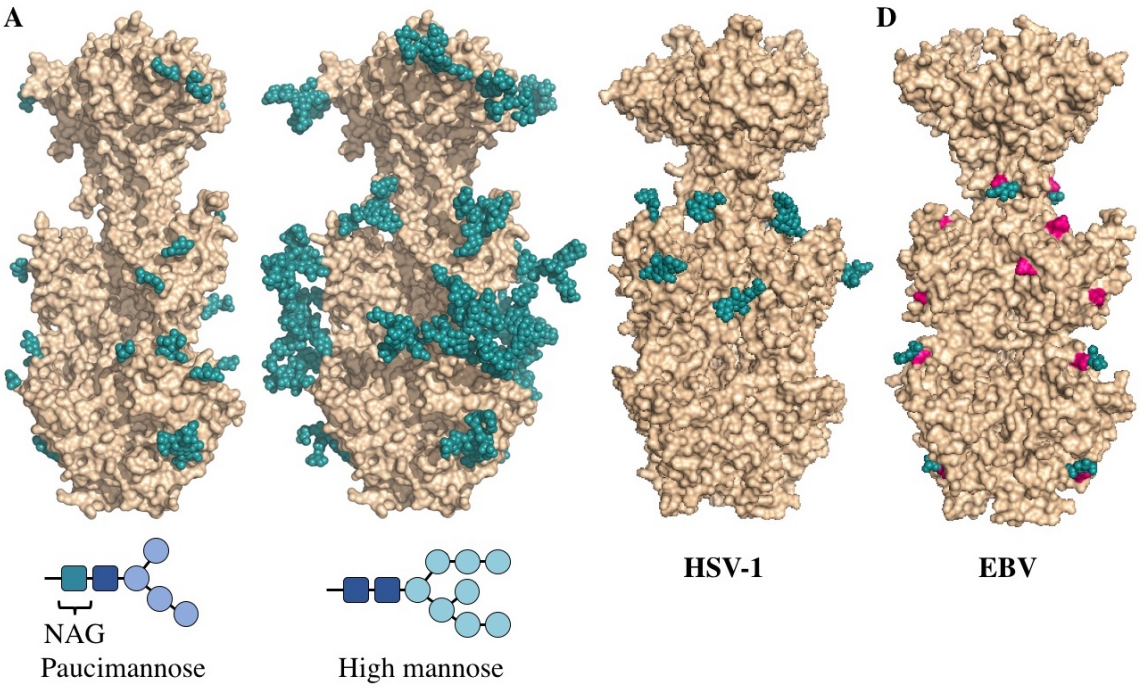

Figure 3.11. Observed glycosylation and fully-glycosylated model of HCMV gB. (A) HCMV gB is shown in surface representation in wheat. Glycans observed in the structure are shown in space-filled representation in teal. Residues shown to be important for antibody binding are colored as in Fig. 4.1. (B) To obtain a glycosylation model representative of mammalian glycosylation, high-mannose type glycans (Man8-GlcNAc2-N-Asn) were modeled onto the structure of gB. Paucimannose and high-mannose are shown schematically. (C) The structure of HSV-1 gB shown in wheat with resolved glycans shown in space-filled representation in teal (unpublished, Cooper and Heldwein). (D) The structure of EBV gB (3FVC trimerized) shown in wheat with resolved glycans shown in space-filled representation in teal and predicted glycosylation sites in hot pink [113].

The major processed N-glycan produced by insect cells is a highly trimmed paucimannose (Man3-GlcNAc2-N-Asn) (reviewed in [205]). To show what gB may look

like on the viral surface, we modeled high-mannose type glycans to generate a fully-glycosylated model of gB (Fig. 3.11B). The model shows that much of the gB surface is shielded by a thick glycan layer. Similar glycan shields have been observed in HIV Env [206], Ebola gp [207], and EBV gp350 [208]. DII is the most heavily glycosylated, with four glycosylation sites in the structure, N383, N405, N409, and N417, plus three predicted glycosylation sites within its unresolved loop, N447, N452, and N465. Four out of five glycosylation sites in DI, N281, N286, N302, and N341, are within its upper pleckstrin homology subdomain. Only one glycosylation site, N208, is within the fusion subdomain of DI, and as described above, this glycan packs against the protein surface and points away from the fusion loops, which is consistent with the need for the fusion loops to be exposed for insertion into the membrane. Within DIV, there are two glycosylation sites, N555 and N585, which are located next to each other at the apexes of the trimer "crown" leaving the top of the crown exposed. The core of the gB trimer, consisting of DIII and DV, is not glycosylated.

There are 6 predicted N-linked glycosylation sites in HSV-1 gB. While there is no density for glycans in the original HSV-1 structure (2GUM) subsequent structures (2NWA and unpublished structures, Cooper) have revealed each of the remaining four sites are indeed glycosylated (Fig. 3.11C) [102, 162]. Three of the four glycans (at N141, N398, and N430) are attached to DII. Thus, this is the most highly glycosylated domain of HSV-1 gB as it is with HCMV gB. One glycan is even conserved between the two homologs (N409 in HCMV and N398 in HSV-1). The forth resolved glycan (at N674) is located in DV as it runs along DII, placing it in the same region as the three DII glycans. The two unresolved glycans are present in disordered regions of HSV-1 gB. One in the

disordered N-terminus and the other in the disordered loop of DII. Thus, the asparagines they are predicted to be attached to are also unresolved.

Of the nine predicted EBV gB glycosylation sites, three (N163, N290, N629) have been shown to in fact be glycosylated with no density confirming the remaining six [113]. Two of the confirmed glycans are located in DI, (N163, N290) and one is in DV (N629) (Fig. 3.11D). DII is also predicted to be the most highly glycosylated domain of EBV gB with five of the nine predicted sites (two in the disordered loop), though none of these glycans are resolved in the structure. The rest of the glycans are more distributed with each domain containing at least one.

3.2 Immunogenicity of gB

3.2.1. Neutralizing antibodies and epitopes.

Antigenic site AD-1, located within DIV, produces the strongest immune response [169-173]. DIV has only two N-linked glycosylation sites, and most of its surface is exposed and available for antibody binding (Figs. 3.12A-B), which likely accounts for its high immunogenicity. To understand the structural determinants for neutralizing ability of some anti-AD-1 Abs, we mapped the locations of residues shown to be important for antibody binding, which were identified in a study that characterized the effect of 600 random mutations, generated in a construct encompassing DIV (residues 484-650), on binding of a panel of anti-AD-1 antibodies [177]. Fifteen mutations (R562C, P577L, S587L, Y588C, G592S, G595D, L601P/H605N, C610Y, L612F, P613Y, Y625C, Y627C, F632L, and K633T) reduced or abolished binding of one or more tested Abs, seven neutralizing and four non-neutralizing [177]. Several of these

residues are buried and inaccessible by antibodies while the rest are surface-exposed and could be directly involved in antibody binding (Fig. 3.12B). Mutations P577L, C610Y, Y627C, and K633T reduced binding of all tested Abs. P577 and Y627 are located next to each other within the DIV core while C610 participates in a conserved disulfide bond. Thus, all three residues likely help maintain the structural integrity of DIV and, therefore, the entire antigenic site AD-1. By contrast, K633 is fully exposed, so it is unclear how K633T mutation would perturb binding of all tested Abs. Each of the other mutations affected binding of a subset of Abs, which suggests that AD-1 contains multiple overlapping epitopes. Unfortunately, the structure does not explain why some antibodies that bind AD-1 are neutralizing while others are not. Most mutations reduce binding of a subset of Abs, which includes both neutralizing and non-neutralizing ones, making it challenging to explain or predict the neutralization capacity. Nevertheless, two mutations, F632L and G595D, specifically reduced binding of several (although not all) neutralizing antibodies without affecting the binding of non-neutralizing Abs. These residues are located on the opposite sides of DIV: G595 is buried at the DIV/DIII interface, and a conformational change would be required to expose it. F632 is partially exposed on the surface. It is tempting to speculate that neutralizing antibodies bind the epitopes exposed in the prefusion state whereas non-neutralizing antibodies probably bind the epitopes that are only accessible in the postfusion state. If so, we would expect both F632 and G595 to be exposed on the surface of the prefusion form of gB. The discernment of the structural basis of neutralization awaits the structures of gB bound to neutralizing vs. non-neutralizing anti-AD-1 Abs.

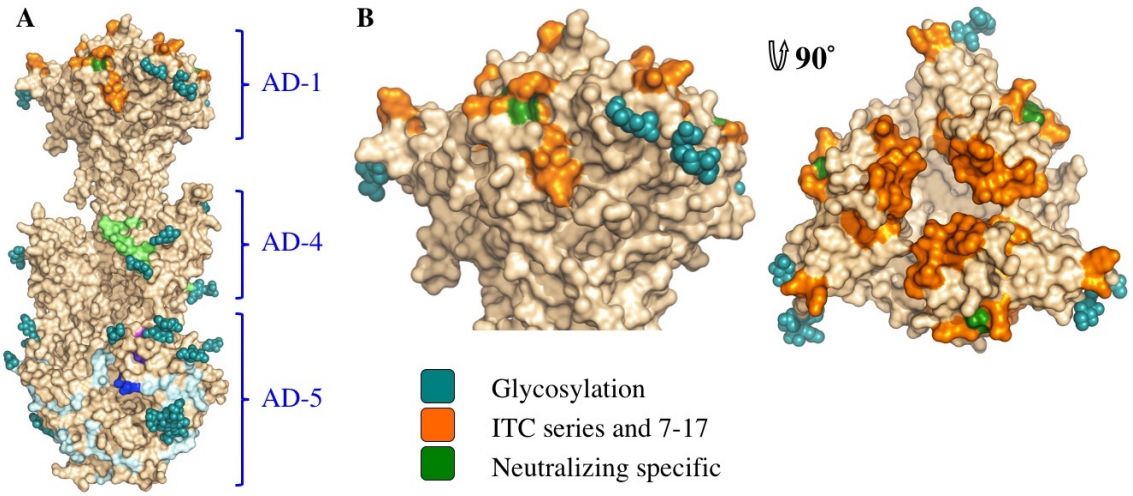

Figure 3.12. AD-1 epitopes. (A) The overall view of the epitopes on the surface of gB. (B) Side and top view of domain IV (AD-1). Residues shown to decrease binding of anti-AD-1 antibodies are shown in orange. Those specific to neutralizing AD-1 antibodies (G595 and F632) are colored forest green.

The two subdomains of antigenic site AD-2, site I (residues 68-77) and site II (residues 50-54), are located within the flexible N-terminus of gB that is absent from the crystallized construct. The sequence of site II is highly variable in clinical strains, while site I is highly conserved and is likely functionally important, which helps explain why antibodies targeting it are neutralizing [209]. Unlike the unglycosylated site II, site I contains 2 conserved predicted glycosylation sites within 10 residues (Fig. 3.6 and S1). Glycans could reduce antibody binding resulting in the observed mild immunogenicity [170, 209].

Antigenic site AD-4 is located within DII (Fig. 3.13) and was defined by the epitope of human neutralizing mAb SM5-1 isolated from B cells of a seropositive patient [170]. The recently published structure of an isolated HCMV gB DII bound to SM5-1 Fab [182] revealed how the antibody binds the narrow epitope at a sharp angle (Fig.

3.13B). But, DII in the crystallized complex was expressed in *E. coli* and lacks glycosylation. The glycan at position N383, located next to the SM5-binding site, is incompatible with SM5-1 binding in the orientation observed in the unglycosylated DII/SM5-1 complex due to a potential clash with the antibody loop CDR H3 (Fig. 3.13B). We hypothesize that in the fully glycosylated gB, the SM5 antibody may bind at an even sharper angle to avoid steric hindrance due to the N383 glycan, which could reduce the surface area of its binding site and thus the affinity.

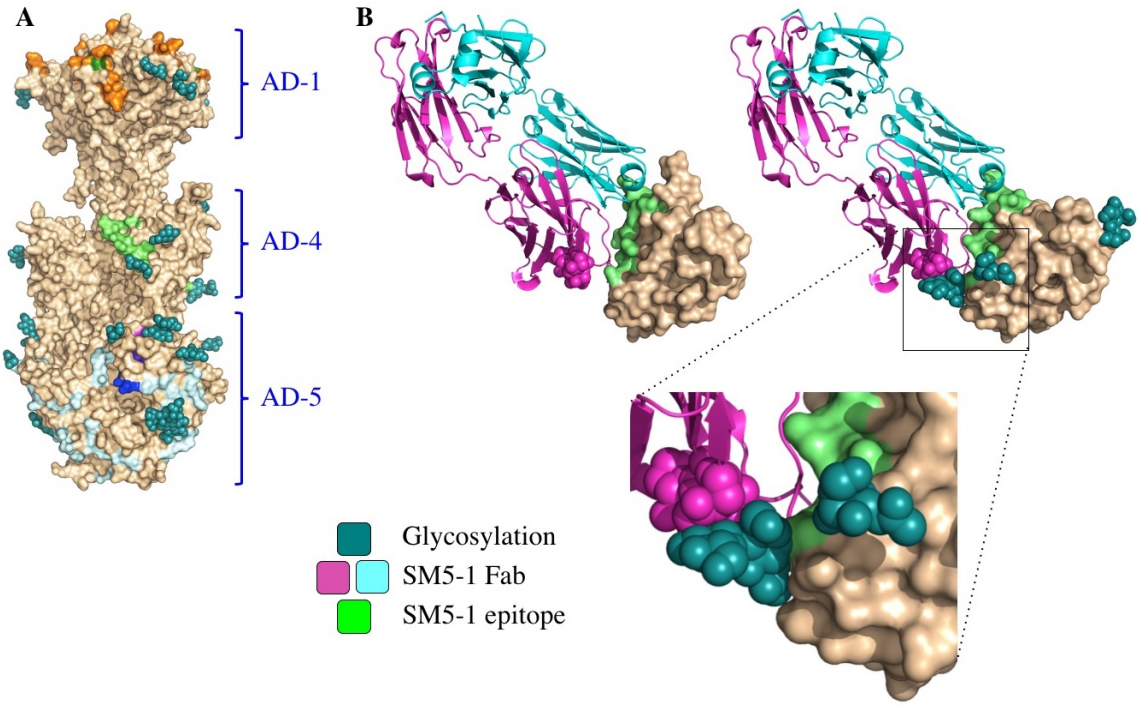

Figure 3.13. AD-4 epitope and DII/SM5-1 Fab structure. (A) The overall view of the epitopes on the surface of gB. (B) Domain II (AD-4) in complex with a human neutralizing Ab, SM5-1 (4OSN and 4OT1) (left) and domain II of gB, chain B, modeled with Fab SM5-1 (right) to illustrate how glycosylation would affect antibody binding. The heavy chain of SM5-1 is colored in magenta, the light chain is in slate, and AD-4 epitope is in lime.

Antigenic site AD-5 is located within DI and contains two distinct epitopes defined by human mAbs 1G2 and 2C2, isolated from two seropositive individuals (Figs. 3.14) [163]. Residues important for the ability of 1G2 or 2C2 to neutralize virus in cell culture, Y280/N284 and Y280/N293/D295, respectively, were identified by mutagenesis [163]. Mutation Y280A reduced neutralization by both Abs, which suggested that Y280 could be directly involved in antibody binding [163]. In the structure, Y280 is almost completely buried, however, and we conclude that instead of interacting with the antibodies directly, Y280 instead buttresses the surface region that is directly involved in binding. All residues involved in binding of anti-AD-5 neutralizing antibodies are conserved amongst the analyzed strains (Fig. 3.8, S1), supporting the idea that this region is functionally important. The residues that define the binding sites of 1G2 and 2C2 are surrounded by glycans, at position N208, N281, N286, N302, which could hinder antibody binding. Neutralization by 1G2 and 2C2 in cell culture increased ~3-fold when N286 was mutated to alanine, despite no obvious increase in antibody binding to gB [163]. The glycan shield could counteract the high neutralizing potency of anti-AD-5 Abs, which could explain why such antibodies are less common. Further mutagenesis and, ultimately, the structures of gB bound to 1G2 or 2C2 would be necessary to pinpoint additional residues involved in binding and help explain how these antibodies avoid glycans.

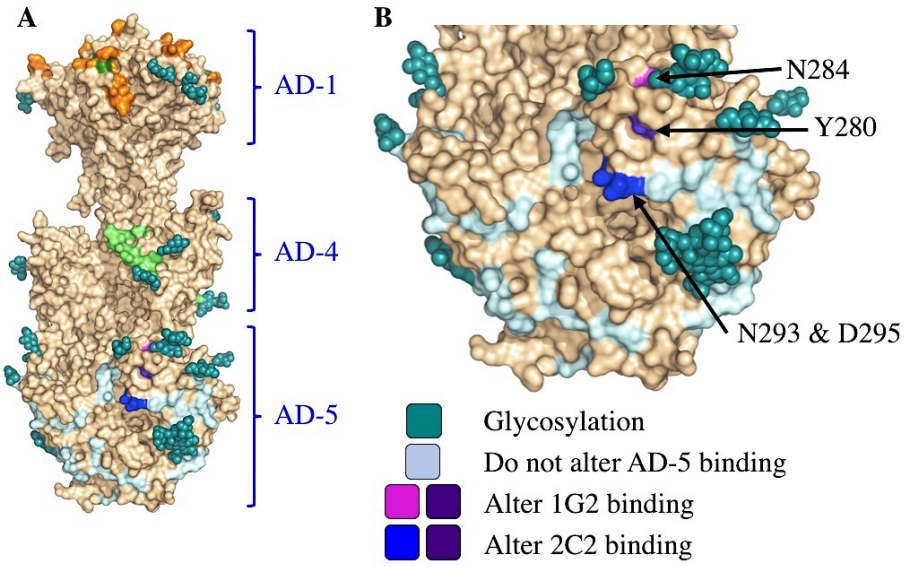

Figure 3.14. AD-5 residues. (A) The overall view of the epitopes on the surface of gB. (B) A close-up view of domain I (AD-5). Residue involved in binding of 1G2 (N284) is colored in magenta, residues involved in binding of 2C2 (N293/D295) are in blue, and residue important for binding of both (Y280) is in purple. Residues shown not to affect binding of 1G2 or 2C2 are colored in pale blue.

3.2.2. Comparison of the HCMV and HSV-1 gB antigenic regions

The immunogenicity of HSV gB has been studied to a similar extent as HCMV gB. While the AD nomenclature is specific to HCMV, mapping of known antigenic sites on HSV gB presents a similar pattern to that of HCMV gB with the majority of antibodies recognizing DI, DII, and DIV (AD-5, AD-4, and AD-1 respectively) (Fig. 3.15) [102, 160]. In DIV of HSV gB, the large epitope of the neutralizing Ab, SS10 (residues 640-670), has been mapped to the side of the domain. While a few HCMV non-neutralizing antibodies have been shown to have decreased binding when residues in this region are mutated, the majority have been mapped to the top of the DIV crown. HCMV

has two glycans located near the SS10 epitope which may preclude antibody binding of the side of the crown while HSV DIV is completely free of glycans. In DII, the epitope of the HSV Ab, H1838 (residues 390-410), overlaps that of the HCMV gB Ab, SM5-1 [155, 182]. Although, the SM5-1 epitope is limited in size by the two glycans buttressing it and thus is smaller and higher than the H1838 epitope. Several additional DII antibody epitopes have been mapped to HSV (H1781 and C226), while SM5 is the only antibody yet isolated against DII of HCMV gB. This is correlated with increased glycosylation of HCMV which has three predicted and four confirmed glycans in DII while HSV-1 only has four. This trend is reflected in DI as well. Three antibodies (1G2, 2C2, SM10) have been shown to bind an overlapping region of HCMV DI, while three distinct regions are bound by seven HSV antibodies (H233, H126, H1375, B4, SS106, SS144, and SS55) in the domain [163]. HCMV has five glycans protecting DI from such extensive antibody recognition while HSV has none.

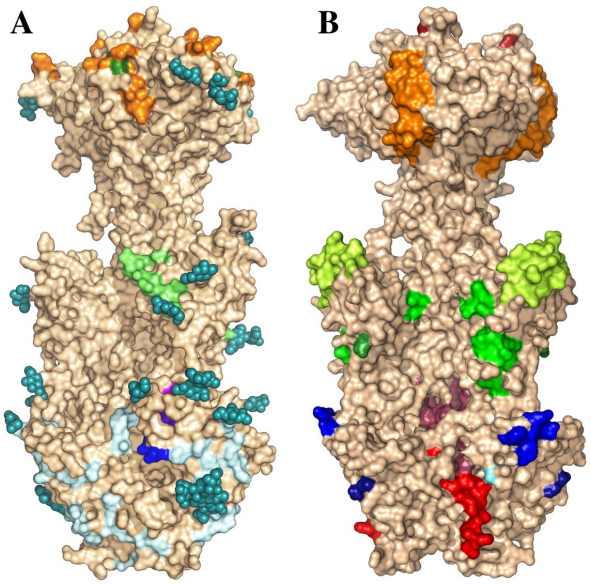

Figure 3.15. Antigenic sites of HCMV and HSV. (A) The structure of HCMV gB colored as in Fig. 3.12-3.14. Briefly, anti-AD-1 colored orange, anti-AD-1 neutralizing (G595 and F632) colored forest green, anti-AD-4 colored lime, anti-AD-5 N284 – magenta, N293/D295 - blue, and Y280 – purple [210]. (B) The structure of HSV gB with important antibody binding residues colored: H233 in Aqua (315 and 328), H126, H1375, B4, and 1435 in blue (303-305, 308), SS106

and SS144 in slate (697-725), SS55 in density (199 and 203), H1838 in green (390-410), H1781 in lime (454-473), C226 in forest (419), B2 and B5 in Firebrick (594), SS10 in orange (640-670).

3.2.3. Comparison of the gB structure to gB/1G2 Fab structure

The structure of gB in complex with 1G2 Fab was determined by Chandramouli, et al. in 2015. Many of the modifications made to obtain our structure of the gB ectodomain were also made by Chandramouli, et al. to obtain the structure of the gB/1G2 complex (5C6T), confirming the reproducibility and emphasizing the importance of each modification for crystallization (Fig. 3.16). They expressed the ectodomain to residue D698 while we expressed it to P706. The last resolved residue in either gB structure was 697. Thus, the additional amino acids in our construct did not provide additional information [102, 211]. They mutated three residues in the fusion loops. When this was not sufficient to limit rosette formation, they added a glycosylation site to fusion loop 2 while we mutated four additional hydrophobic fusion loop residues. Results from limited proteolysis of gB with subtilisin E prompted the group to truncate the N-terminus gB to residue T86, just as trypsin proteolysis prompted us to truncate gB to residue Y78. While we replaced the furin cleavage site with another cleavage sequence, they simply mutated two of the four cleavage residues to serines. Both approaches abolished heterogeneous cleavage during expression. Differences in our methodologies included their use of the "clinical" strain, Merlin instead of our use of the "laboratory" strain, AD169, mammalian expression rather than insect cell, and their deglycosylation with sendoff. The later was not necessary after expression in insect cells. This may have been due to the lack of variability of glycosylation types generated by insect cells, while mammalian cell glycans vary extensively. The single gB chain (A) in the gB/1G2 structure aligns well with each

of the three chains of our gB structure (5CXF, A-C) with low RMSD values around 1.6-1.7 (Table 3.3). By comparison, the RMSD values of each chain compared to the others (A-C) are 1.01-1.03.

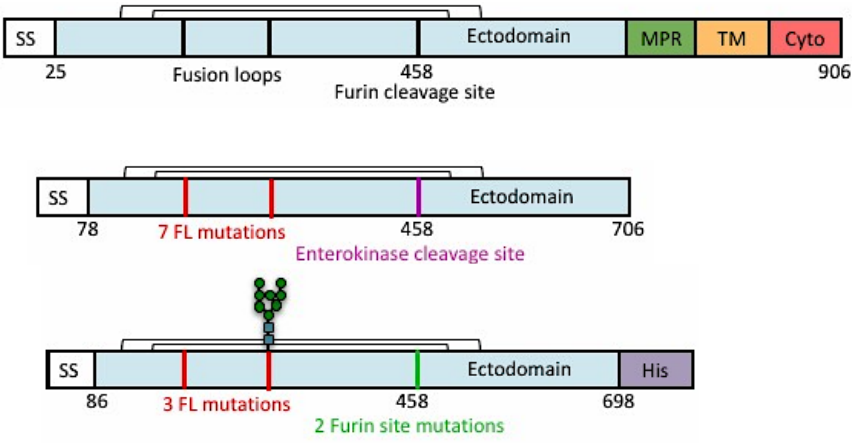

Figure 3.16. Comparison of gB vs. gB/1G2 Fab constructs. (A) Schematic representation of full-length gB (top), our gB construct (gB78-706-7M-E) (middle) and the construct created by Chandramouli, et al. (gB-698glyco) (bottom).

Structure		**gB**/1G2 (5C6T)	gB (5CXF)		
	Chain	A	A	B	C
gB/1G2 (5C6T)	A	-			
	A	1.60	-		
gB (5CXF)	B	1.68	1.01	-	
	C	1.71	1.02	1.03	-

Table 3.3 Comparison of gB/1G2 gB protomer to gB protomers. The RMSD values comparing the single gB chain in the gB/1G2 structure (5C6T) to each of the three gB protomers (5CXF) [210, 211]. The three gB (5CXF) protomers were also compared to each other for reference.

3.3 DISCUSSION

The 3.6-Å crystal structure of the HCMV gB ectodomain reported here and the 3.6-Å crystal structure of the HCMV gB/1G2 Fab complex are the first structures of any

glycoprotein from a betaherpesvirus [211]. HCMV gB structure resembles the postfusion structures of HSV-1 and EBV homologs, making it a member of the new class III viral fusogens. Despite structural similarities, each gB has a unique domain arrangement, demonstrating that gB has structural plasticity which may serve to accommodate virus-specific functional requirements. By contrast, the postfusion forms of G homologs from Vesicular Stomatitis Virus [152] and Chandipura virus [212], which also belong to class III viral fusogens, have very similar structures, including domain orientations. These observations suggest different constraints on class III fusogens from different viral families, which may reflect differences either in their mode of activation (pH for vesiculovirus G vs. interaction with additional viral glycoproteins for herpesvirus gB), or in the architecture and the stabilization of their pre-fusion conformations, or both.

The structure illustrates how most of the gB surface is shielded by a thick glycan layer. Viruses commonly use glycosylation to escape immune recognition (reviewed in [213]). Glycosylation alteration in HIV-1 Env has been proposed as a mechanism of immune escape [214]. The high conservation of the glycosylation pattern in HCMV gB suggests another mechanism. HCMV is a dsDNA virus making its genome less error-prone as the RNA genome of the retrovirus, HIV. Thus, it is unlikely to mutate as readily making glycan escape less frequent. Therefore, instead of escape, HCMV utilizes extensive glycosylation to shield functionally important regions from immune recognition. DI and DII are the most heavily glycosylated, and all antibodies against the antigenic sites located in these domains are neutralizing. Although the functional roles of domains DI and DII in HCMV gB have not yet been elucidated, these domains have been proposed to bind gH/gL in HSV-1 gB [215], and in HCMV gB could, perhaps, interact

with the gH/gL pentamer or the trimer. Carbohydrates may be shielding antigenic sites within these domains from immune recognition as a means of avoiding neutralization, which could explain why antibodies against AD-4 and AD-5 are relatively rare compared to those against AD-1. Many neutralizing HSV antibodies recognize DI and DII as well, though the locations of their epitopes are more spread out than those of HCMV. This reflects the differences in glycosylation. HCMV gB has up to eleven glycans on the two domains while HSV has up to four. This increase in glycan density limits the area antibodies can bind HCMV gB, suggesting the glycan shield is an effective method of decreasing the immunogenicity of a protein region.

The core of the gB trimer, consisting of DIII and DV, is not glycosylated. These regions are expected to undergo large-scale refolding during the prefusion-to-postfusion transition [196]. Fusion subunits of other viral fusogens such as HIV Env [206] and Ebola gp [207] are shielded by heavily glycosylated domains in the prefusion conformation. This could be a common strategy for immune evasion. No antibodies against DIII or DV have yet been isolated, and we expect that DIII and DV in the prefusion form of gB to be protected from the immune response by the glycan shields of DI and DII.

Although HCMV gB elicits a strong immune response in humans and induces the production of neutralizing Abs, most anti-gB antibodies are non-neutralizing and target the immunodominant antigenic site AD-1 [166, 170]. The limited glycosylation of DIV, containing AD-1, could account for this immunodominance (Fig. 3.12). Structure analysis is consistent with the presence of multiple overlapping epitopes within AD-1 but does not explain why most antibodies that bind AD-1 are non-neutralizing. One plausible

explanation is that neutralizing antibodies bind the epitopes exposed in the prefusion state whereas non-neutralizing antibodies probably bind the epitopes that are only accessible in the postfusion state. The HSV-1 envelope may display both the prefusion and the postfusion form of gB [216, 217], which raises the possibility that the postfusion form of gB could be present on the surface of HCMV. By presenting the postfusion form with its fully exposed AD-1, HCMV could divert the immune response towards production of non-neutralizing Abs.

In summary, the crystal structure of HCMV gB ectodomain provides an important framework for elucidating the immunogenic determinants and establishes HCMV gB as the viral fusogen. The glycan distribution in HCMV gB revealed by its structure suggests that antigenic sites that elicit neutralizing antibodies are more heavily glycosylated than those that elicit non-neutralizing Abs. By using glycans to shield neutralizing epitopes while exposing regions that elicit non-neutralizing Abs, gB could be redirecting the immune response.

Figure 3S1. (Below) Sequence alignment of gB from clinical and laboratory-adapted HCMV strains. (Below) Sixty HCMV gB sequences from clinical and laboratory-adapted strains, downloaded from NCBI's RefSeq database, were aligned and analyzed using ClustalW2 [194] and ESPript 3.x [195]. Identical residues are shown as white text on red background and similar residues are highlighted in yellow.

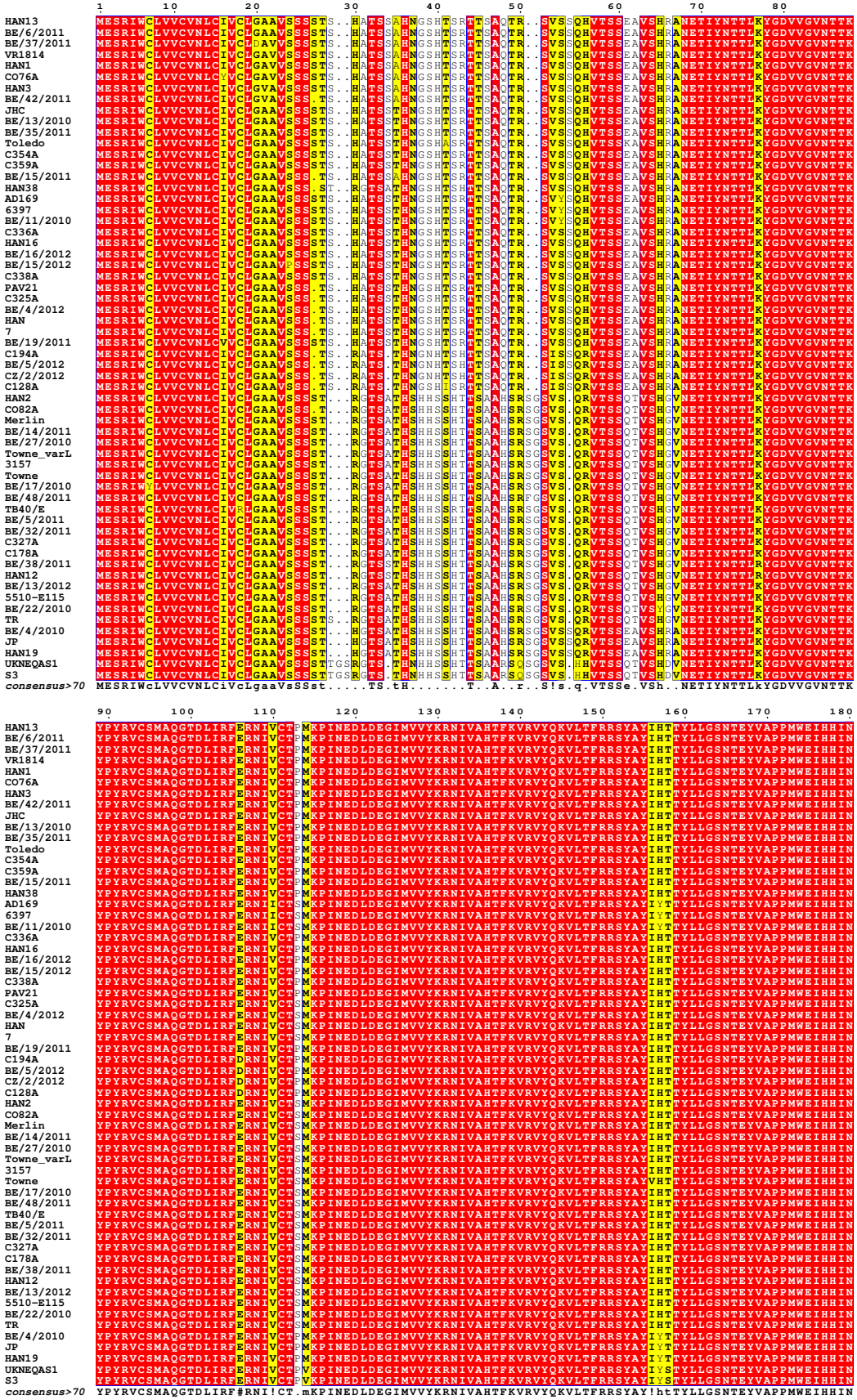

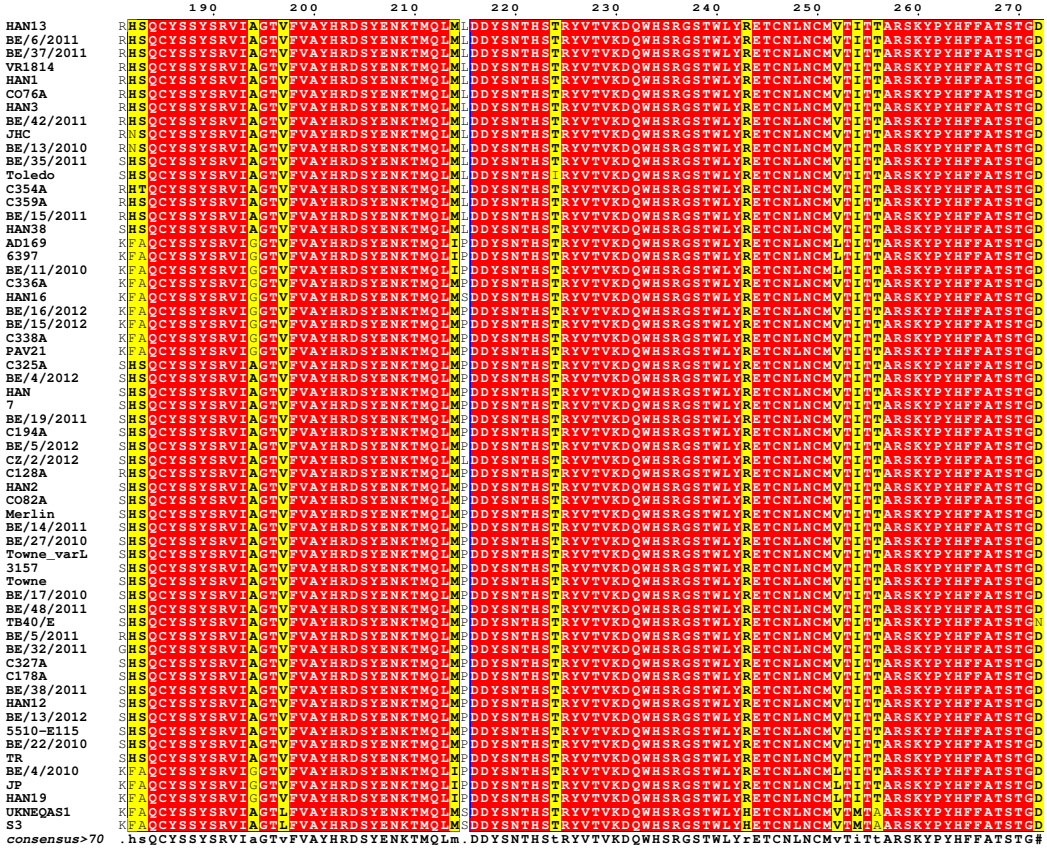
190 200 210 220 230 240 250 260 270
HAN13 RHSQCYSSYSRVIAGTVFVAYHRDSYENKTMQLMLDDYSNTHSTRYVTVKDQWHSRGSTWLYRETCNLNCMVTITTARSKYPYHFFATSTGD
BE/6/2011 RHSQCYSSYSRVIAGTVFVAYHRDSYENKTMQLMLDDYSNTHSTRYVTVKDQWHSRGSTWLYRETCNLNCMVTITTARSKYPYHFFATSTGD
BE/37/2011 RHSQCYSSYSRVIAGTVFVAYHRDSYENKTMQLMLDDYSNTHSTRYVTVKDQWHSRGSTWLYRETCNLNCMVTITTARSKYPYHFFATSTGD
VR1814 RHSQCYSSYSRVIAGTVFVAYHRDSYENKTMQLMLDDYSNTHSTRYVTVKDQWHSRGSTWLYRETCNLNCMVTITTARSKYPYHFFATSTGD
HAN1 RHSQCYSSYSRVIAGTVFVAYHRDSYENKTMQLMLDDYSNTHSTRYVTVKDQWHSRGSTWLYRETCNLNCMVTITTARSKYPYHFFATSTGD
CO76A RHSQCYSSYSRVIAGTVFVAYHRDSYENKTMQLMLDDYSNTHSTRYVTVKDQWHSRGSTWLYRETCNLNCMVTITTARSKYPYHFFATSTGD
HAN3 RHSQCYSSYSRVIAGTVFVAYHRDSYENKTMQLMLDDYSNTHSTRYVTVKDQWHSRGSTWLYRETCNLNCMVTITTARSKYPYHFFATSTGD
BE/42/2011 RHSQCYSSYSRVIAGTVFVAYHRDSYENKTMQLMLDDYSNTHSTRYVTVKDQWHSRGSTWLYRETCNLNCMVTITTARSKYPYHFFATSTGD
JHC RNSQCYSSYSRVIAGTVFVAYHRDSYENKTMQLMLDDYSNTHSTRYVTVKDQWHSRGSTWLYRETCNLNCMVTITTARSKYPYHFFATSTGD
BE/13/2010 RNSQCYSSYSRVIAGTVFVAYHRDSYENKTMQLMLDDYSNTHSTRYVTVKDQWHSRGSTWLYRETCNLNCMVTITTARSKYPYHFFATSTGD
BE/35/2011 SHSQCYSSYSRVIAGTVFVAYHRDSYENKTMQLMLDDYSNTHSTRYVTVKDQWHSRGSTWLYRETCNLNCMVTITTARSKYPYHFFATSTGD
Toledo SHSQCYSSYSRVIAGTVFVAYHRDSYENKTMQLMLDDYSNTHSIRYVTVKDQWHSRGSTWLYRETCNLNCMVTITTARSKYPYHFFATSTGD
C354A RHTQCYSSYSRVIAGTVFVAYHRDSYENKTMQLMLDDYSNTHSTRYVTVKDQWHSRGSTWLYRETCNLNCMVTITTARSKYPYHFFATSTGD
C359A RHSQCYSSYSRVIAGTVFVAYHRDSYENKTMQLMLDDYSNTHSTRYVTVKDQWHSRGSTWLYRETCNLNCMVTITTARSKYPYHFFATSTGD
BE/15/2011 RHSQCYSSYSRVIAGTVFVAYHRDSYENKTMQLMLDDYSNTHSTRYVTVKDQWHSRGSTWLYRETCNLNCMVTITTARSKYPYHFFATSTGD
HAN38 SHSQCYSSYSRVIAGTVFVAYHRDSYENKTMQLMLDDYSNTHSTRYVTVKDQWHSRGSTWLYRETCNLNCMVTITTARSKYPYHFFATSTGD
AD169 KFAQCYSSYSRVIGGTVFVAYHRDSYENKTMQLIPDDYSNTHSTRYVTVKDQWHSRGSTWLYRETCNLNCLITITTARSKYPYHFFATSTGD
6397 KFAQCYSSYSRVIGGTVFVAYHRDSYENKTMQLIPDDYSNTHSTRYVTVKDQWHSRGSTWLYRETCNLNCLITITTARSKYPYHFFATSTGD
BE/11/2010 KFAQCYSSYSRVIGGTVFVAYHRDSYENKTMQLIPDDYSNTHSTRYVTVKDQWHSRGSTWLYRETCNLNCLITITTARSKYPYHFFATSTGD
C336A KFAQCYSSYSRVIGGTVFVAYHRDSYENKTMQLMPDDYSNTHSTRYVTVKDQWHSRGSTWLYRETCNLNCMVTITTARSKYPYHFFATSTGD
HAN16 KFAQCYSSYSRVIGGTVFVAYHRDSYENKTMQLMSDDYSNTHSTRYVTVKDQWHSRGSTWLYRETCNLNCMVTITTARSKYPYHFFATSTGD
BE/16/2012 KFAQCYSSYSRVIGGTVFVAYHRDSYENKTMQLMPDDYSNTHSTRYVTVKDQWHSRGSTWLYRETCNLNCMVTITTARSKYPYHFFATSTGD
BE/15/2012 KFAQCYSSYSRVIGGTVFVAYHRDSYENKTMQLMPDDYSNTHSTRYVTVKDQWHSRGSTWLYRETCNLNCMVTITTARSKYPYHFFATSTGD
C338A KFAQCYSSYSRVIGGTVFVAYHRDSYENKTMQLMPDDYSNTHSTRYVTVKDQWHSRGSTWLYRETCNLNCMVTITTARSKYPYHFFATSTGD
PAV21 KFAQCYSSYSRVIGGTVFVAYHRDSYENKTMQLMPDDYSNTHSTRYVTVKDQWHSRGSTWLYRETCNLNCMVTITTARSKYPYHFFATSTGD
C325A SHSQCYSSYSRVIAGTVFVAYHRDSYENKTMQLMPDDYSNTHSTRYVTVKDQWHSRGSTWLYRETCNLNCMVTITTARSKYPYHFFATSTGD
BE/4/2012 SHSQCYSSYSRVIAGTVFVAYHRDSYENKTMQLMPDDYSNTHSTRYVTVKDQWHSRGSTWLYRETCNLNCMVTITTARSKYPYHFFATSTGD
HAN SHSQCYSSYSRVIAGTVFVAYHRDSYENKTMQLMPDDYSNTHSTRYVTVKDQWHSRGSTWLYRETCNLNCMVTITTARSKYPYHFFATSTGD
7 SHSQCYSSYSRVIAGTVFVAYHRDSYENKTMQLMPDDYSNTHSTRYVTVKDQWHSRGSTWLYRETCNLNCMVTITTARSKYPYHFFATSTGD
BE/19/2011 SHSQCYSSYSRVIAGTVFVAYHRDSYENKTMQLMPDDYSNTHSTRYVTVKDQWHSRGSTWLYRETCNLNCMVTITTARSKYPYHFFATSTGD
C194A SHSQCYSSYSRVIAGTVFVAYHRDSYENKTMQLMPDDYSNTHSTRYVTVKDQWHSRGSTWLYRETCNLNCMVTITTARSKYPYHFFATSTGD
BE/5/2012 SHSQCYSSYSRVIAGTVFVAYHRDSYENKTMQLMPDDYSNTHSTRYVTVKDQWHSRGSTWLYRETCNLNCMVTITTARSKYPYHFFATSTGD
CZ/2/2012 SHSQCYSSYSRVIAGTVFVAYHRDSYENKTMQLMPDDYSNTHSTRYVTVKDQWHSRGSTWLYRETCNLNCMVTITTARSKYPYHFFATSTGD
C128A RHSQCYSSYSRVIAGTVFVAYHRDSYENKTMQLMPDDYSNTHSTRYVTVKDQWHSRGSTWLYRETCNLNCMVTITTARSKYPYHFFATSTGD
HAN2 SHSQCYSSYSRVIAGTVFVAYHRDSYENKTMQLMPDDYSNTHSTRYVTVKDQWHSRGSTWLYRETCNLNCMVTITTARSKYPYHFFATSTGD
CO82A SHSQCYSSYSRVIAGTVFVAYHRDSYENKTMQLMPDDYSNTHSTRYVTVKDQWHSRGSTWLYRETCNLNCMVTITTARSKYPYHFFATSTGD
Merlin SHSQCYSSYSRVIAGTVFVAYHRDSYENKTMQLMPDDYSNTHSTRYVTVKDQWHSRGSTWLYRETCNLNCMVTITTARSKYPYHFFATSTGD
BE/14/2011 SHSQCYSSYSRVIAGTVFVAYHRDSYENKTMQLMPDDYSNTHSTRYVTVKDQWHSRGSTWLYRETCNLNCMVTITTARSKYPYHFFATSTGD
BE/27/2010 SHSQCYSSYSRVIAGTVFVAYHRDSYENKTMQLMPDDYSNTHSTRYVTVKDQWHSRGSTWLYRETCNLNCMVTITTARSKYPYHFFATSTGD
Towne_varL SHSQCYSSYSRVIAGTVFVAYHRDSYENKTMQLMPDDYSNTHSTRYVTVKDQWHSRGSTWLYRETCNLNCMVTITTARSKYPYHFFATSTGD
3157 SHSQCYSSYSRVIAGTVFVAYHRDSYENKTMQLMPDDYSNTHSTRYVTVKDQWHSRGSTWLYRETCNLNCMVTITTARSKYPYHFFATSTGD
Towne SHSQCYSSYSRVIAGTVFVAYHRDSYENKTMQLMPDDYSNTHSTRYVTVKDQWHSRGSTWLYRETCNLNCMVTITTARSKYPYHFFATSTGD
BE/17/2010 SHSQCYSSYSRVIAGTVFVAYHRDSYENKTMQLMPDDYSNTHSTRYVTVKDQWHSRGSTWLYRETCNLNCMVTITTARSKYPYHFFATSTGD
BE/48/2011 SHSQCYSSYSRVIAGTVFVAYHRDSYENKTMQLMPDDYSNTHSTRYVTVKDQWHSRGSTWLYRETCNLNCMVTITTARSKYPYHFFATSTGD
TB40/E SHSQCYSSYSRVIAGTVFVAYHRDSYENKTMQLMPDDYSNTHSTRYVTVKDQWHSRGSTWLYRETCNLNCMVTITTARSKYPYHFFATSTGN
BE/5/2011 RHSQCYSSYSRVIAGTVFVAYHRDSYENKTMQLMPDDYSNTHSTRYVTVKDQWHSRGSTWLYRETCNLNCMVTITTARSKYPYHFFATSTGD
BE/32/2011 GHSQCYSSYSRVIAGTVFVAYHRDSYENKTMQLMPDDYSNTHSTRYVTVKDQWHSRGSTWLYRETCNLNCMVTITTARSKYPYHFFATSTGD
C327A SHSQCYSSYSRVIAGTVFVAYHRDSYENKTMQLMPDDYSNTHSTRYVTVKDQWHSRGSTWLYRETCNLNCMVTITTARSKYPYHFFATSTGD
C178A SHSQCYSSYSRVIAGTVFVAYHRDSYENKTMQLMPDDYSNTHSTRYVTVKDQWHSRGSTWLYRETCNLNCMVTITTARSKYPYHFFATSTGD
BE/38/2011 SHSQCYSSYSRVIAGTVFVAYHRDSYENKTMQLMPDDYSNTHSTRYVTVKDQWHSRGSTWLYRETCNLNCMVTITTARSKYPYHFFATSTGD
HAN12 SHSQCYSSYSRVIAGTVFVAYHRDSYENKTMQLMPDDYSNTHSTRYVTVKDQWHSRGSTWLYRETCNLNCMVTITTARSKYPYHFFATSTGD
BE/13/2012 SHSQCYSSYSRVIAGTVFVAYHRDSYENKTMQLMPDDYSNTHSTRYVTVKDQWHSRGSTWLYRETCNLNCMVTITTARSKYPYHFFATSTGD
5510-E115 SHSQCYSSYSRVIAGTVFVAYHRDSYENKTMQLMPDDYSNTHSTRYVTVKDQWHSRGSTWLYRETCNLNCMVTITTARSKYPYHFFATSTGD
BE/22/2010 SHSQCYSSYSRVIAGTVFVAYHRDSYENKTMQLMPDDYSNTHSTRYVTVKDQWHSRGSTWLYRETCNLNCMVTITTARSKYPYHFFATSTGD
TR SHSQCYSSYSRVIAGTVFVAYHRDSYENKTMQLMPDDYSNTHSTRYVTVKDQWHSRGSTWLYRETCNLNCMVTITTARSKYPYHFFATSTGD
BE/4/2010 KFAQCYSSYSRVIGGTVFVAYHRDSYENKTMQLIPDDYSNTHSTRYVTVKDQWHSRGSTWLYRETCNLNCLITITTARSKYPYHFFATSTGD
JP KFAQCYSSYSRVIGGTVFVAYHRDSYENKTMQLIPDDYSNTHSTRYVTVKDQWHSRGSTWLYRETCNLNCLITITTARSKYPYHFFATSTGD
HAN19 KFAQCYSSYSRVIGGTVFVAYHRDSYENKTMQLIPDDYSNTHSTRYVTVKDQWHSRGSTWLYRETCNLNCLITITTARSKYPYHFFATSTGD
UKNEQAS1 KFAQCYSSYSRVIAGTLFVAYHRDSYENKTMQLMSDDYSNTHSTRYVTVKDQWHSRGSTWLYHETCNLNCMVTMMAARSKYPYHFFATSTGD
S3 KFAQCYSSYSRVIAGTLFVAYHRDSYENKTMQLMSDDYSNTHSTRYVTVKDQWHSRGSTWLYHETCNLNCMVTMMAARSKYPYHFFATSTGD
consensus>70 .hsQCYSSYSRVIaGTvFVAYHRDSYENKTMQLm.DDYSNTHStRYVTVKDQWHSRGSTWLYrETCNLNCMvTiTtARSKYPYHFFATSTG#
280 290 300 310 320 330 340 350 360
HAN13 VVDISPFYNGTNRNISYFGENADKFFIFPNYTIVSDFGRANSAPETHRLVAFLERADSVISWDIQDEKNVTCQLTFWEASERTIRSEAEDSY
BE/6/2011 VVDISPFYNGTNRNISYFGENADKFFIFPNYTIVSDFGRANSAPETHRLVAFLERADSVISWDIQDEKNVTCQLTFWEASERTIRSEAEDSY
BE/37/2011 VVDISPFYNGTNRNISYFGENADKFFIFPNYTIVSDFGRANSAPETHRLVAFLERADSVISWDIQDEKNVTCQLTFWEASERTIRSEAEDSY
VR1814 VVDISPFYNGTNRNISYFGENADKFFIFPNYTIVSDFGRANSAPETHRLVAFLERADSVISWDIQDEKNVTCQLTFWEASERTIRSEAEDSY
HAN1 VVDISPFYNGTNRNISYFGENADKFFIFPNYTIVSDFGRANSAPETHRLVAFLERADSVISWDIQDEKNVTCQLTFWEASERTIRSEAEDSY
CO76A VVDISPFYNGTNRNISYFGENADKFFIFPNYTIVSDFGRANSAPETHRLVAFLERADSVISWDIQDEKNVTCQLTFWEASERTIRSEAEDSY
HAN3 VVDISPFYNGTNRNISYFGENADKFFIFPNYTIVSDFGRANSAPETHRLVAFLERADSVISWDIQDEKNVTCQLTFWEASERTIRSEAEDSY
BE/42/2011 VVDISPFYNGTNRNISYFGENADKFFIFPNYTIVSDFGRANSAPETHRLVAFLERADSVISWDIQDEKNVTCQLTFWEASERTIRSEAEDSY
JHC VVDISPFYNGTNRNISYFGENADKFFIFPNYTIVSDFGRANSAPETHRLVAFLERADSVISWDIQDEKNVTCQLTFWEASERTIRSEAEDSY
BE/13/2010 VVDISPFYNGTNRNISYFGENADKFFIFPNYTIVSDFGRANSAPETHRLVAFLERADSVISWDIQDEKNVTCQLTFWEASERTIRSEAEDSY
BE/35/2011 VVDISPFYNGTNRNISYFGENADKFFIFPNYTIVSDFGRANSAPETHRLVAFLERADSVISWDIQDEKNVTCQLTFWEASERTIRSEAEDSY
Toledo VVDISPFYNGTNRNISYFGENADKFFIFPNYTIVSDFGRANSAPETHRLVAFLERADSVISWDIQDEKNVTCQLTFWEASERTIRSEAEDSY
C354A VVDISPFYNGTNRNISYFGENADKFFIFPNYTIVSDFGRANSAPETHRLVAFLERADSVISWDIQDEKNVTCQLTFWEASERTIRSEAEDSY
C359A VVDISPFYNGTNRNISYFGENADKFFIFPNYTIVSDFGRANSAPETHRLVAFLERADSVISWDIQDEKNVTCQLTFWEASERTIRSEAEDSY
BE/15/2011 VVDISPFYNGTNRNISYFGENADKFFIFPNYTIVSDFGRANSAPETHRLVAFLERADSVISWDIQDEKNVTCQLTFWEASERTIRSEAEDSY
HAN38 VVDISPFYNGTNRNISYFGENADKFFIFPNYTIVSDFGRANSAPETHRLVAFLERADSVISWDIQDEKNVTCQLTFWEASERTIRSEAEDSY
AD169 VVYISPFYNGTNRNASYFGENADKFFIFPNYTIVSDFGRPNAAPETHRLVAFLERADSVISWDIQDEKNVTCQLTFWEASERTIRSEAEDSY
6397 VVDISPFYNGTNRNASYFGENADKFFIFPNYTIVSDFGRPNAAPETHRLVAFLERADSVISWDIQDEKNVTCQLTFWEASERTIRSEAEDSY
BE/11/2010 VVDISPFYNGTNRNASYFGENADKFFIFPNYTIVSDFGRPNAAPETHRLVAFLERADSVISWDIQDEKNVTCQLTFWEASERTIRSEAEDSY
C336A VVDISPFYNGTNRNASYFGENADKFFIFPNYTIVSDFGRPNAAPETHRLVAFLERADSVISWDIQDEKNVTCQLTFWEASERTIRSEAEDSY
HAN16 VVDISPFYNGTNRNASYFGENADKFFIFPNYTIVSDFGRPNAAPETHRLVAFLERADSVISWDIQDEKNVTCQLTFWEASERTIRSEAEDSY
BE/16/2012 VVDISPFYNGTNRNASYFGENADKFFIFPNYTIVSDFGRPNAAPETHRLVAFLERADSVISWDIQDEKNVTCQLTFWEASERTIRSEAEDSY
BE/15/2012 VVDISPFYNGTNRNASYFGENADKFFIFPNYTIVSDFGRPNAAPETHRLVAFLERADSVISWDIQDEKNVTCQLTFWEASERTIRSEAEDSY
C338A VVDISPFYNGTNRNASYFGENADKFFIFPNYTIVSDFGRPNAAPETHRLVAFLERADSVISWDIQDEKNVTCQLTFWEASERTIRSEAEDSY
PAV21 VVDISPFYNGTNRNASYFGENADKFFIFPNYTIVSDFGRPNAAPETHRLVAFLERADSVISWDIQDEKNVTCQLTFWEASERTIRSEAEDSY
C325A VVDISPFYNGTNRNASYFGENADKFFIFPNYTIVSDFGRPNSAPETHRSVAFLERADSVISWDIQDEKNVTCQLTFWEASERTIRSEAEDSY
BE/4/2012 VVDISPFYNGTNRNASYFGENADKFFIFPNYTIVSDFGRPNSALETHRSVAFLERADSVISWDIQDEKNVTCQLTFWEASERTIRSEAEDSY
HAN VVDISPFYNGTNRNASYFGENADKFFIFPNYTIVSDFGRPNSALETHRSVAFLERADSVISWDIQDEKNVTCQLTFWEASERTIRSEAEDSY
7 VVDISPFYNGTNRNASYFGENADKFFIFPNYTIVSDFGRPNSALETHRSVAFLERADSVISWDIQDEKNVTCQLTFWEASERTIRSEAEDSY
BE/19/2011 VVDISPFYNGTNRNASYFGENADKFFIFPNYTIVSDFGRPNSALETHRLVAFLERADSVISWDIQDEKNVTCQLTFWEASERTIRSEAEDSY
C194A VVDISPFYNGTNRNASYFGENADKFFIFPNYTIVSDFGRPNSALETHRLVAFLERADSVISWDIQDEKNVTCQLTFWEASERTIRSEAEESY
BE/5/2012 VVDISPFYNGTNRNASYFGENADKFFIFPNYTIVSDFGRPNSALETHRLVAFLERADSVISWDIQDEKNVTCQLTFWEASERTIRSEAEESY
CZ/2/2012 VVDISPFYNGTNRNASYFGENADKFFIFPNYTIVSDFGRPNSALETHRLVAFLERADSVISWDIQDEKNVTCQLTFWEASERTIRSEAEESY
C128A VVDISPFYNGTNRNASYFGENADKFFIFPNYTIVSDFGRPNSALETHRLVAFLERADSVISWDIQDEKNVTCQLTFWEASERTIRSEAEESY
HAN2 VVDISPFYNGTNRNASYFGENADKFFIFPNYTIVSDFGRPNSALETHRLVAFLERADSVISWDIQDEKNVTCQLTFWEASERTIRSEAEDSY
CO82A VVDISPFYNGTNRNASYFGENADKFFIFPNYTIVSDFGRPNSALETHRLVAFLERADSVISWDIQDEKNVTCQLTFWEASERTIRSEAEDSY
Merlin VVDISPFYNGTNRNASYFGENADKFFIFPNYTIVSDFGRPNSALETHRLVAFLERADSVISWDIQDEKNVTCQLTFWEASERTIRSEAEDSY
BE/14/2011 VVDISPFYNGTNRNASYFGENADKFFIFPNYTIVSDFGRPNSALETHRLVAFLERADSVISWDIQDEKNVTCQLTFWEASERTIRSEAEDSY
BE/27/2010 VVDISPFYNGTNRNASYFGENADKFFIFPNYTIVSDFGRPNSALETHRLVAFLERADSVISWDIQDEKNVTCQLTFWEASERTIRSEAEDSY
Towne_varL VVDISPFYNGTNRNASYFGENADKFFIFPNYTIVSDFERPNSALETHRLVAFLERADSVISWDIQDEKNVTCQLTFWEASERTIRSEAEDSY
3157 VVDISPFYNGTNRNASYFGENADKFFIFPNYTIVSDFGRPNSALETHRLVAFLERADSVISWDIQDEKNVTCQLTFWEAPERTIRSEAEDSY
Towne VVDISPFYNGTNRNASYFGENADKFFIFPNYTIVSDFGRPNSALETHRLVAFLERADSVISWDIQDEKNVTCQLTFWEASERTIRSEAEDSY
BE/17/2010 VVDISPFYNGTNRNASYFGENADKFFIFPNYTIVSDFGRPNSALETHRLVAFLERADSVISWDIQDEKNVTCQLTFWEASERTIRSEAEDSY
BE/48/2011 VVDISPFYNGTNRNASYFGENADKFFIFPNYTIVSDFGRPNSALETHRLVAFLERADSVISWDIQDEKNVTCQLTFWEASERTIRSEAEDSY
TB40/E VVDISPFYNGTNRNASYFGENADKFFIFPNYTIVSDFGRPNSALETHRLVAFLERADSVISWDIQDEKNVTCQLTFWEASERTIRSEAEDSY
BE/5/2011 VVDISPFYNGTNRNASYFGENADKFFIFPNYTIVSDFGRPNSALETHRLVAFLERADSVISWDIQDEKNVTCQLTFWEASERTIRSEAEDSY
BE/32/2011 VVDISPFYNGTNRNASYFGENADKFFIFPNYTIVSDFGRPNSALETHRLVAFLERADSVISWDIQDEKNVTCQLTFWEASERTIRSEAEDSY
C327A VVDISPFYNGTNRNASYFGENADKFFIFPNYTIVSDFGRPNSALETHRLVAFLERADSVISWDIQDEKNVTCQLTFWEASERTIRSEAEDSY
C178A VVDISPFYNGTNRNASYFGENADKFFIFPNYTIVSDFGRPNSALETHRLVAFLERADSVISWDIQDEKNVTCQLTFWEASERTIRSEAEDSY
BE/38/2011 VVDISPFYNGTNRNASYFGENADKFFIFPNYTIVSDFGRPNSALETHRLVAFLERADSVISWDIQDEKNVTCQLTFWEASERTIRSEAEDSY
HAN12 VVDISPFYNGTNRNASYFGENADKFFIFPNYTIVSDFGRPNSALETHRLVAFLERADSVISWDIQDEKNVTCQLTFWEASERTIRSEAEDSY
BE/13/2012 VVDISPFYNGTNRNASYFGENADKFFIFPNYTIVSDFGRPNSALETHRLVAFLERADSVISWDIQDEKNVTCQLTFWEASERTIRSEAEDSY
5510-E115 VVDISPFYNGTNRNASYFGENADKFFIFPNYTIVSDFGRANSAPETHRLVAFLERADSVISWDIQDEKNVTCQLTFWEASERTIRSEAEDSY
BE/22/2010 VVDISPFYNGTNRNASYFGENADKFFIFPNYTIVSDFGRPNSALETHRLVAFLERADSVISWDIQDEKNVTCQLTFWEASERTIRSEAEDSY
TR VVDISPFYNGTNRNASYFGENADKFFIFPNYTIVSDFGRPNSALETHRLVAFLERADSVISWDIQDEKNVTCQLTFWEASERTIRSEAEDSY
BE/4/2010 VVDISPFYNGTNRNASYFGENADKFFIFPNYTIVSDFGRPNAAPETHRLVAFLERADSVISWDIQDEKNVTCQLTFWEASERTIRSEAEDSY
JP VVDISPFYNGTNRNASYFGENADKFFIFPNYTIVSDFGRPNAAPETHRLVAFLERADSVISWDIQDEKNVTCQLTFWEASERTIRSEAEDSY
HAN19 VVDISPFYNGTNRNASYFGENADKFFIFPNYTIVSDFGRPNAAPETHRLVAFLERADSVISWDIQDEKNVTCQLTFWEASERTIRSEAEDSY
UKNEQAS1 VVDISPFYNGTNRNISYFGENADKFFIFPNYTIVSDFGRPNAAQETHRLVAFLERADSVISWDIQDEKNVTCQLTFWEASERTIRSEAKDSY
S3 VVDISPFYNGTNRNISYFGENADKFFIFPNYTIVSDFGRPNAAQETHRLVAFLERADSVISWDIQDEKNVTCQLTFWEASERTIRSEAKDSY
consensus>70 VVdISPFYNGTNRNaSYFGENADKFFIFPNYTIVSDFgRpNsA.ETHRlVAFLERA#SVISWDIQDEKNVTCQLTFWEAsERTIRSEAe#SY


370 380 390 400 410 420 430 440 450
HAN13 HFSSAKMTATFLSKKQEVNMSDPVLDCVRDQALNKLQQIFNASYNQTYEKYGNVSVFETTGGLVVFWQGIKQKSLELERLANSSGVNFTR.
BE/6/2011 HFSSAKMTATFLSKKQEVNMSDPVLDCVRDQALNKLQQIFNASYNQTYEKYGNVSVFETTGGLVVFWQGIKQKSLELERLANSSGVNFTE.
BE/37/2011 HFSSAKMTATFLSKKQEVNMSDPVLDCVRDQALNKLQQIFNASYNQTYEKYGNVSVFETTGGLVVFWQGIKQKSLELERLANSSGVNFTE.
VR1814 HFSSAKMTATFLSKKQEVNMSDPVLDCVRDQALNKLQQIFNASYNQTYEKYGNVSVFETTGGLVVFWQGIKQKSLELERLANSSGVNFTE.
HAN1 HFSSAKMTATFLSKKQEVNMSDPVLDCVRDQALNKLQQIFNASYNQTYEKYGNVSVFETTGGLVVFWQGIKQKSLELERLANSSGVNFTE.
CO76A HFSSAKMTATFLSKKQEVNMSDPVLDCVRDQALNKLQQIFNASYNQTYEKYGNVSVFETTGGLVVFWQGIKQKSLELERLANSSGVNFTR.
HAN3 HFSSAKMTATFLSKKQEVNMSDPVLDCVRDQALNKLQQIFNASYNQTYEKYGNVSVFETTGGLVVFWQGIKQKSLELERLANSSGVNFTR.
BE/42/2011 HFSSAKMTATFLSKKQEVNMSDPVLDCVRDQALNKLQQIFNASYNQTYEKYGNVSVFETTGGLVVFWQGIKQKSLELERLANSSGVNFTR.
JHC HFSSAKMTATFLSKKQEVNMSDPVLDCVRDQALNKLQQIFNASYNQTYEKYGNVSVFETTGGLVVFWQGIKQKSLELERLANSSGVNFTR.
BE/13/2010 HFSSAKMTATFLSKKQEVNMSDPVLDCVRDQALNKLQQIFNASYNQTYEKYGNVSVFETTGGLVVFWQGIKQKSLELERLANSSGVNFTR.
BE/35/2011 HFSSAKMTATFLSKKQEVNMSDPVLDCVRNQALNKLQQIFNASYNQTYEKYGNVSVFETTGGLVVFWQGIKQKSLELERLANSSGVNFTR.
Toledo HFSSAKMTATFLSKKQEVNMSDPVLDCVRNQALDKLQQIFNASYNQTYEKYGNVSVFETTGGLVVFWQGIKQKSLELERLANSSGVNFTR.
C354A HFSSAKMTATFLSKKQEVNMSDPVLDCVRNQALNKLQQIFNASYNQTYEKYGNVSVFETTGGLVVFWQGIKQKSLELERLANSSGVNFTR.
C359A HFSSAKMTATFLSKKQEVNMSDPMLDCVRDQALNKLQQIFNASYNQTYEKYGNVSVFETTGGLVVFWQGIKQKSLELERLANSSGVNFTR.
BE/15/2011 HFSSAKMTATFLSKKQEVNMSDPVLDCVRDQALNKLQQIFNASYNQTYEKYGNVSVFETTGGLVVFWQGIKQKSLELERLANSSGVNFTR.
HAN38 HFSSAKMTATFLSKKQEVNMSDPVLDCVRNQALNKLQQIFNASYNQTYEKYGNVSVFETTGGLVVFWQGIKQKSLELERLANSSGVNFTR.
AD169 HFSSAKMTATFLSKKQEVNMSDSALDCVRDEAINKLQQIFNTSYNQTYEKYGNVSVFETSGGLVVFWQGIKQKSLVELERLANRSSLNTTH.
6397 HFSSAKMTATFLSKKQEVNMSDSALDCVRDEAINKLQQIFNTSYNQTYEKYGNVSVFETSGGLVVFWQGIKQKSLVELERLANRSSLNTTH.
BE/11/2010 HFSSAKMTATFLSKKQEVNMSDSALDCVRDEAINKLQQIFNTSYNQTYEKYGNVSVFETSGGLVVFWQGIKQKSLVELERLANRSSLNTTH.
C336A HFSSAKMTATFLSKKQEVNMSDSALDCVRDEAINKLQQIFNTSYNQTYEKYGNVSVFETSGGLVVFWQGIKQKSLVELERLANRSSLNTTH.
HAN16 HFSSAKMTATFLSKKQEVNMSDSALDCVRDEAINKLQQIFNTSYNQTYEKYGNVSVFETSGGLVVFWQGIKQKSLVELERLANRSSLNTTH.
BE/16/2012 HFSSAKMTATFLSKKQEVNMSDSALDCVRVEAINKLQQIFNTSYNQTYEKYGNVSVFETSGGLVVFWQGIKQKSLVELERLANRSSLNTTH.
BE/15/2012 HFSSAKMTATFLSKKQEVNMSDSALDCVRVEAINKLQQIFNTSYNQTYEKYGNVSVFETSGGLVVFWQGIKQKSLVELERLANRSSLNTTH.
C338A HFSSAKMTATFLSKKQEVNMSDSALDCVRDEAINKLQQIFNTSYNQTYEKYGNVSVFETSGGLVVFWQGIKQKSLVELERLANRSSLNTTH.
PAV21 HFSSAKMTATFLSKKQEVNMSDSALDCVRDEAINKLQQIFNISYNQTYEKYGNVSVFETSGGLVVFWQGIKQKSLVELERLANRSSLNTTH.
C325A HFSSAKMTATFLSKKQEVNMSDSALDCVRDEAINKLQQIFNISYNQTYEKYGNVSVFETSGGLVVFWQGIKQKSLVELERLANRSSLNTTH.
BE/4/2012 HFSSAKMTATFLSKKQEVNMSDSALDCVRDEAINKLQQIFNISYNQTYEKYGNVSVFETTGGLVVFWQGIKQKSLVELERLANRSSLNTTHN
HAN HFSSAKMTATFLSKKQEVNMSDSALDCVRDEAINKLQQIFNISYNQTYEKYGNVSVFETTGGLVVFWQGIKQKSLVELERLANRSSLNTTHN
7 HFSSAKMTATFLSKKQEVNMSDSALDCVRDEAINKLQQIFNISYNQTYEKYGNVSVFETTGGLVVFWQGIKQKSLVELERLANRSSLNTTHN
BE/19/2011 HFSSAKMTATFLSKKQEVNMSDSALDCVRDEAINKLQQIFNASYNQTYEKYGNVSVFETTGGLVVFWQGIKQKSLVELERLANRSSLNTTHN
C194A HFSSAKMTATFLSKKQEVNMSDSALDCVRDEAINKLQQIFNASYNQTYEKYGNVSVFETTGGLVVFWQGIKQKSLVELERLANRSSLNTTHS
BE/5/2012 HFSSAKMTATFLSKKQEVNMSDSALDCVRDEAINKLQQIFNASYNQTYEKYGNVSVFETTGGLVVFWQGIKQKSLVELERLANRSSLNTTHS
CZ/2/2012 HFSSAKMTATFLSKKQEVNMSDSALDCVRDEAINKLQQIFNASYNQTYEKYGNVSVFETTGGLVVFWQGIKQKSLVELERLANRSSLNTTHS
C128A HFSSAKMTATFLSKKQEVNMSDSALDCVRDEAINKLQQIFNTSYNQTYEKYGNVSVFETTGGLVVFWQGIKQKSLVELERLANRSSLNTTHS
HAN2 HFSSAKMTATFLSKKQEVNMSDSALDCVRDEAINKLQQIFNTSYNQTYEKYGNVSVFETTGGLVVFWQGIKQKSLVELERLANRSSLNTTHN
CO82A HFSSAKMTATFLSKKQEVNMSDSALDCVRDEAINKLQQIFNTSYNQTYEKYGNVSVFETTGGLVVFWQGIKQKSLVELERLANRSSLNTTHN
Merlin HFSSAKMTATFLSKKQEVNMSDSALDCVRDEAINKLQQIFNTSYNQTYEKYGNVSVFETTGGLVVFWQGIKQKSLVELERLANRSSLNTTHN
BE/14/2011 HFSSAKMTATFLSKKQEVNMSDSALDCVRDEAINKLQQIFNTSYNQTYEKYGNVSVFETTGGLVVFWQGIKQKSLVELERLANRSSLNTTHN
BE/27/2010 HFSSAKMTATFLSKKQEVNMSDSALDCVRDEAINKLQQIFNTSYNQTYEKYGNVSVFETTGGLVVFWQGIKQKSLVELERLANRSSLNTTHN
Towne_varL HFSSAKMTATFLSKKQEVNMSDSALDCVRDEAINKLQQIFNTSYNQTYEKYGNVSVFETTGGLVVFWQGIKQKSLVELERLANRSSLNTTHN
3157 HFSSAKMTATFLSKKQEVNMSDSALDCVRDEAINKLQQIFNTSYNQTYEKYGNVSVFETTGGLVVFWQGIKQKSLVELERLANRSSLNTTHN
Towne HFSSAKMTATFLSKKQEVNMSDSALDCVRDEAINKLQQIFNTSYNQTYEKYGNVSVFETTGGLVVFWQGIKQKSLVELERLANRSSLNTTHN
BE/17/2010 HFSSAKMTATFLSKKQEVNMSDSALDCVRDEAINKLQQIFNTSYNQTYEKYGNVSVFETTGGLVVFWQGIKQKSLVELERLANRSSLNTTHN
BE/48/2011 HFSSAKMTATFLSKKQEVNMSDSALDCVRDEAINKLQQIFNTSYNQTYEKYGNVSVFETTGGLVVFWQGIKQKSLVELERLANRSSLNTTHN
TB40/E HFSSAKMTATFLSKKQEVNMSDSALDCVRDEAINKLQQIFNTSYNQTYEKYGNVSVFETTGGLVVFWQGIKQKSLVELERLANRSSLNTTHN
BE/5/2011 HFSSAKMTATFLSKKQEVNMSDSALDCVRDEAINKLQQIFNTSYNQTYEKYGNVSVFETTGGLVVFWQGIKQKSLVELERLANRSSLNTTHN
BE/32/2011 HFSSAKMTATFLSKKQEVNMSDSALDCVRDEAINKLQQIFNTSYNQTYEKYGNVSVFETTGGLVVFWQGIKQKSLVELERLANRSSLNTTHN
C327A HFSSAKMTATFLSKKQEVNMSDSVLDCVRDEAINKLQQIFNTSYNQTYEKYGNVSVFETTGGLVVFWQGIKQKSLVELERLANRSSLNTTHN
C178A HFSSAKMTATFLSKKQEVNMSDSVLDCVRDEAINKLQQIFNTSYNQTYEKYGNVSVFETTGGLVVFWQGIKQKSLVELERLANRSSLNTTHN
BE/38/2011 HFSSAKMTATFLSKKQEVNMSDSALDCVRDEAINKLQQIFNTSYNQTYEKYGNVSVFETTGGLVVFWQGIKQKSLVELERLANRSSLNTTHN
HAN12 HFSSAKMTATFLSKKQEVNMSDSALDCVRDEAINKLQQIFNTSYNQTYEKYGNVSVFETTGGLVVFWQGIKQKSLVELERLANRSSLNTTHN
BE/13/2012 HFSSAKMTATFLSKKQEVNMSDSALDCVRDEAINKLQQIFNTSYNQTYEKYGNVSVFETTGGLVVFWQGIKQKSLVELERLANRSSLNTTHN
5510-E115 HFSSAKMTATFLSKKQEVNMSDSVLDCVRDEAINKLQQIFNTSYNQTYEKYGNVSVFETTGGLVVFWQGIKQKSLVELERLANRSSLNTTHS
BE/22/2010 HFSSAKMTATFLSKKQEVNMSDSALDCVRDEAINKLQQIFNTSYNQTYEKYGNVSVFETTGGLVVFWQGIKQKSLVELERLANRSSLNTTHS
TR HFSSAKMTATFLSKKQEVNMSDSALDCVRDEAINKLQQIFNTSYNQTYEKYGNVSVFETTGGLVVFWQGIKQKSLVELERLANRSSLNTTHS
BE/4/2010 HFSSAKMTATFLSKKQEVNMSDSALDCVRDEAINKLQQIFNISYNQTYEKYGNVSVFETSGGLVVFWQGIKQKSLVELERLANRSSLNTTH.
JP HFSSAKMTATFLSKKQEVNMSDSALDCVRDEAINKLQQIFNISYNQTYEKYGNVSVFETSGGLVVFWQGIKQKSLVELERLANRSSLNTTH.
HAN19 HFSSAKMTATFLSKKQEVNMSDSALDCVRDEAINKLQQIFNISYNQTYEKYGNVSVFETSGGLVVFWQGIKQKSLVELERLANRSSLNTTH.
UKNEQAS1 HFSSAKMTATFLSKKQEVNMSDPVLDCVRDQALNKLQQIFNASYNQTYEKYGNVSVFETTGGLVVFWQGIKQKSLVELERLANSSGVNATR.
S3 HFSSAKMTATFLSKKQEVNMSDPVLDCVRDQALNKLQQIFNASYNQTYEKYGNVSVFETTGGLVVFWQGIKQKSLVELERLANSSGVNATR.
consensus>70 HFSSAKMTATFLSKKQEVNMSDs.LDCVRd#A.#KLQQIFN.SYNQTYEKYGNVSVFETtGGLVVFWQGIKQKSLvELERLANrSslN.Th.
460 470 480 490 500 510 520 530 540
HAN13 RTKRST.GNTTTLSLESESVRNVLYAQLQFTYDTLRSYINRALAQIAEAWCVDQRRTLEVFKELSKINPSAILSAIYNKPIAARFMGDVLGL
BE/6/2011 RTKRST.GNTTTLSLESESVRNVLYAQLQFTYDTLRSYINRALAQIAEAWCVDQRRTLEVFKELSKINPSAILSAIYNKPIAARFMGDVLGL
BE/37/2011 RTKRST.GNTTTLSLESESVRNVLYAQLQFTYDTLRSYINRALAQIAEAWCVDQRRTLEVFKELSKINPSAILSAIYNKPIAARFMGDVLGL
VR1814 RTKRST.GNTTTLSLESESVRNVLYAQLQFTYDTLRSYINRALAQIAEAWCVDQRRTLEVFKELSKINPSAILSAIYNKPIAARFMGDVLGL
HAN1 RTKRST.GNTTTLSLESESVRNVLYAQLQFTYDTLRSYINRALAQIAEAWCVDQRRTLEVFKELSKINPSAILSAIYNKPIAARFMGDVLGL
CO76A RTKRST.GNTTTLSLESESVRNVLYAQLQFTYDTLRSYINRALAQIAEAWCVDQRRTLEVFKELSKINPSAILSAIYNKPIAARFMGDVLGL
HAN3 RTKRST.GNTTTLSLESESVRNVLYAQLQFTYDTLRSYINRALAQIAEAWCVDQRRTLEVFKELSKINPSAILSAIYNKPIAARFMGDVLGL
BE/42/2011 RTKRST.GNTTTLSLESESVRNVLYAQLQFTYDTLRSYINRALAQIAEAWCVDQRRTLEVFKELSKINPSAILSAIYNKPIAARFMGDVLGL
JHC RTKRST.GNTTTLSLESESVRNVLYAQLQFTYDTLRSYINRALAQIAEAWCVDQRRTLEVFKELSKINPSAILSAIYNKPIAARFMGDVLGL
BE/13/2010 RTKRST.GNTTTLSLESESVRNVLYAQLQFTYDTLRSYINRALAQIAEAWCVDQRRTLEVFKELSKINPSAILSAIYNKPIAARFMGDVLGL
BE/35/2011 RTKRST.GNTTTLSLESESVRNVLYAQLQFTYDTLRSYINRALAQIAEAWCVDQRRTLEVFKELSKINPSAILSAIYNKPIAARFMGDVLGL
Toledo RTKRST.GNTTTLSPESESVRNVLYAQLQFTYDTLRSYINRALAQIAEAWCVDQRRTLEVFKELSKINPSAILSAIYNKPIAARFMGDVLGL
C354A RTKRST.GNTTTLSLESESVRNVLYAQLQFTYDTLRSYINRALAQIAEAWCVDQRRTLEVFKELSKINPSAILSAIYNKPIAARFMGDVLGL
C359A RTKRST.GNTTTLSPESESVRNVLYAQLQFTYDTLRSYINRALAQIAEAWCVDQRRTLEVFKELSKINPSAILSAIYNKPIAARFMGDVLGL
BE/15/2011 RTKRST.GNTTTLSLENESVRNVLYAQLQFTYDTLRSYINRALAQIAEAWCVDQRRTLEVFKELSKINPSAILSAIYNKPIAARFMGDVLGL
HAN38 RTKRST.GNTTTLSLESESVRNVLYAQLQFTYDTLRSYINRALAQIAEAWCVDQRRTLEVFKELSKINPSAILSAIYNKPIAARFMGDVLGL
AD169 RTRRSTSDNNTTHLSSMESVHNLVYAQLQFTYDTLRGYINRALAQIAEAWCVDQRRTLEVFKELSKINPSAILSAIYNKPIAARFMGDVLGL
6397 RTRRSTSDNNTTHLSSMESVHNLVYAQLQFTYDTLRGYINRALAQIAEAWCVDQRRTLEVFKELSKINPSAILSAIYNKPIAARFMGDVLGL
BE/11/2010 RTRRSTSDNNTTHLSSMESVHNLVYAQLQFTYDTLRGYINRALAQIAEAWCVDQRRTLEVFKELSKINPSAILSAIYNKPIAARFMGDVLGL
C336A RTRRSTSDNNTTHLSSMESVHNLVYAQLQFTYDTLRGYINRALAQIAEAWCVDQRRTLEVFKELSKINPSAILSAIYNKPIAARFMGDVLGL
HAN16 RTRRSTSDNNTTHLSSMESVHNLVYAQLQFTYDTLRGYINRALAQIAEAWCVDQRRTLEVFKELSKINPSAILSAIYNKPIAARFMGDVLGL
BE/16/2012 RTRRSTSDNNTTHLSSMESVHNLVYAQLQFTYDTLRGYINRALAQIAEAWCVDQRRTLEVFKELSKINPSAILSAIYNKPIAARFMGDVLGL
BE/15/2012 RTRRSTSDNNTTHLSSMESVHNLVYAQLQFTYDTLRGYINRALAQIAEAWCVDQRRTLEVFKELSKINPSAILSAIYNKPIAARFMGDVLGL
C338A RTRRSTSDNNTTHLSSMESVHNLVYAQLQFTYDTLRGYINRALAQIAEAWCVDQRRTLEVFKELSKINPSAILSAIYNKPIAARFMGDVLGL
PAV21 RTRRSTSDNNTTHLSSMESVHNLVYAQLQFTYDTLRGYINRALAQIAEAWCVDQRRTLEVFKELSKINPSAILSAIYNKPIAARFMGDVLGL
C325A RTKRSTNGNNATHLSNMESVHNLVYAQLQFTYDTLRGYINRALAQIAEAWCVDQRRSLEVFRELSKINPSAILSAIYNKPIAARFMGDVLGL
BE/4/2012 RTKRSTNGNNATHLSNMESVHNLVYAQLQFTYDTLRGYINRALAQIAEAWCVDQRRSLEVFRELSKINPSAILSAIYNKPIAARFMGDVLGL
HAN RTKRSTNGSNATHLSNMESVHNLVYAQLQFTYDTLRGYINRALAQIAEAWCVDQRRSLEVFRELSKINPSAILSAIYNKPIAARFMGDVLGL
7 RTKRSTNGSNATHLSNMESVHNLVYAQLQFTYDTLRGYINRALAQIAEAWCVDQRRSLEVFRELSKINPSAILSAIYNKPIAARFMGDVLGL
BE/19/2011 RTKRSTDGNNATHLSNMESVHNLVYAQLQFTYDTLRGYINRALAQIAEAWCVDQRRTLEVFKELSKINPSAILSAIYNKPIAARFMGDVLGL
C194A RTRRSTDGTNVTHLSNMDSVHNLVYAQLQFTYDTLRGYINRALTQIAEAWCVDQRRTLEVFKELSKINPSAILSAIYNKPIAARFMGDVLGL
BE/5/2012 RTRRSTDGTNVTHLSNMDSVHNLVYAQLQFTYDTLRGYINRALTQIAEAWCVDQRRTLEVFKELSKINPSAILSAIYNKPIAARFMGDVLGL
CZ/2/2012 RTRRSTDGTNVTHLSNMDSVHNLVYAQLQFTYDTLRGYINRALTQIAEAWCVDQRRTLEVFKELSKINPSAILSAIYNKPIAARFMGDVLGL
C128A RTRRSTDGTNVTHLSNMDSVHNLVYAQLQFTYDTLRGYINRALTQIAEAWCVDQRRTLEVFKELSKINPSAILSAIYNKPIAARFMGDVLGL
HAN2 RTKRSTDGNNATHLSNMESVHNLVYAQLQFTYDTLRGYINRALAQIAEAWCVDQRRTLEVFKELSKINPSAILSAIYNKPIAARFMGDVLGL
CO82A RTKRSTDGNNATHLSNMESVHNLVYAQLQFTYDTLRGYINRALAQIAEAWCVDQRRTLEVFKELSKINPSAILSAIYNKPIAARFMGDVLGL
Merlin RTKRSTDGNNATHLSNMESVHNLVYAQLQFTYDTLRGYINRALAQIAEAWCVDQRRTLEVFKELSKINPSAILSAIYNKPIAARFMGDVLGL
BE/14/2011 RTKRSTDGNNATHLSNMESVHNLVYAQLQFTYDTLRGYINRALAQIAEAWCVDQRRTLEVFKELSKINPSAILSAIYNKPIAARFMGDVLGL
BE/27/2010 RTKRSTDGNNATHLSNMESVHNLVYAQLQFTYDTLRGYINRALAQIAEAWCVDQRRTLEVFKELSKINPSAILSAIYNKPIAARFMGDVLGL
Towne_varL RTKRSTDGNNATHLSNMESVHNLVYAQLQFTYDTLRGYINRALAQIAEAWCVDQRRTLEVFKELSKINPSAILSAIYNKPIAARFMGDVLGL
3157 RTKRSTDGNNATHLSNMESVHNLVYAQLQFTYDTLRGYINRALAQIAEAWCVDQRRTLEVFKELSKINPSAILSAIYNKPIAARFMGDVLGL
Towne RTKRSTDGNNATHLSNMESVHNLVYAQLQFTYDTLRGYINRALAQIAEAWCVDQRRTLEVFKELSKINPSAILSAIYNKPIAARFMGDVLGL
BE/17/2010 RTKRSTDGNNATHLSNMESVHNLVYAQLQFTYDTLRGYINRALAQIAEAWCVDQRRTLEVFKELSKINPSAILSAIYNKPIAARFMGDVLGL
BE/48/2011 RTKRSTDGNNATHLSNMESVHNLVYAQLQFTYDTLRGYINRALAQIAEAWCVDQRRTLEVFKELSKINPSAILSAIYNKPIAARFMGDVLGL
TB40/E RTKRSTDGNNATHLSNMESVHNLVYAQLQFTYDTLRGYINRALAQIAEAWCVDQRRTLEVFKELSKINPSAILSAIYNKPIAARFMGDVLGL
BE/5/2011 RTKRSTDGNNATHLSNMESVHNLVYAQLQFTYDTLRGYINRALAQIAEAWCVDQRRTLEVFKELSKINPSAILSAIYNKPIAARFMGDVLGL
BE/32/2011 RTKRSTDGNNATHLSNMESVHNLVYAQLQFTYDTLRGYINRALAQIAEAWCVDQRRTLEVFKELSKINPSAILSAIYNKPIAARFMGDVLGL
C327A RTKRSTDGNNATHLSNMESVHNLVYAQLQFTYDTLRGYINRALAQIAEAWCVDQRRTLEVFKELSKINPSAILSAIYNKPIAARFMGDVLGL
C178A RTKRSTDGNNATHLSNMESVHNLVYAQLQFTYDTLRGYINRALAQIAEAWCVDQRRTLEVFKELSKINPSAILSAIYNKPIAARFMGDVLGL
BE/38/2011 RTKRSIDGNNATHLSNMESVHNLVYAQLQFTYDTLRGYINRALAQIAEAWCVDQRRTLEVFKELSKINPSAILSAIYNKPIAARFMGDVLGL
HAN12 RTKRSIDGNNATHLSNMESVHNLVYAQLQFTYDTLRGYINRALAQIAEAWCVDQRRTLEVFKELSKINPSAILSAIYNKPIAARFMGDVLGL
BE/13/2012 RTKRSTDGNNATHLSNMESVHNLVYAQLQFTYDTLRGYINRALAQIAEAWCVDQRRSLEVFKELSKINPSAILSAIYNKPIAARFMGDVLGL
5510-E115 RAKRSADGNNTTHLSNMESVHNLVYAQLQFTYDTLRGYINRALAQIAEAWCVDQRRSLEVFRELSKINPSAILSAIYNKPIAARFMGDVLGL
BE/22/2010 RTKRSTDGNNATHLSNMESVHNLVYAQLQFTYDTLRGYINRALAQIAEAWCVDQRRSLEVFRELSKINPSAILSAIYNKPIAARFMGDVLGL
TR RTKRSADGNNATHLSSMESVHNLVYAQLQFTYDTLRGYINRALAQIAEAWCVDQRRSLEVFKELSKINPSAILSAIYNKPIAARFMGDVLGL
BE/4/2010 RTRRSTSDNNTTHLSSMESVHNLVYAQLQFTYDTLRGYINRALAQIAEAWCVDQRRTLEVFKELSKINPSAILSAIYNKPIAARFMGDVLGL
JP RTRRSTSDNNTTHLSSMESVHNLVYAQLQFTYDTLRGYINRALAQIAEAWCVDQRRTLEVFKKLSKINPSAILSAIYNKPIAARFMGDVLGL
HAN19 RTRRSTSDNNTTHLSSMESVHNLVYAQLQFTYDTLRGYINRALAQIAEAWCVDQRRTLEVFKELSKINPSAILSAIYNKPIAARFMGDVLGL
UKNEQAS1 RSKRSTNNTTTLSLEN.DSVRSVLYAQLQFTYDTLRNYINRALAQIAEAWCVDQRRTLEVFKELSKINPSAILSAIYNKPIAARFMGDVLGL
S3 RSKRSTNNTTTLSLEN.DSVRSVLYAQLQFTYDTLRNYINRALAQIAEAWCVDQRRTLEVFKELSKINPSAILSAIYNKPIAARFMGDVLGL
consensus>70 RtkRSt.gnn.thlsnm#SVhnlvYAQLQFTYDTLRgYINRALaQIAEAWCVDQRRtLEVFkeLSKINPSAILSAIYNKPIAARFMGDVLGL


550 560 570 580 590 600 610 620 630
HAN13 BE/6/2011 BE/37/2011 VR1814 HAN1 CO76A HAN3 BE/42/2011 JHC BE/13/2010 BE/35/2011 Toledo C354A C359A BE/15/2011 HAN38 AD169 6397 BE/11/2010 C336A HAN16 BE/16/2012 BE/15/2012 C338A PAV21 C325A BE/4/2012 HAN 7 BE/19/2011 C194A BE/5/2012 CZ/2/2012 C128A HAN2 CO82A Merlin BE/14/2011 BE/27/2010 Towne_varL 3157 Towne BE/17/2010 BE/48/2011 TB40/E BE/5/2011 BE/32/2011 C327A C178A BE/38/2011 HAN12 BE/13/2012 5510-E115 BE/22/2010 TR BE/4/2010 JP HAN19 UKNEQAS1 S3
consensus>70
640 650 660 670 680 690 700 710 720
HAN13 BE/6/2011 BE/37/2011 VR1814 HAN1 CO76A HAN3 BE/42/2011 JHC BE/13/2010 BE/35/2011 Toledo C354A C359A BE/15/2011 HAN38 AD169 6397 BE/11/2010 C336A HAN16 BE/16/2012 BE/15/2012 C338A PAV21 C325A BE/4/2012 HAN 7 BE/19/2011 C194A BE/5/2012 CZ/2/2012 C128A HAN2 CO82A Merlin BE/14/2011 BE/27/2010 Towne_varL 3157 Towne BE/17/2010 BE/48/2011 TB40/E BE/5/2011 BE/32/2011 C327A C178A BE/38/2011 HAN12 BE/13/2012 5510-E115 BE/22/2010 TR BE/4/2010 JP HAN19 UKNEQAS1 S3
consensus>70

Chapter Four: gB/Antibody Complexes

4.1 Isolated Human Neutralizing gB Antibodies

4.1.1. TRL345, a Human Neutralizing AD-2 Specific Antibody

Antibodies against AD-2 (site I), AD-4, and AD-5 are of interest and are in some stage of development for use as mAb therapeutics. The structure of gB in complex with an anti-AD-4 antibody (SM5-1) is available [182]. However, there remains limited structural information for AD-2 and AD-5. Structural knowledge of AD-2 is particularly lacking as it is located in the disordered N-terminus which was not included in the crystallization construct for the gB ectodomain and the corresponding regions in HSV-1 and EBV gB were unresolved. Site I of AD-2 (residues 68-77) is completely conserved (Fig. 3.S1), is protected with two glycosylation sites (Fig. 3.9), and likely has functional importance consistent with the high neutralizing capacity of antibodies that target it [209]. Furthermore, its poor immunogenicity may improve the efficacy of an AD-2 mAb with protection in patients since preexisting immunity is less likely to interfere with binding. With this rationale in mind, antibodies against AD-2, site I were isolated from human B cells. One of the most potent, TRL345 has been characterized with the intent of developing it as a mAb therapeutic [58]. No structural information is available for AD-2 to inform the linear epitopes mechanism of neutralization as it is located in the disordered N-terminus.

4.1.2. 1G2, a Human Neutralizing AD-5 Specific Antibody

The antigenic region, AD-5, is located in DI of gB. DI contains the two fusion loops, a PH domain, may interact with gH/gL and is heavily glycosylated [210]. How anti-AD-5 antibodies cope with glycosylation and through which mechanism they

achieve neutralization is yet unclear. Results from alanine surface scanning mutations identified four residues that were detrimental to antibody when mutated, two affected binding of 1G2 (Y280/N284) and three affected binding of 2C2 and SM10 (Y280/N293/D295) [163]. The structure of gB indicated that the area around N284 is densely glycosylated and mutational analysis can be misleading. Thus, the structure of gB in complex with 1G2 would improve our understanding of the 1G2 epitope and structural determinates affecting it.

4.2. TRL345 in Complex with gB

4.2.1 gB/TRL345 Fab complex

To enhance our understanding of the structural determinants of AD-2, we sought to determine the crystal structure of TRL345 in complex with gB. TRL345 IgG was kindly provided by Trellis Bioscience. It was necessary to cleave IgG to generate Fab so that the flexible constant regions did not interfere with crystallization. The protease papain was used to cleave IgG into the Fc and Fab fragments. However, papain cleavage was inefficient in doing so, leaving ~50% IgG uncleaved despite optimization efforts (Fig. 4.1A). Fc and IgG can be separated from Fab using protein A beads which recognize the constant region of IgG antibodies. The protein A beads did not remove all of the uncleaved IgG or Fc from the papain digestion, thus did not provide pure Fab. Some Fab was also present in the protein A eluate. It appears that TRL345 Fab bound non-specifically to protein A beads as well, a common occurrence for IgG subclass 3 (IgG3) antibodies, giving incomplete separation of Fab from Fc and IgG. Thus, partially cleaved TRL345 containing IgG, Fc, and Fab were run over SEC to separate the IgG

from the Fc and the Fab. Then, gB was used to isolate the Fab from the Fc and form the complex, followed by running over SEC to remove Fc and unbound Fab (Fig. 4.1B).

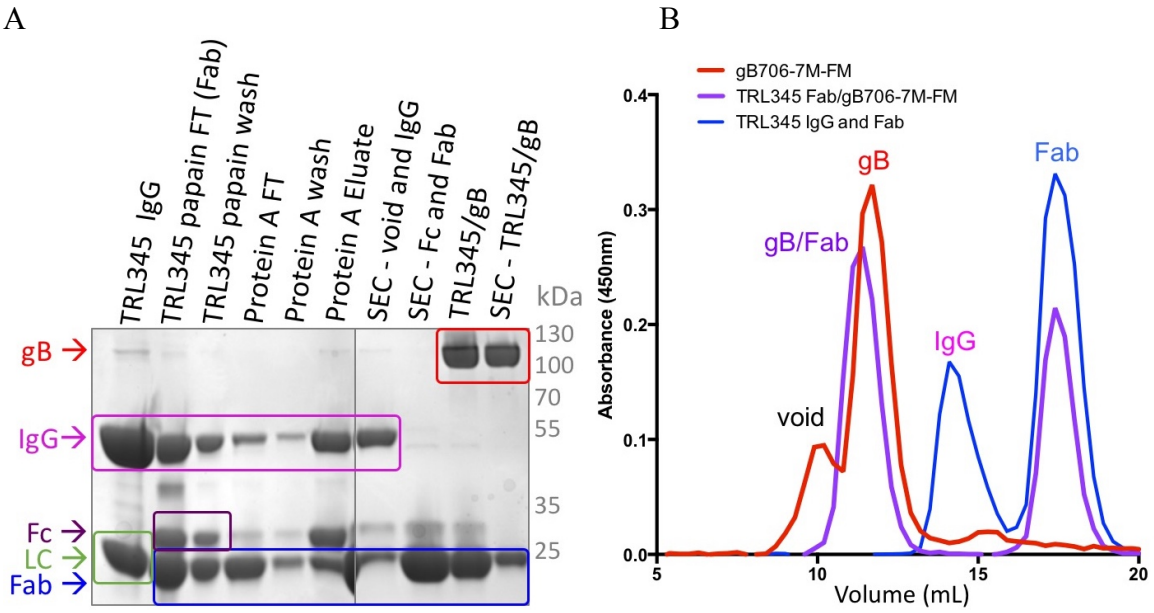

Figure 4.1 Preparation and formation of gB/TRL345 Fab. (A) Coomassie gel with samples from the preparation of gB/TRL345 Fab complex. Incomplete papain cleavage of TRL345 IgG (pink box and green box for light chain) to Fab (blue box) and Fc (purple box), followed by incomplete removal of Fc from Fab using protein A beads (FT = flow-through). Subsequently, the papain digest was run over size exclusion chromatography (SEC) to separate uncleaved IgG from Fab and Fc. gB (red box) was bound to Fab/Fc fraction and the complex was run over Agarose/dextran SEC (B) SEC spectra of TRL345 Fab purification (blue) and gB/TRL345 complex (purple) with gB (red) for comparison.

New gB constructs had to be created that contained the seven fusion loop mutations and deletion of the furin cleavage site while still maintaining site 1 in the N-terminus. The furin cleavage site was mutated to four serines (RRRK→SSSS) in the full-length ectodomain construct, gB706-7M, since cleavage of the loop was not necessary for crystallization (gB706-7M-FM). This construct expressed well and TRL345 bound to it at

a ratio of 3:1 Fab to gB trimer. The complex was subjected to 960 crystallization conditions, all of which failed to generate crystals. Many conditions formed oils, indicating the protein was attempting to come together in those conditions, yet something was preventing it from doing so. This was likely presence of the intact N-terminus which prevented crystal contacts from forming with gB alone. We had hoped that TRL345 would stabilize this region allowing contacts to form while having the complete N-terminus intact. Unfortunately, this was not the case.

Irregular, snowflake-like crystals were obtained when trypsin cleaved after residues R50, R66, and K77 (Section 3.1.2). Truncation to residue Y78 reduced this irregularity; however, it was unclear if this was the result of the removal of the disordered region or the reduction in protein heterogeneity. Thus, gB was truncated to residue S51 to keep as much of the N terminus intact while still potentially allowing crystal contacts to form by removing some of the disordered N terminus. This construct expressed poorly and precipitated when concentrated. Low yields allowed for only 192 crystallization conditions to be tested. We obtained one hit, but crystals were too small to test diffraction (Fig. 4.2). Because there is no obvious reason for the location of the truncation being detrimental, alternative truncations should be tested. The sequence conservation of the of the region could be used as a guide in designing such truncations (Fig. 4.3). The sequence is highly conserved beginning at site I. Upstream of N68 (site I), there are a few conserved residues: V57 to S60, V63, and S64 (Fig. 4.3). Truncations based on sequence conservation could include constructs starting at V63 or V57. It is encouraging that crystals were obtained from a rather limited screen of the gB51-706-7M-FM/TRL345

complex. Construct optimization and extensive crystallization screening will likely generate crystals leading to the structure of the complex.

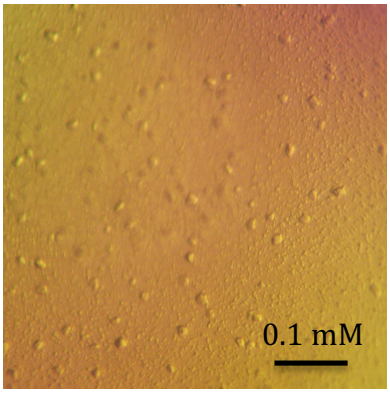

Figure 4.2 Crystallization of gB/TRL345 Fab. (left) Crystals of gB51-706-7M-FM/TRL345 Fab grown in PEG 8000, 0.1 M NaH_2PO_4, pH 6.2, and $(NH_4)_2SO$.

Figure 4.3. Sequence Conservation of AD-2. (Right) Identical residues are shown as white text on red background, similar residues are highlighted in yellow and (.) indicates no conservation or insertion. Sites I (residues 68-77) and site II (residues 50-54) are boxed. (*) indicates possible truncation sites.

4.3. 1G2 in Complex with gB

4.3.1. Crystallization of the gB/1G2 Fab complex

We sought to determine the structure of gB in complex with the anti-AD-5 human neutralizing antibody, 1G2 to clarify the epitope and examine the effect of glycans. The Fab of 1G2 binds the gB ectodomain in a ratio of one gB trimer to three 1G2 antibodies. AD-5 contains the two fusion loops in which seven mutations were made to decrease rosette formation. These mutations (gB706-7M) do not interfere with binding of 1G2 Fab and thus interactions with the fusion loops are not likely the mechanism of 1G2 neutralization (Fig. 4.4), which is in agreement with previous mutational analysis [163]. 1G2 Fab in complex with various gB constructs formed crystals readily in many

crystallization conditions (Table 4.1). The complex of 1G2 Fab bound to trypsin cleaved gB706-7M had 5 crystal hits obtained from screening 960 conditions. Two of which were reproducible by hanging drop vapor diffusion crystallization (Fig. 4.5A, B). 1G2 bound to trypsin cleaved gB78-706-7M crystallized in five different crystal screen conditions, one of which was reproducible (Fig. 4.5C). Finally, the Fab fragment of 1G2 in complex with gB78-706-7M-E crystallized in 16 screen conditions, 7 reproducibly (Fig. 4.5D-F). Most crystallization conditions generated crystals did not diffract at all (22 crystals diffracted out 180 tested). Those that did diffract, did so poorly. Modifications to gB that resulted in improved diffraction also improved diffraction of the gB/1G2 complex, though not to the same extent. The best resolution obtained was 8.8-Å from the 1G2 Fab in complex with gB78-706-7M-E, crystallized in 8% polyethylene glycol (PEG) 8000, 0.1 M Tris pH 8.5, and 0.1 M ammonium sulfate. Many crystals grown in this condition were tested with only one diffracting to 8.8-Å.

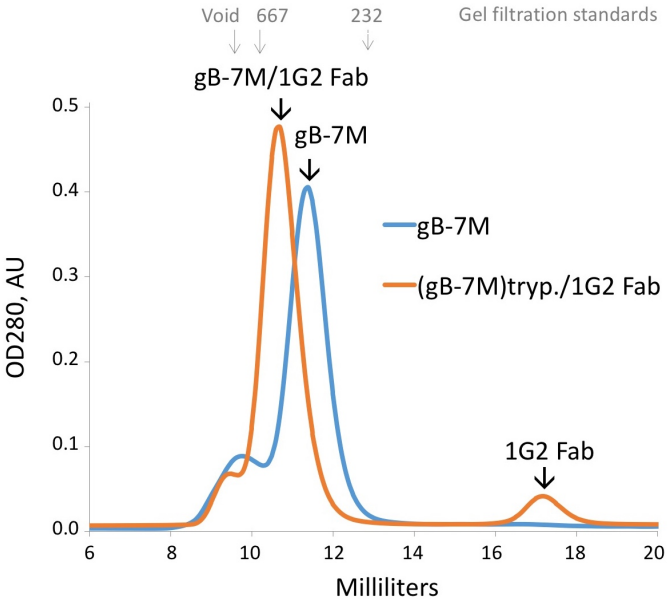

Figure 4.4. SEC Spectrum of gB/1G2 Fab Complex. 1G2 was bound to gB78-706-7M-E at a molar ratio of 1.3:1 Fab to gB protomer to achieve saturation of gB. The complex was run over Agarose/ dextran SEC to remove excess Fab (orange). The complex elutes slightly before gB alone (blue), ~1 ml after the void. A peak corresponding to excess 1G2 Fab confirms that gB was saturated with Fab.

gB Construct	Precipitant	Buffer	pH	Additive	Reproducible	Diffraction
(gB707-7M)trypsin	PEG 5000	Tris	6.5	-	No	
	PEG 12000	HEPES	7.0	-	No	
	PEG 20000	HEPES	7.0	-	No	
	PEG 8000	NaH_2PO_4	6.5	-	Yes	
	PEG 8000	Na Citrate	6.5	NaCl	Yes	none
(gB78-707-7M)trypsin	PEG 1500	MMT Buffer	6.5	-	No	
	PEG 2000	Tris	7.5	$(CH_3)_3NO$	No	
	PEG 3350	NaH_2 Citrate	6.5	-	No	
	PEG 8000	HEPES	7.5	$(CH_2OH)_2$	No	
	PEG 8000	NaH_2PO_4	6.5	-	Yes	~15-Å
gB78-706-7M-E	PEG 1000	NaH_2PO_4	6.5	NaCl	No	
	PEG 3000	NaH_2PO_4	6.2	-	No	
	PEG 8000	NaH_2PO_4	6.5	-	No	
	PEG 4000	Tris	8.0	$(NH_4)_2SO_4$	No	
	PEG 8000	Tris	7.0	MgCl2	No	
	PEG 20000	Tris	8.0	NaCl	No	
	PEG 20000	Bicine	9.0	Dioxane	No	
	Glascol W13	K Citrate	7.0	-		
	Sokalan CP7	HEPES	7.0	KCl		
	Sokalan CP5	HEPES	7.0	NH_4HCO_2	Yes	none
	Sokalan CP5	Tris	8.5	-	Yes	none
	PEG 3000	Imidazole	8.0	Li2SO4	Yes	none
	Polyacrylate 5100	Tris	8.0	NaCl	Yes	none
	PEG 4000	Tris	8.5	$(NH_4)_2SO_4$	Yes	none
	PEG 8000	Tris	8.5	-	Yes	~30-Å
	PEG 8000	Tris	8.5	$(NH_4)_2SO_4$	Yes	8.8-Å

Table 4.1 gB/1G2 Crystallization Screen Hits. 1G2 Fab was bound to three gB ectodomain constructs: trypsin cleaved gB with 7 fusion loop mutations ((gB706-7M)trypsin), trypsin cleaved gB, truncated to residue 78 with 7 fusion loop mutations ((gB78-706-7M)trypsin), and gB, truncated to residue 78 with 7 fusion loop mutations, and the furin cleavage site replaced with an enterokinase cleavage site (gB78-706-7M-E). A "-" indicates no additive included. If blank, the condition was not tested.

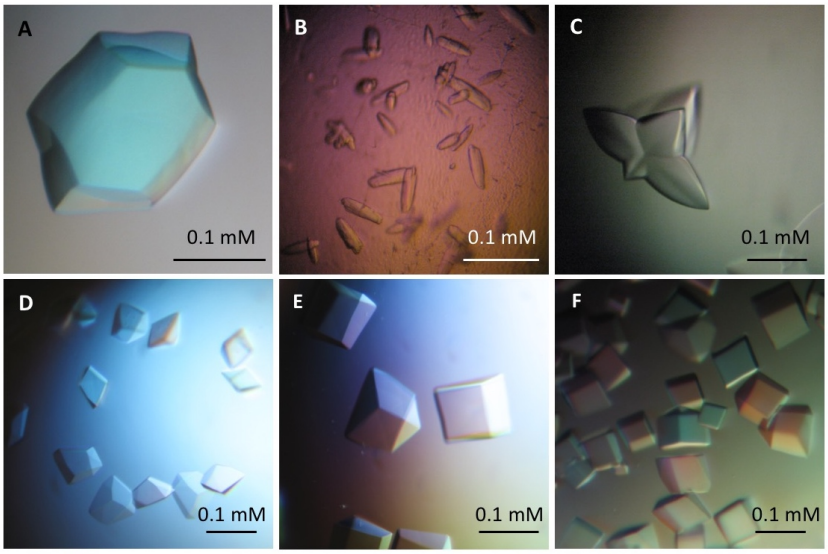

Figure 4.5. gB/1G2 Fab Crystals. A) Trypsin cleaved gB706-7M/1G2 Fab crystallized in 8-9% PEG 8000, 0.1 M Na citrate, pH 6.5, 0.2 M NaCl. **B)** Trypsin cleaved gB706-7M/1G2 Fab crystallized in 10% PEG 8000, 0.1 M NaH2PO4, pH 6.5. **C)** Trypsin cleaved gB78-706-7M/1G2 Fab crystallized in 8-10% PEG 8K, 0.1 M NaH2PO4, pH 6.5. **D)** gB78-706-7M-E/1G2 Fab crystallized in 20% Sokalan CP 5, 0.1 M HEPES pH 7, 0.3 M ammonium formate. **E)** gB78-706-7M-E/1G2 Fab crystallized in 10% PEG 3000, 0.1 M Imidazole pH 8, 0.2 M Li2SO4. **F)** gB78-706-7M-E/1G2 Fab crystallized in 8% PEG 8K, 0.1 Tris pH 8.5, 0.1 ammonium sulfate.

4.3.2. Molecular replacement of gB in gB/1G2 Fab dataset

Molecular replacement (MR) was run on the 8.8-Å data set using the gB structure as a search model. MR with gB was successful, however, there was no density for the Fab (Fig. 4.6A). Despite crystallizing in very similar conditions to gB alone (PEG 8000, Tris pH 6.5, 0.1 mM ammonium sulfate vs. PEG 8000, Tris pH 7-8.5, 0.15 mM magnesium nitrate, respectively), the complex crystallized in the space group R3, which is drastically different from the gB crystallization space group, $P2_12_12_1$. Furthermore, crystal packing allows ample space between molecules of gB for three 1G2 Fabs to bind, suggesting the

Fab is present in the crystals. This was further confirmed by running the gB78-706-7M-E/1G2 Fab crystals on an SDS page gel (Fig. 4.6B). The phasing power may be too low for the Fab to be resolved.

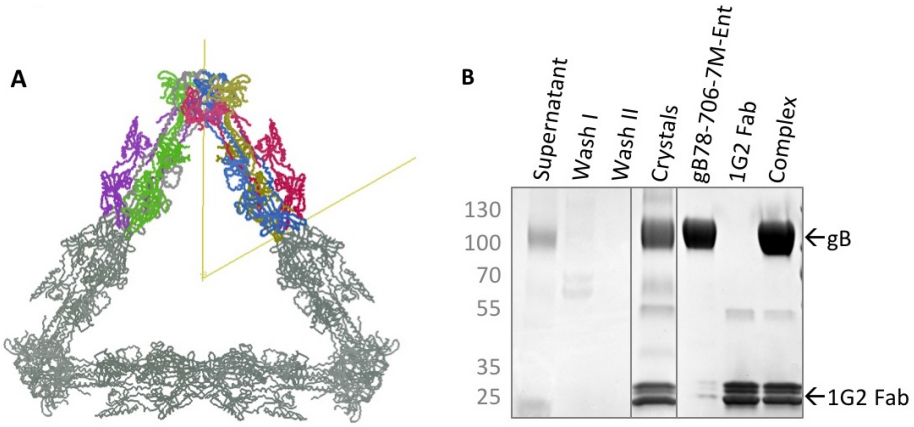

Figure 4.6. The presence of 1G2 Fab in gB/1G2 Fab Crystals. (A) MR solution of gB using the 8.8-Å dataset of gB78-706-7M-E/1G2 Fab crystals grown in 10% PEG 8000, Tris pH 6.5, and 0.1 mM ammonium sulfate. (B) gB/1G2 Fab crystals were collected, washed, and run over an SDS page gel then stained with Coomassie to determine if the Fab was present in the crystals despite the lack of density. One band for gB is present above 100 kDa, and two additional bands for 1G2 Fab heavy and light chains are present at just above and below 25 kDa.

4.3.3. The 1G2 Epitope

The recently published structure of gB in complex with 1G2 Fab and subsequent mutational analysis revealed the gB residues actually involved in 1G2 binding [211]. Interestingly, the gB/1G2 structure revealed that 1G2 does not make contact with N284 as the alanine mutation suggested [163, 211]. Rather, the 1G2 epitope roughly consists of gB residues 280-301, making hydrogen/disulfide bonds, salt bridges, or covalent linkages with Y280, G282, R285, F290, G291, and A294 (Fig. 4.7B). This emphasizes the need

for structural information regarding antibody epitopes rather than relying on mutational analysis which can give misleading results due to indirect effects.

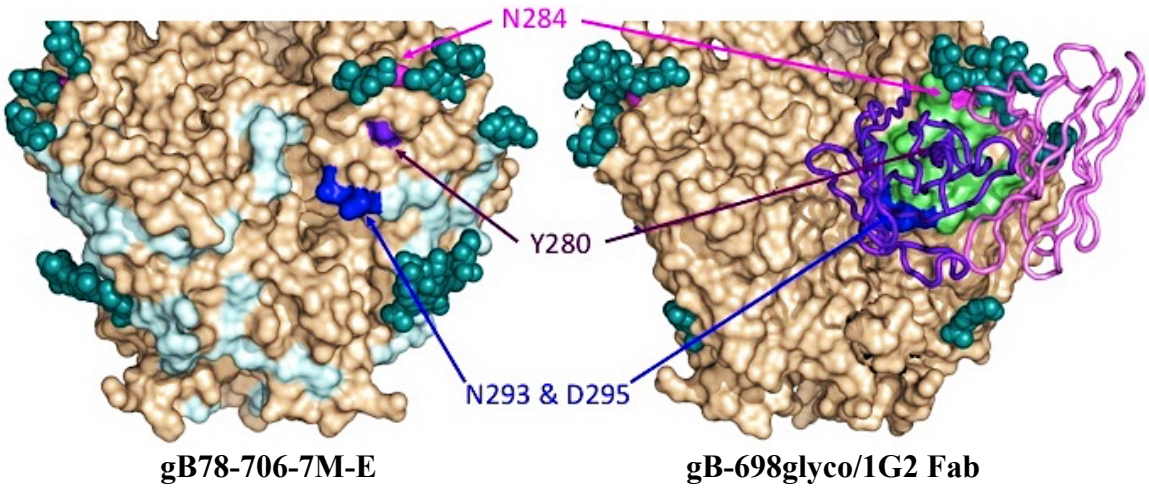

Figure 4.7 AD-5 comparison of gB vs. gB/1G2 Fab. Structure of gB DI (5CXF) (left) compared to gB/1G2 Fab (5C6T) (right), re-rendered from [211]. gB structures are in wheat with surface representation. 1G2 Fab is shown in ribbon with the heavy chain colored purple and the light colored pink. Glycans are shown as spheres in teal. N284, shown to decrease 1G2 binding when mutated, is colored pink. N293 and D295, shown to decrease binding of 2C2 and SM10 when mutated are colored blue. Y280 shown to decrease binding of 1G2, 2C2, and SM10 when mutated is colored purple [163].

4.4 Discussion

gB (along with gH/gL and the pentamer, gH/gL/UL128/UL130/UL131) elicits a strong immune response in humans and induces the production of neutralizing antibodies, though most anti-gB antibodies are non-neutralizing [166, 170]. gB is the most highly conserved among the HCMV entry glycoproteins and is required for entry into all cell types whereas the pentamer is necessary for entry into epithelial and endothelial cells but

not fibroblasts. Furthermore, anti-gB IgG could protect human trophoblast progenitor cells (TBPCs), the precursors to placental cells, while anti-pentamer IgG could not [167]. Therefore, gB may represent a better antigenic target for monoclonal immunoglobulin therapy and an understanding of the structural factors of immunogenicity aids in these efforts.

The gB AD-5 specific antibody 1G2 is one such promising mAb therapeutic candidate. The structure published by Chandramouli, et al. confirmed the antibody bound gB in a 1:3 molar ratio and that Y280 was involved in both antibody binding and the structural integrity of the epitope [163, 211]. The addition residue N284 reported to be important for 1G2 binding from mutational analysis likely had only an indirect effect on the epitope. This is consistent with the observation that N284 is located between to glycans, making antibody binding challenging. 1G2 binds gB on the conserved face of DI (Fig. 3.14) just below a thick glycan ridge and just above the stabilized glycan at N208. 1G2, and likely 2C2 and SM10, bind the narrow conserved region between theses glycans on this functionally important domain. Thus, antibodies that recognize this patch on gB would likely be broadly neutralizing and make an excellent therapeutic.

While the structural information provided by the AD-4 and AD-5 antibody complexes is useful, AD-2 is still lacking. Determining the structure of TRL345 in complex with gB would illuminate how the antibody is able to bind the linear epitope ($_{68}$NETIYNTTLK$_{77}$) in the disordered N-terminus while avoiding the two predicted site I glycans (cyan). The structure may also provide insights into how this flexible stretch of residues interacts in a functionally relevant manner with the whole of gB. Additional truncations to the N-terminus that maintain site I may reduce precipitation of gB51-706-

7M-FM while improving crystal contact formation. Doing so should lead to the determination of the structure.

In summary, the HCMV gB structure presented in chapter 3 and the structure of gB in complex with the neutralizing antibodies SM5-1 and 1G2 provide valuable insights into the structural determinants of the immunogenicity of gB. This gives us a framework from which to re-design recombinant gB vaccines and isolate potent mAbs for therapeutics. The glycan distribution in HCMV gB revealed by its structure suggests that antigenic sites that elicit neutralizing antibodies are more heavily glycosylated than those that elicit non-neutralizing antibodies. For instance, glycans could be used to shield the non-neutralizing epitopes of AD-1 thereby designing recombinant gB to redirecting the immune response to elicit neutralizing antibodies only.

Chapter Five: Maternal Antibodies and HCMV Infection Protection

5.1. gB epitope location and protection from infection

5.1.1. Protective capacity of different gB antigenic regions

There is a great deal of interest in developing a mAb therapy for treatment of HCMV [155, 218, 219], yet this goal remains elusive. Given that there are four ADs on gB that generate antibodies with varying degrees of neutralizing capabilities in cell culture, it is necessary to determine which of these domains elicits antibodies that will provide the greatest protection in patients. Genetic variation in immunity has been shown to result in the variation of gB antibody responsiveness [220] and may correlate with variation in protection as well. Additionally, antibodies rather than cellular immunity were associated with protection from disease in a recombinant gD HSV-2 clinical trial [221]. Both HSV-2 gD and gB are surface glycoproteins involved in viral entry; thus, it is possible that anti-gB antibodies may play a larger role in protection from HMCV.

5.1.2. CMVIG prophylaxis study with premature neonates

Prior to the 1990's, donated blood was not screened for HCMV putting premature infants receiving blood transfusions at a higher risk. In an effort to protect transfused premature neonates from HCMV infection, a clinical trial was conducted to test the efficacy of prophylaxis immunoglobulin from HCMV seropositive individuals with high anti-HCMV titers (CMVIG). Premature infants enrolled in the study were separated at random into two groups, those receiving CMVIG or placebo. Sera were taken from the mothers at the time of birth to test HCMV serostatus as well as from the infants at various time points. The infants were followed for six months. During that time it was determined if they had no HCMV infection, viruria (HCMV positive urine), positive ELISA at six

months (indicating an infant immune response to infection), HCMV syndrome (disease), or death [57]. Various other information was gathered on the infants such as gestational age and weight, breastfed, etc. We are particularly interested in the maternal sera from these studies, which presumably contain naturally occurring anti-gB antibodies. Because premature infants have immature immune systems [222], this set of samples offers a unique opportunity to dissect the importance of the naturally occurring maternal antibodies in protection from HCMV infection in the absence of cellular immunity. Such analysis will provide a correlation between an antibody's ability to neutralize HCMV in cell culture vs. to protect neonates from disease.

5.2 Correlational Analysis

5.2.1. Maternal anti-gB ELISA levels

Forty maternal samples from the placebo group (not given CMVIG) were analyzed to identify the antigenic specificity of any anti-gB antibodies present in the maternal sera and to correlate it with protection from infection and disease in neonates. ELISA with immobilized gB706-7M (soluble, but maintaining the N terminus and furin cleavage site) was conducted on with serial dilutions of each maternal serum sample. An anti-human secondary antibody was used to determine the overall level of anti-gB antibodies in each sample (Fig. 5.1). The dilution versus absorbance curves were plotted and a Kd of each curve was determined using prism (graphpad.com). One sample could not be tested due to low volume. The other 39 maternal samples were grouped into the following 3 categories: Kd <999 = low anti-gB antibody levels, Kd of 1000-2999 = mid-

anti-gB levels, and Kd >3000 = high anti-gB levels. The samples distributed evenly with 33% in each category or 13/39 each (summarized in Table 5.2).

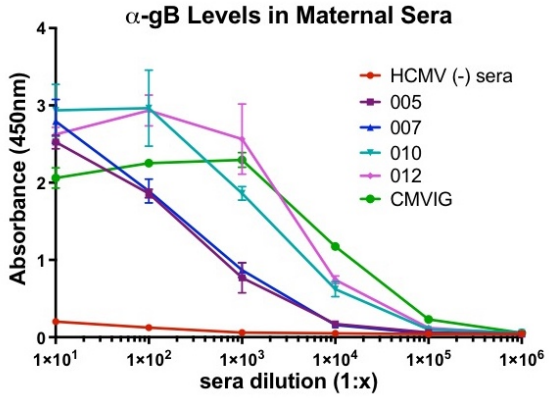

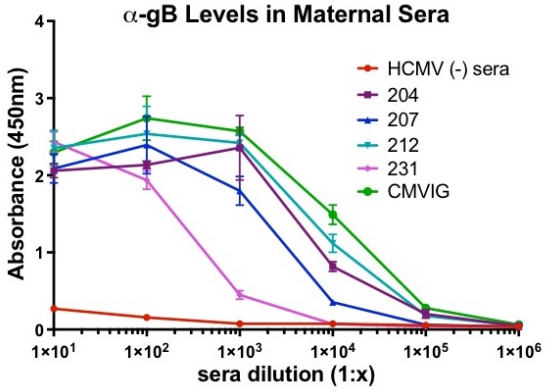

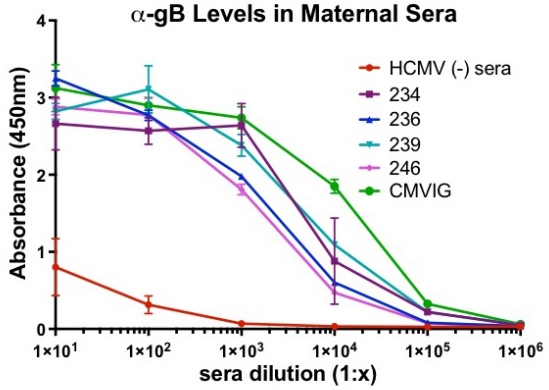

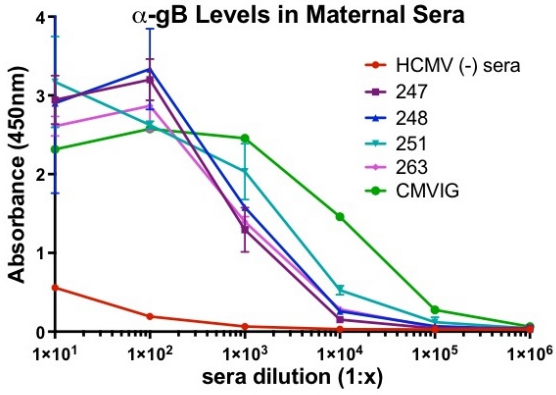

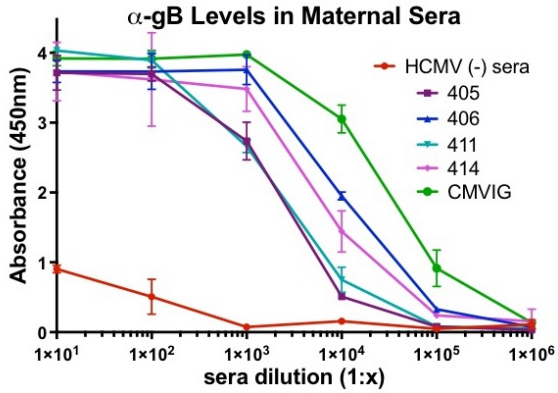

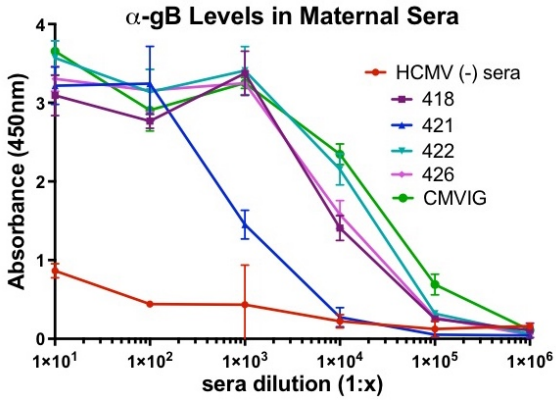

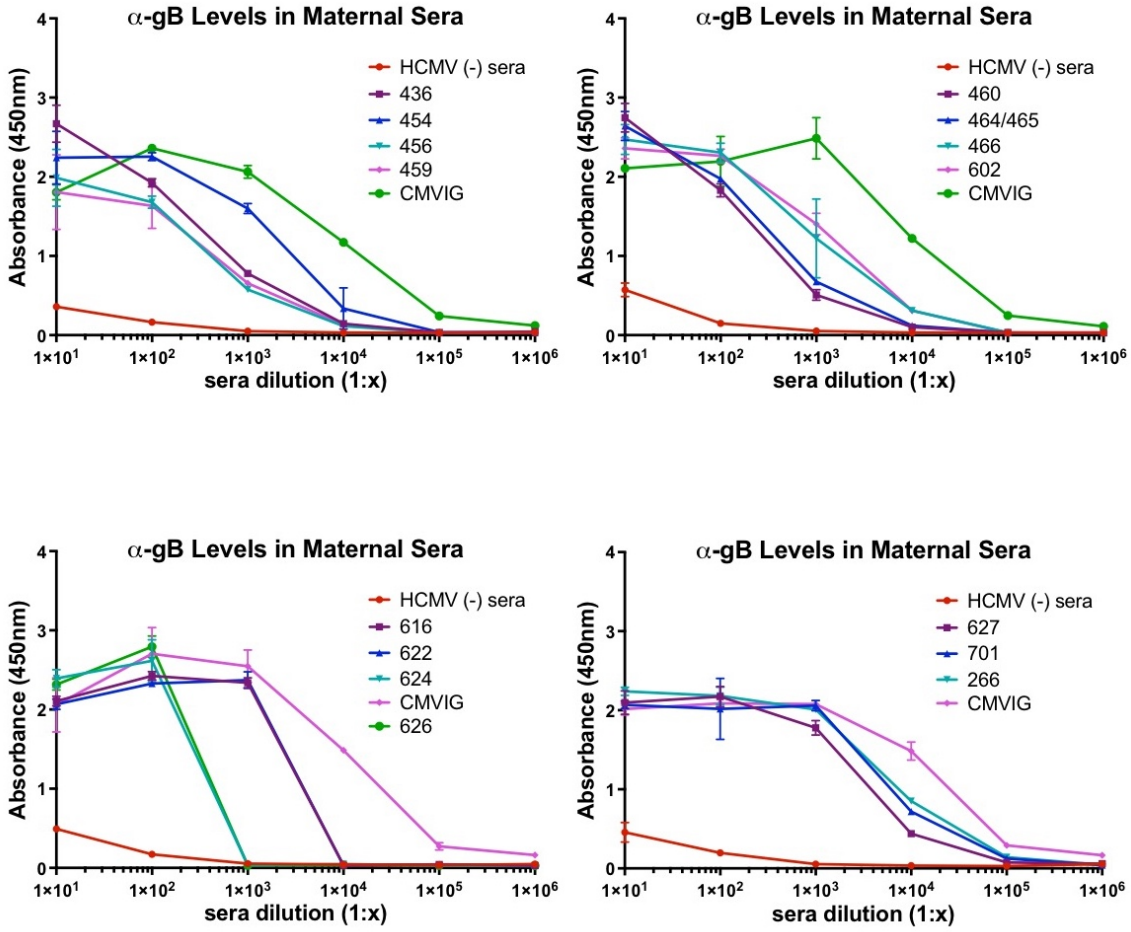

Figure 5.1. Anti-gB ELISA Curves. Curves of the ELISA determining the level of total anti-gB antibodies in sera samples. Four samples were tested per ELISA plate and are grouped as such. The positive CMVIG control is always colored green and the seronegative serum negative control is always in red. Graphs created in Prism (graphpad.com).

5.2.2. Blocking ELISA Design

To determine the gB domain specificity of the antibodies in each serum sample, a blocking ELISA was designed (described in Section 2.5.2 and diagramed in Fig. 5.2). This assay determined the level of mAb blocking each serum sample was capable of against four AD-specific mAbs (Table 5.1), establishing the repertoire of gB antibodies

for each mother (Fig. 5.3). Blocking of AD-1 was tested with the non-neutralizing antibody, 27-156, while the neutralizing Ab TRL345 was used to test blocking of AD-2 [58, 223]. SM5-1, a human neutralizing Ab, is a member of a set of antibodies from the same individual that are currently the only isolated antibodies with recognition of HCMV gB AD-4 [155, 182]. 1G2 is the most characterized of three antibodies isolated against AD-5 to date [155, 163, 211]. Therefore, SM5-1 and 1G2 were used to assess binding of AD-4 and AD-5. A decrease in binding of a mAb to a specific gB AD served as an indicator that the serum contains antibodies that recognize an overlapping epitope.

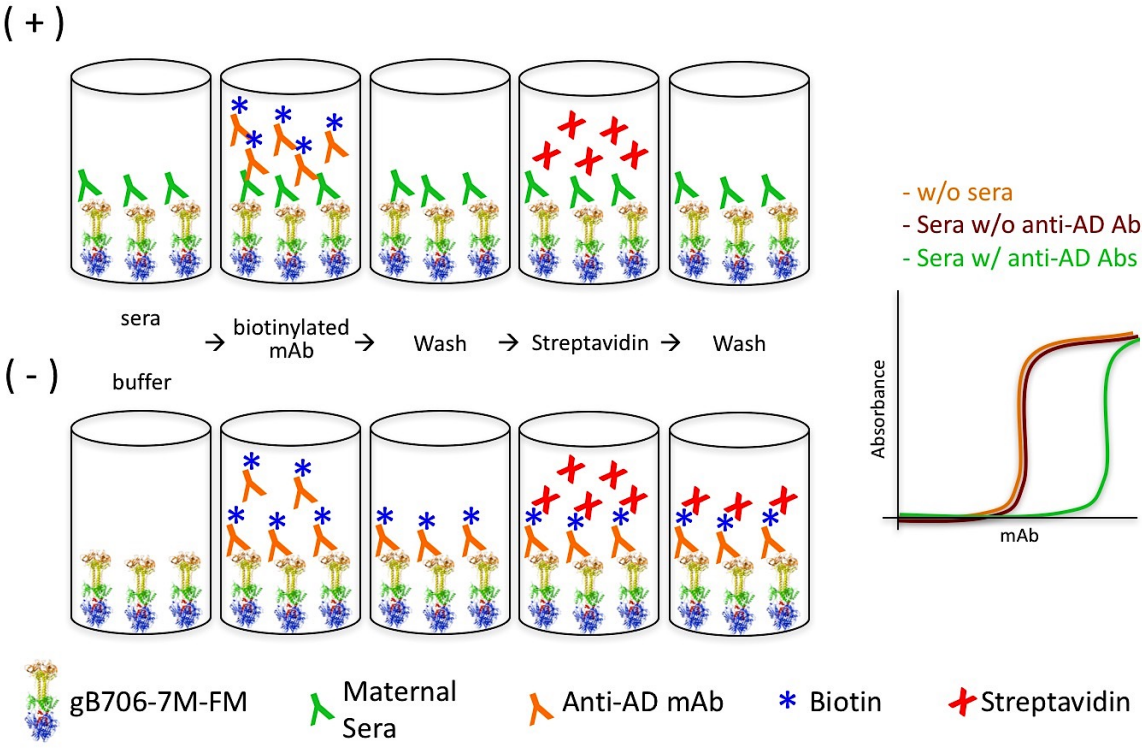

Figure 5.2. Blocking ELISA Design. Blocking ELISA steps as described in materials and methods (section 2.5.2). Briefly, gB (rainbow) is immobilized in ELISA wells, then incubated with serum sample (green Abs). Wells are washed and one biotinylated (blue) mAb (orange Abs) (testing AD-1, AD-2, AD-4, or AD-5) is added. Unbound mAb is washed away and streptavidin

(red) is added and developed using HRP substrate chemiluminescence. The absorbance of wells can be measured and percent inhibition compared to buffer only can be calculated.

Antigenic Region	Structural Domain	Monoclonal Antibody	Immunogenicity (% of sera)	Neutralizing (% of Abs)
AD-1	DIV	27-156	100	7
AD-2	N term	TRL345	57	50
AD-3	Cyto	N/A	N/A	N/A
AD-4	DII	SM5-1	95	100
AD-5	DI	1G2	95	100

Table 5.1. Set of mAbs used for blocking ELISA. mAbs against AD-1, AD-2, AD-4, and AD-5 were selected based on high affinity and availability. Most are neutralizing mAbs with the exception of anti-AD-1 (27-156) which reflects the nature of most antibodies against AD-1. Abbreviations: N term – N terminus, cyto – cytoplasmic domain. References for mAb: 27-156 [223], TRL345 [58], SM5-1 [182], 1G2 [163].

5.2.3. Sera blocking levels

The antibodies present in the sera were classified into antigenic groups by calculating the percentage of mAb blocking using Kd from the generated blocking curves for each sample (Fig. 5.4). The level of blocking was categorized and summarized in Table 5.2 as none - 0-24.9% (-), weak – 25-49.9% (+), moderate 50-74.9% (++), and strong 75-100% (+++), summarized in Table 5.2. Moderate to strong (>50%) blocking of the anti-AD-1 antibody was observed in 65% (26/40) of the maternal serum samples. Moderate to strong blocking of the anti-AD-2 antibody was found in 42.5% (17/40) of the maternal serum samples. 35% (14/40) of the maternal serum samples had moderate to strong blocking of the anti-AD-4 antibody and 37.5% (15/40) of the anti-AD-4 antibody.

Samples 005, 007, 010, and 012:

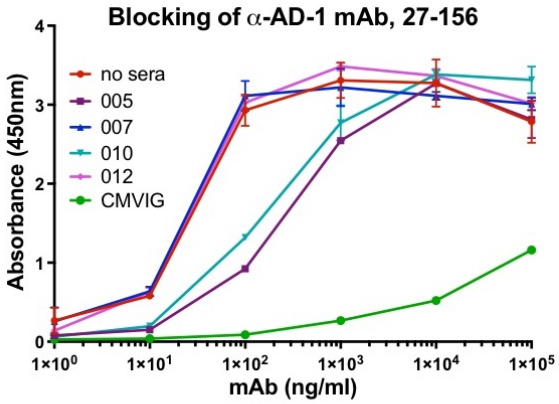

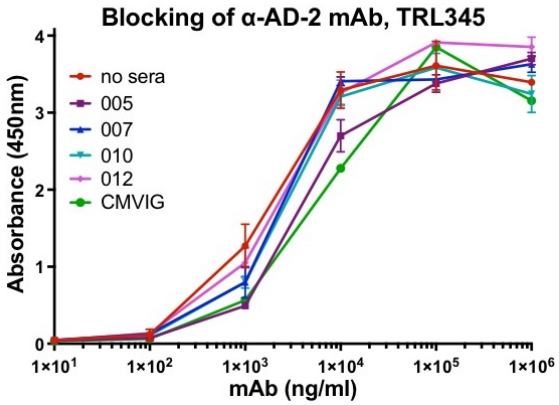

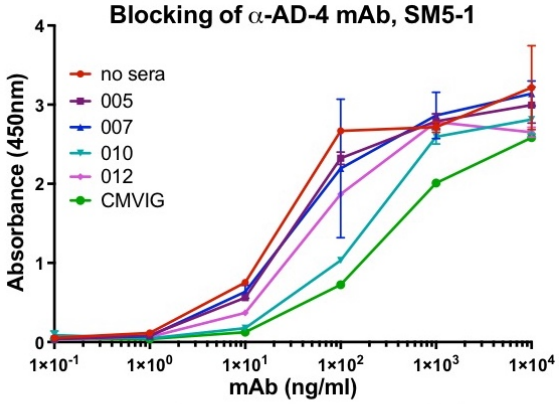

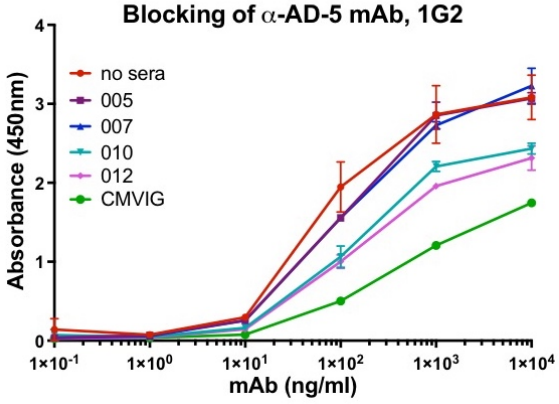

Samples 234, 236, 239, and 246:

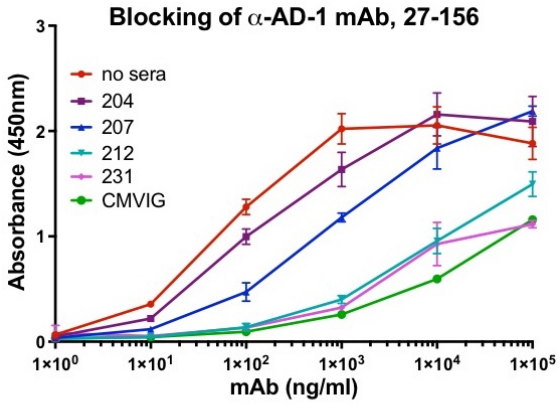

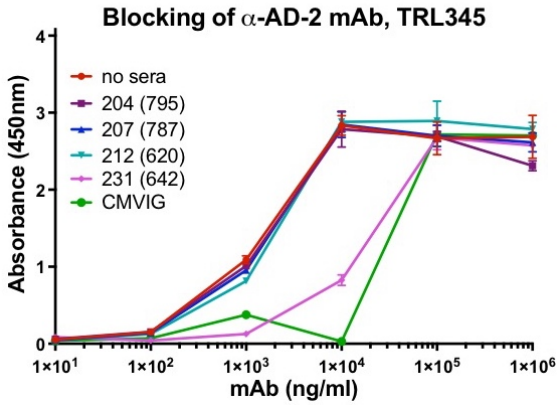

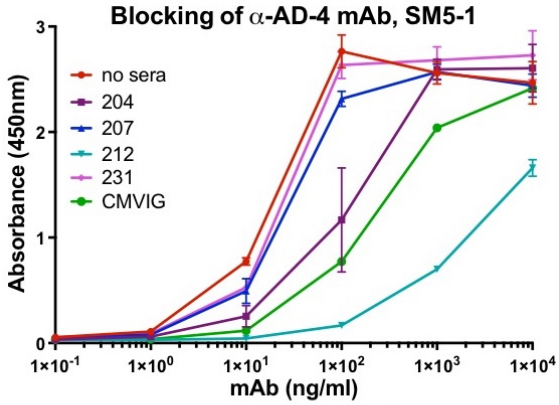

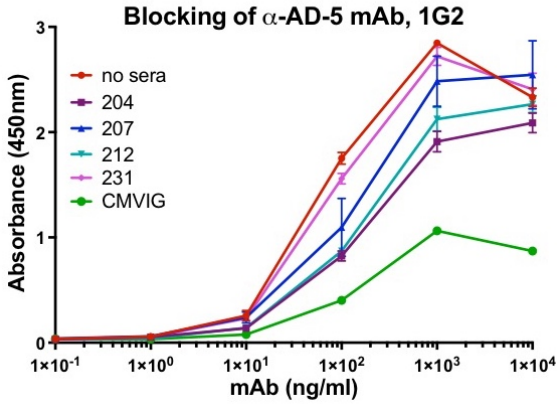

Samples 234, 236, 239, and 246:

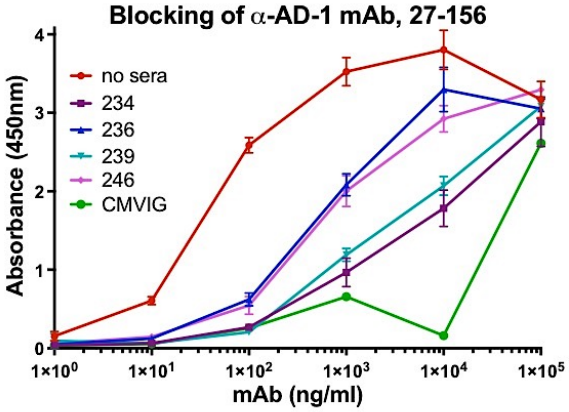

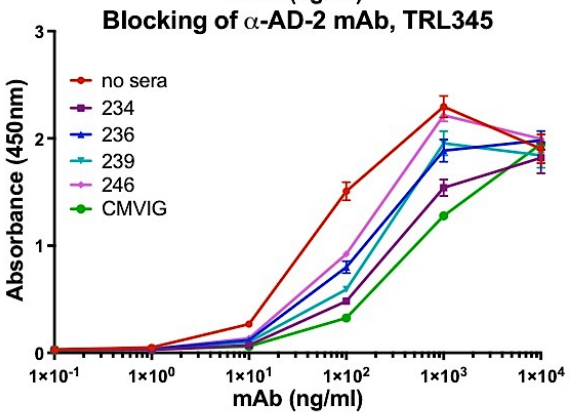

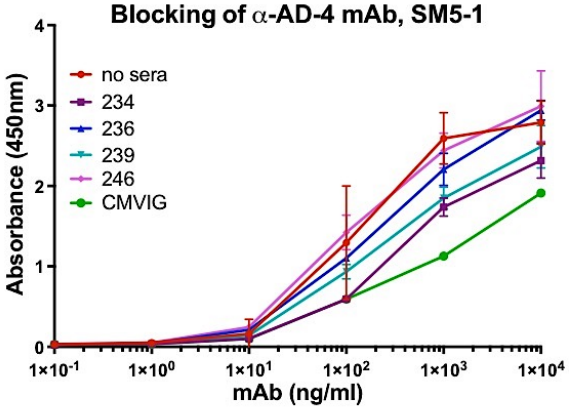

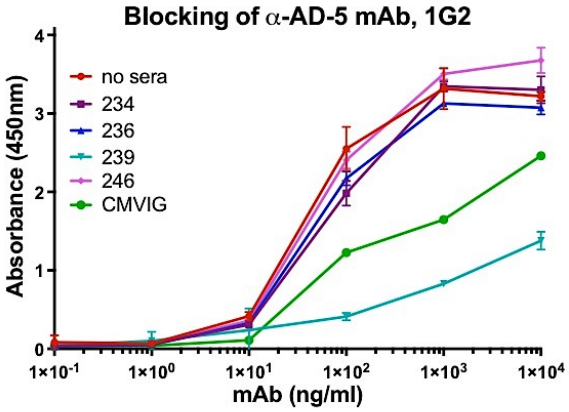

Samples 247, 251, 248, and 263:

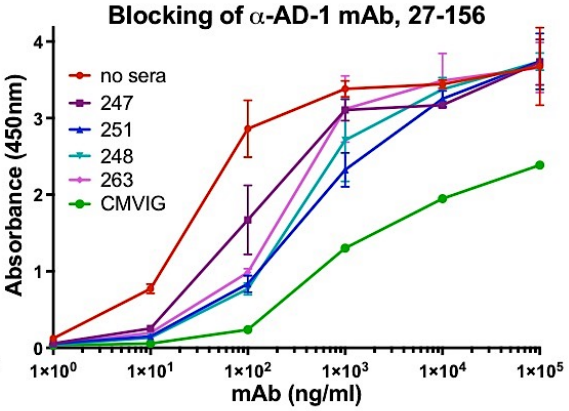

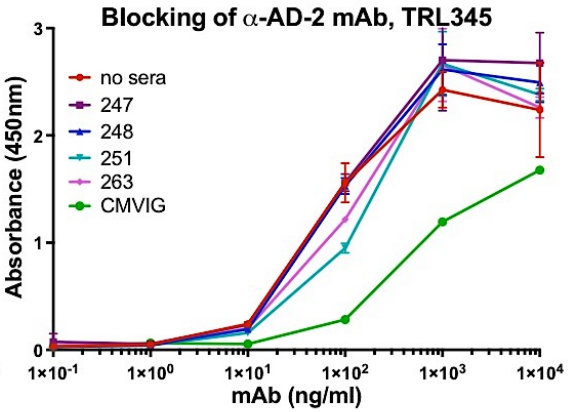

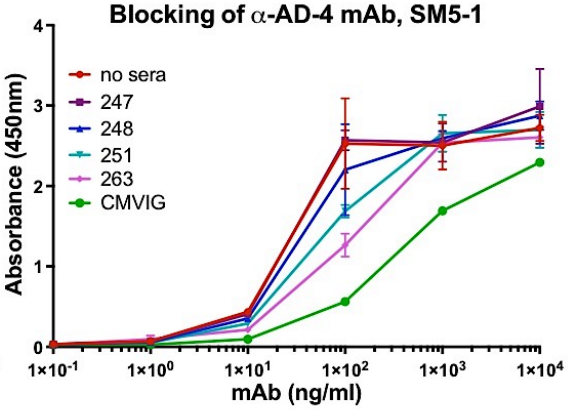

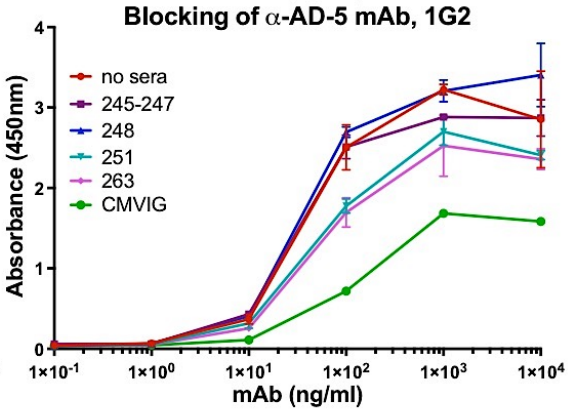

Samples 405, 406, 411, and 414:

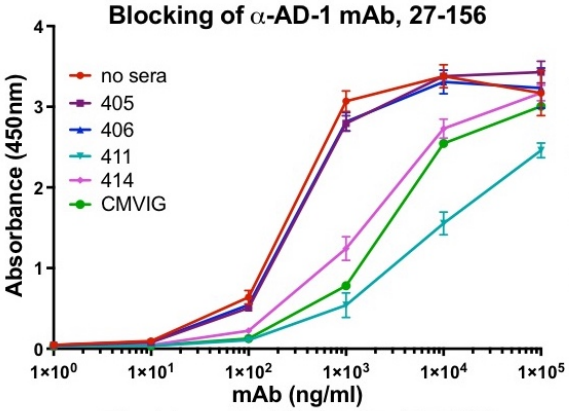

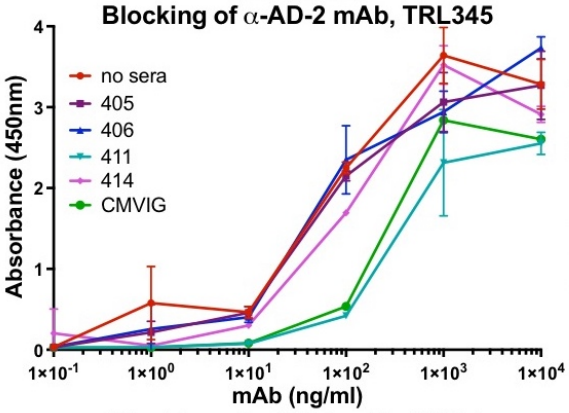

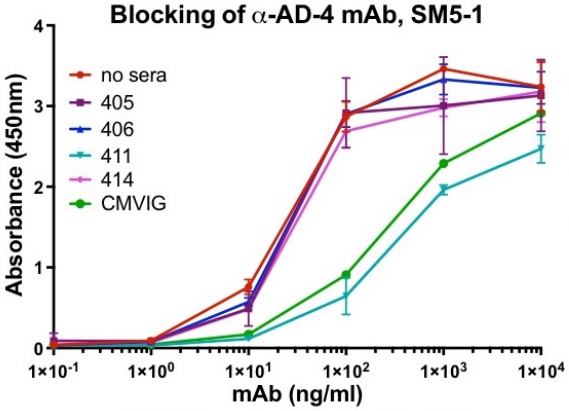

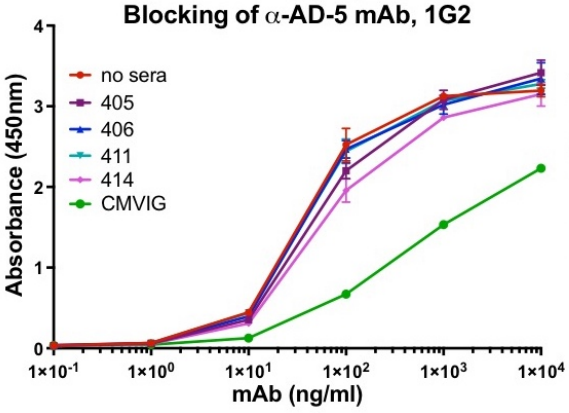

Samples 418, 421, 422, and 426:

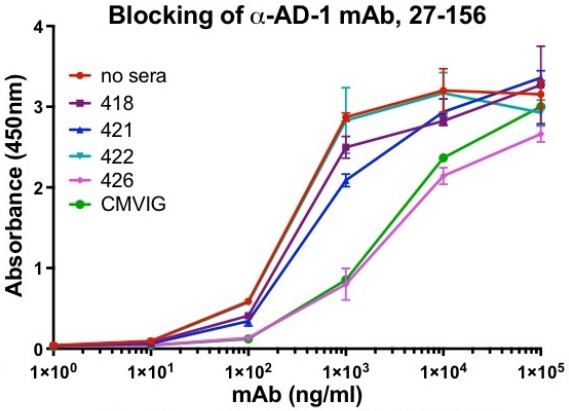

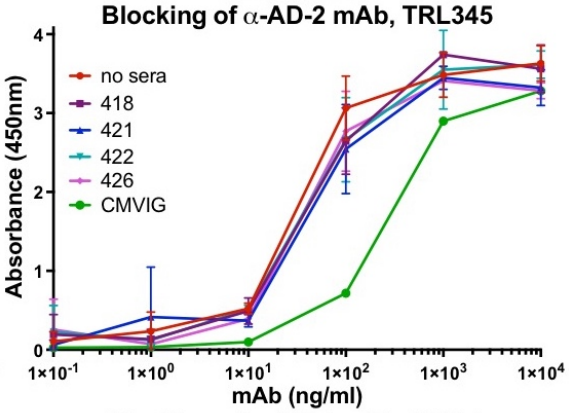

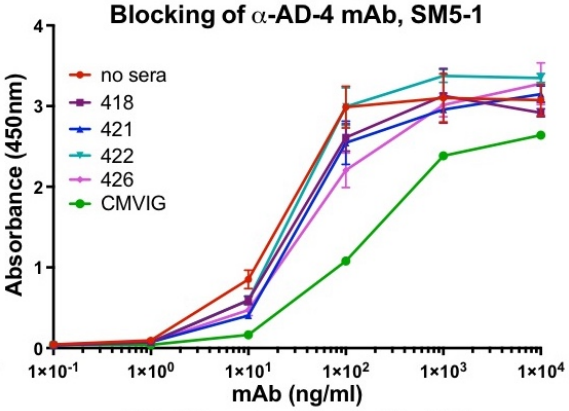

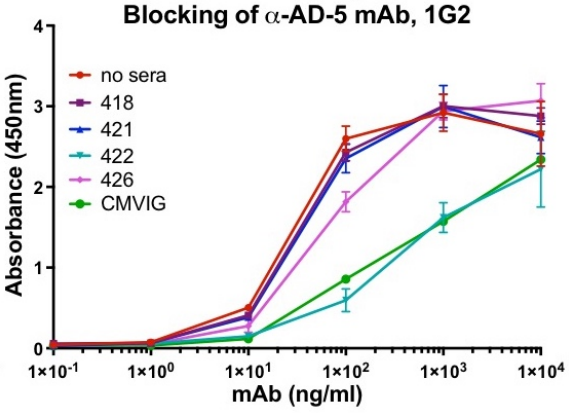

Samples 616, 617, 622, and 624:

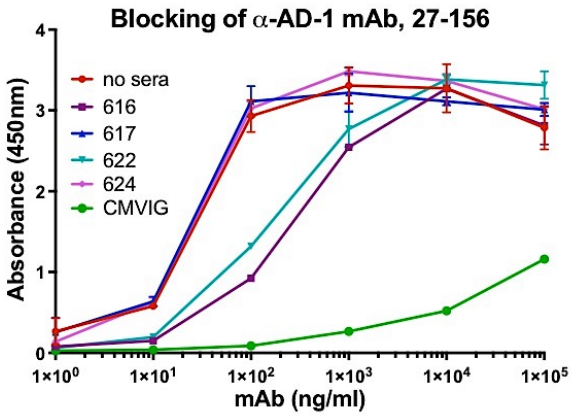

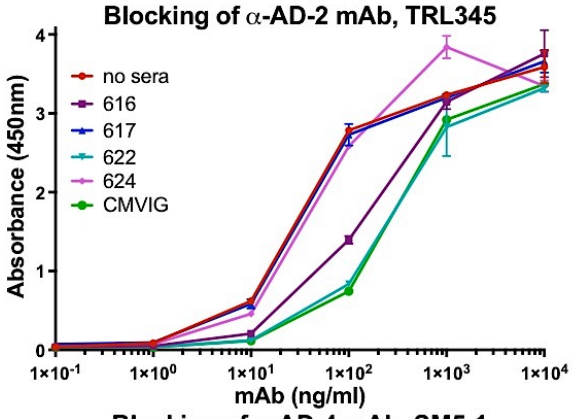

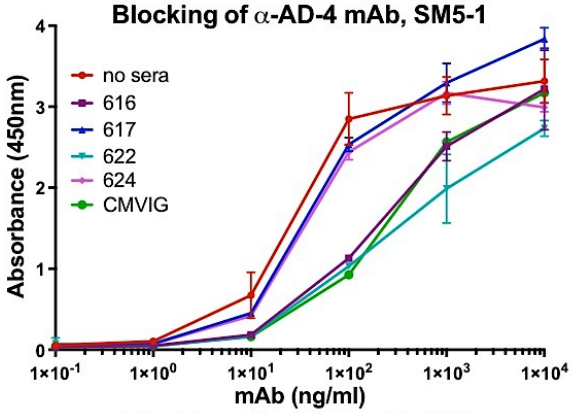

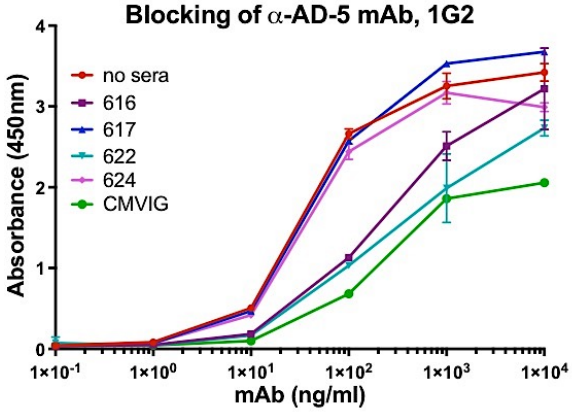

Samples 626, 627, 701, and repeats:

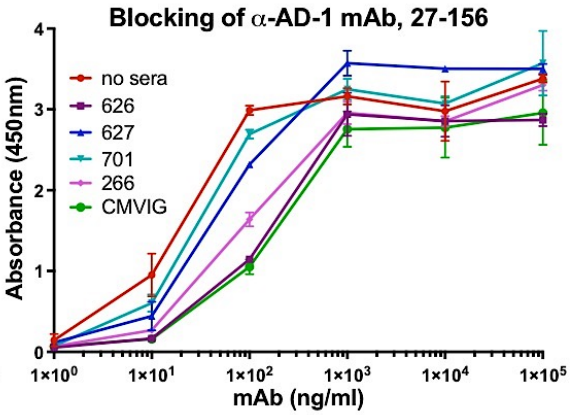

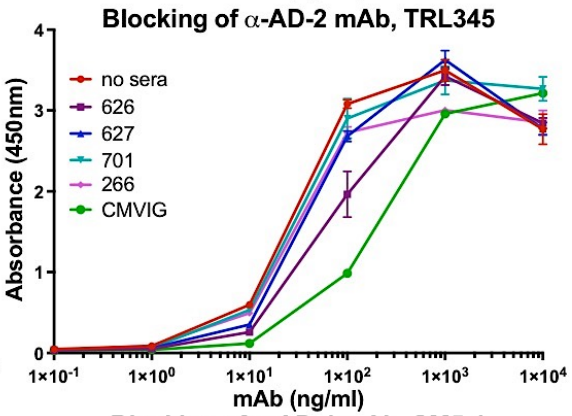

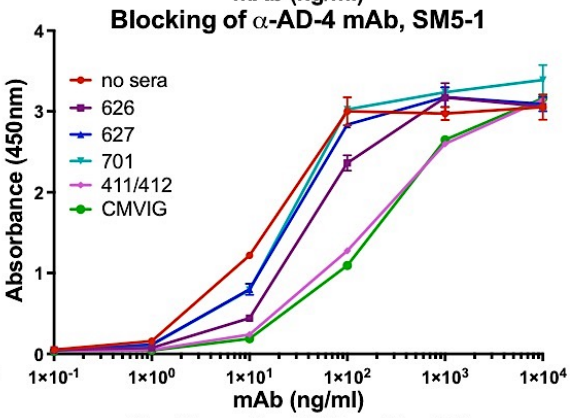

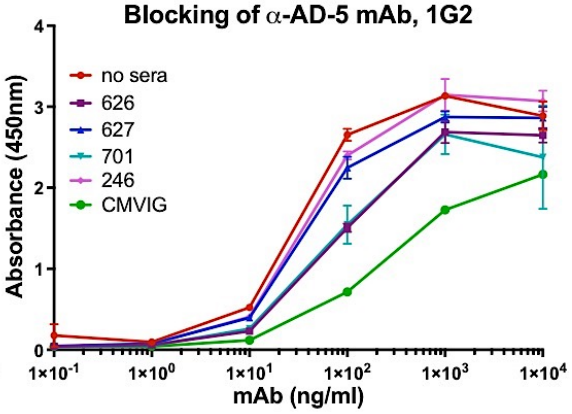

Figure 5.3. Antibody Blocking ELISA Curves (previous 5 pages). Four samples were tested per ELISA plate and are grouped as such. Graphs of blocking ELISAs showing the curve of blocking mAb (AD-1-5) are tiled with anti-AD-1 (27-156) in the top left, anti-AD-2 (TRL345) in the top right, anti-AD-4 (SM5-1) in the bottom left, and anti-AD-5 (1G2) in the bottom right. The no sera control from which the level of percent blocking was calculated is always red while the CMVIG positive control is always green. Graphs created in Prism (GraphPad).

Figure 5.4. Percent blocking by Sera (following page). Bar graphs comparing the level of blocking for the complete set of mAb organized by sera samples calculated as described in Materials and Methods. Red bars indicate anti-AD-1 mAb blocking (27-156). Orange bars indicate blocking of anti-AD-2 mAb (TLR345). Green bars indicate anti-AD-4 mAb blocking (SM5-1). Blue bars indicate blocking of anti-AD-5 mAb (1G2). Prism was used to calculate Kd and graph (GraphPad).

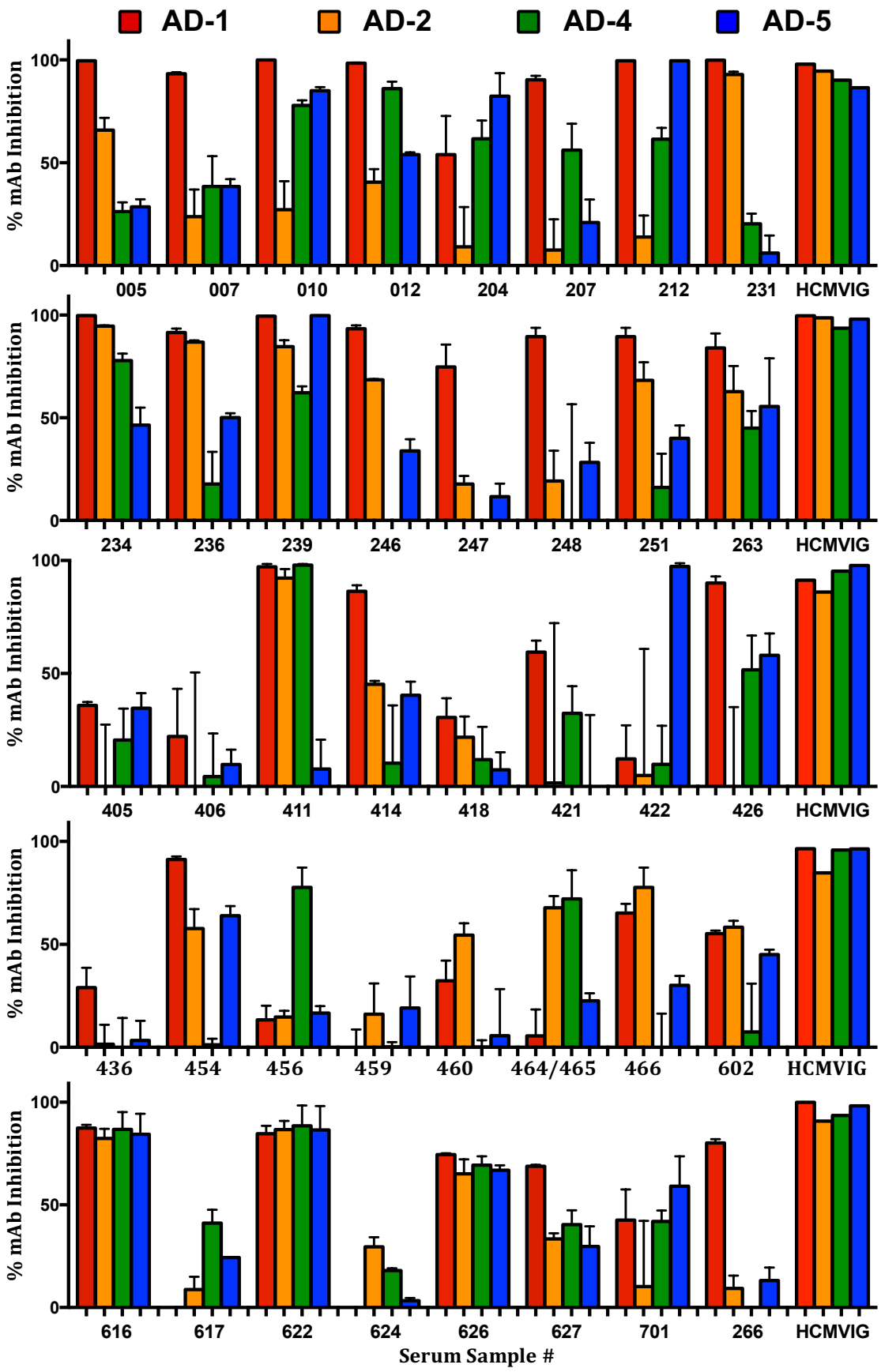
AD-1
AD-2
AD-4
AD-5
% mAb Inhibition
100
50
0
005
007
010
012
204
207
212
231
HCMVIG
234
236
239
246
247
248
251
263
405
406
411
414
418
421
422
426
436
454
456
459
460
464/465
466
602
616
617
622
624
626
627
701
266
Serum Sample #

5.2.4. Infant outcome

The outcomes of the infants are also listed in Table 5.2. Viruria (V) as an outcome indicates HCMV was detected in the urine of the infant, and thus, the infant was infected. Viruria is considered the most conclusive method of confirming HCMV infection. All infants in the study were shown to be negative for viruria at the time of birth, establishing that they were not congenitally infected while in the womb. The infants had possible exposure to HCMV during birth, through their mother's breast milk, or from multiple blood transfusions, many of which were HCMV positive. Seven infants tested positive for viruria after birth indicating they were infected with HCMV. Another possible outcome is a positive ELISA test at six months of age (E) which demonstrates the infant was infected and mounted an immune response to HCMV once its immune system matured. There were five infants that had anti-HCMV antibodies at six months, indicating seroconversion and infection. Four of these infants also tested positive for viruria. One infant only had a positive ELISA test, bringing the total number of infected infants to eight. The infants can also display symptoms of HCMV syndrome which means that after a positive viruria result, the infant suffered some indication of disease such as fever, leukopenia, thrombocytopenia, hepatitis, cerebritis, and pneumonia [57]. Six of the seven viruria positive infants also had HCMV syndrome. Viruria and syndrome are thought to be indicators of high viral load while a positive ELISA test alone is thought to be an indicator of low viral load. One infant (#247) died after eight days without confirmation of HCMV status, thus was removed from our correlational analysis.

5.2.5. Trends in antibody protection

Finally, maternal serum antigenic specificity was tested for correlation with protection from HCMV disease in the neonates. The percentage of blocking of the maternal sera samples were grouped by infected versus non-infected infants and viruria versus no viruria and plotted (Fig. 5.5). A Welch's t test was used to determine the P values to test if there was a difference between the two groups for blocking of each mAb. No significant difference was observed, but AD-1 did have the lowest P values with both infection and viruria. The average blocking of mAbs against AD-1, AD-2, and AD-4 was greater in the maternal samples of infected infants than the non-infected infants suggesting that none of these antibodies are beneficial for protection if they have any effect at all. However, the average AD-5 blocking was greater in the maternal samples of infants with viruria than the average of those without viruria. This suggests there may be some protection from anti-AD-5 antibodies, although the significance of this is low.

A.

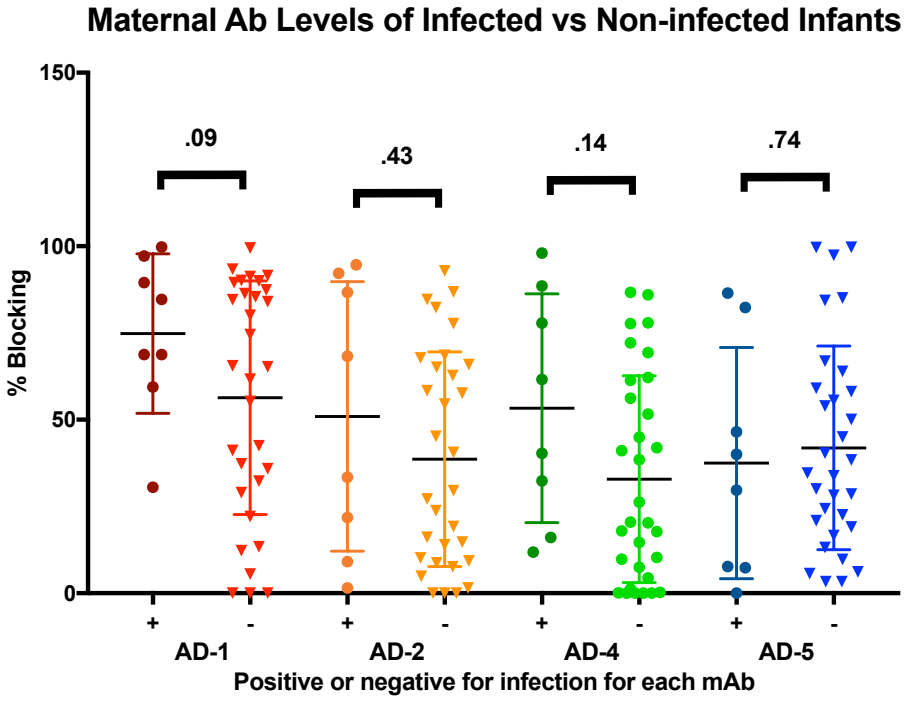

B.

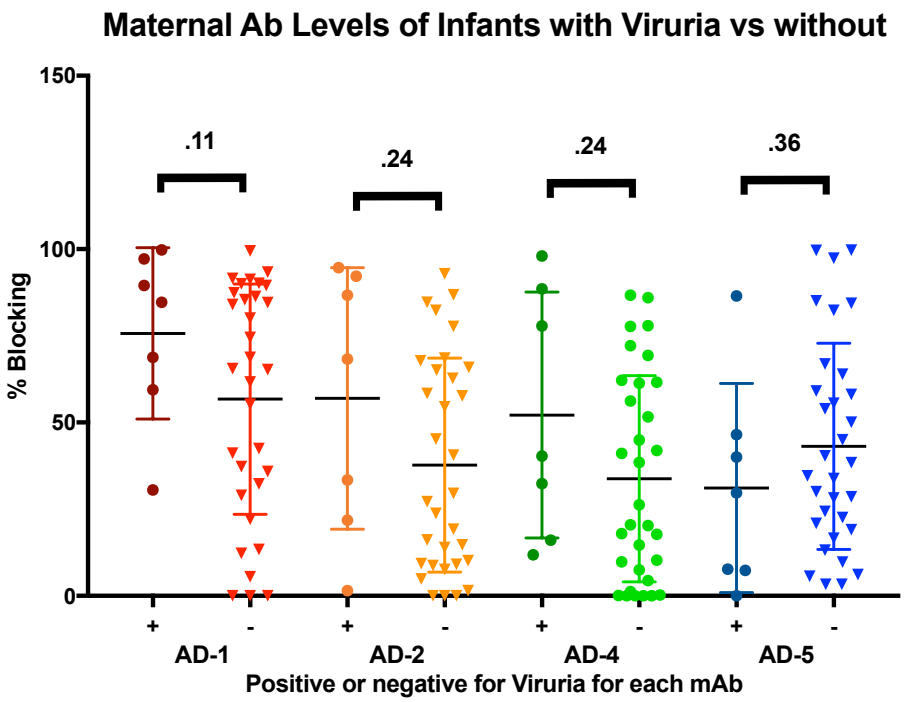

Figure 5.5. Blocking of Anti-AD Antibodies Grouped by Infant Infection Status. Blocking levels of mAbs by maternal serum samples were grouped and plotted by their infant's infection status, **(A)** infected (circles) versus non-infected (triangles) and **(B)** positive viruria (circles) versus negative viruria tests (triangles). Anti-AD-1 mAb blocking is shown in red, anti-AD-2 mAb blocking is shown in orange, anti-AD-4 mAb blocking is shown in green, and anti-AD-5 mAb blocking is shown in blue. Welch's t test comparing +/- is displayed above each pair. Graphs and analysis were done using Prism (GraphPad).

The results of the ELISA experiments are noisy, and some low-level blocking may be due to this giving a false positive for the presence of antibodies against a specific domain in the maternal sera. Samples with greater than 50% blocking tend to have distinctly different curves compared to the no-blocking buffer controls. To test for a correlation with moderately to strongly blocking samples, a Fisher's exact test calculator

(graphpad.com) was used to determine two-tailed P values for each AD with infection and each of the three sub-outcomes, ELISA, viruria, and syndrome (Table 5.3). None were statistically significant likely due to low sample size; however, there were two observed trends identified with P values ranging from 0.07 to 0.22 ($P < 0.05$ considered significant). The first and stronger trend involved anti-AD-1 antibodies. The sera of the mothers of all five infants with a positive ELISA test at six months of age blocked the anti-AD-1 mAb binding by more than 50% with a P value of 0.14. The six infants with HCMV syndrome all had mothers whose sera blocked the anti-AD-1 mAb binding by more than 50% as well. This provided the lowest P value (0.07) of the set indicating a possible correlation between the presence of anti-AD-1 antibody in maternal sera and a positive HCMV syndrome in infants which means the presence of anti-AD-1 antibodies may be detrimental to protection from disease. This correlational trend did not hold for viruria due to one infant who was infected without despite low levels of maternal anti-AD-1 antibodies (#418), giving a P value of 0.39 for viruria and P value of 0.22 for overall infection. The mother had little blocking capacity for any of the four mAbs (7.4-30.6%), although she did have high anti-gB levels in her serum. She may have anti-AD-1 antibodies that are not blocked by 27-156, or the infant may not have had adequate HCMV exposure to cause infection. The infant was not breastfed by its mother so it was not exposed by that mood, though it did receive 108.6 units of HCMV positive blood. Regardless of the reason, the HCMV infection in the infant did not progress to disease as the other six viruria positive infants did which means the correlational trend between anti-AD-1 antibodies and HCMV disease is not affected by this infant.

The second trend identified indicated the possibility of a correlation between the presence of anti-AD-5 antibodies and protection from viruria. Six of the seven infants that tested positive for viruria had <50% blocking of the anti-AD-5 Ab, giving a P value of 0.22 which again, is not statistically significant possibly due to low sample size. This suggests that AD-5 antibodies may be correlated with protection from infection. The one remaining infant with viruria (#622) had all markers of disease (viruria, +ELISA, and syndrome), yet the mother had high levels of antibodies against each AD. The infant was not protected by its mother's antibodies despite being breastfed. The mother of the eighth infected infant (#204) who only had a positive ELISA test, also had high levels of anti-AD-5 Abs. A closer examination of these infants' maternal antibody repertoire revealed that the level of anti-AD-1 antibodies was >50% in both. Thus, the lack of protection by anti-AD-5 antibodies in those two infants could have been caused by the presence of anti-AD-1 antibodies. Thus, I hypothesize that the two trends may work against each other, with the negative effect of anti-AD-1 antibodies on protection being stronger than the positive effect of anti-AD-5 antibodies. Nevertheless, a larger sample size would need to be tested to confirm these correlations.

Sample #	*α-gB*	*α-AD-1*	*α-AD-2*	*α-AD-4*	*α-AD-5*	*Outcome*
005	Low	+	++	+	+	-
007	Low	+	-	+	+	-
010	Mid	++	+	+++	+++	-
012	High	+++	+	+++	++	-
207	Mid	++	-	++	-	-
212	High	+++	-	++	+++	-
231	Low	+++	+++	-	-	-
236	Mid	+++	+++	-	++	-
239	High	+++	+++	++	+++	-
246	Mid	+++	++	-	+	-
247	Low	++	-	-	-	D – 8 days
248	Mid	+++	-	-	+	-
263	Mid	+++	++	+	++	-
405	Mid	+	-	-	+	-
406	High	-	-	-	-	-
414	High	+++	+	-	+	-
422	High	-	-	-	+++	-
426	High	+++	-	++	++	-
436	Low	+	-	-	-	-
454	Mid	+++	++	-	++	-
456	Low	-	-	+++	-	-
459	Low	-	-	-	-	-
460	Low	+	++	-	-	-
464	Low	-	++	++	-	-
466	Low	++	+++	-	+	-
602	Mid	++	++	-	+	-
616	Mid	+++	+++	+++	+++	-
617	ND	-	-	+	-	-
624	Low	-	+	-	-	-
626	Low	++	++	++	++	-
701	High	+	-	+	++	-
266	High	+++	-	-	-	-
204	High	++	-	++	+++	E
418	High	+	-	-	-	V
627	High	++	+	+	+	V/S
234	High	+++	+++	++	+	V/S
421	Low	++	-	+	-	E/V/S
411	Mid	+++	+++	+++	-	E/V/S
622	Mid	+++	+++	+++	+++	E/V/S
251	Mid	+++	++	-	+	E/V/S
<50%		13	21	23	24	V – 7
>50%		25	17	15	14	E/S – 5

Table 5.2. Levels of mAb blocking and outcome of premature infants. Results from the anti-gB ELISAs are categorized as low = <9999, mid (midrange) = 1000-2999, or high = >3000. Results from the blocking ELISAs are categorized as none = 0-24.9% blocking (-), low = 25-

49.9% blocking (+), moderate = 50-74.9% blocking (++), and strong = 75-100% blocking (+++). The outcome of the premature infants includes: positive infant ELISA at six months (E), viruria (V), HCMV syndrome (S), or no infection (-). Totals of none to low (<50%) and moderate to high (>50%) and the number of infants with each outcome are listed at the bottom of each column.

AD of mAb	Viruria	+ELISA	Syndrome	Infection (all)
AD-1	0.3863	**0.1392**	**0.0705**	**0.2179**
AD-2	1	1	0.679	0.7089
AD-4	0.6857	0.3289	0.6472	0.4237
AD-5	**0.2159**	1	0.3758	0.4499

Table 5.3. Summary of significance. To test for a correlation with protection, two-tailed P values were calculated for each antigenic region versus infant outcome using a Fisher's exact test 2x2 calculator (GraphPad). Lowest P values are bold.

5.2.6. Prefusion model of HCMV gB

AD-1 and AD-5 are on opposite ends of gB in the postfusion structure [210, 211] and anti-AD-1 antibodies are unlikely to be able to interfere with AD-5 antibodies in this conformation (Fig. 5.6). This is most likely not the case in the undetermined prefusion conformation. In fact, the prefusion conformation of the type III viral fusogen, VSV G, is folded in such a manner that DIV and DI are next to each other [151]. A homology model of HCMV prefusion gB was generated by Samuel Stampfer based on the postfusion gB structure and the prefusion VSV G structure (unpublished results). This predicts that DIV and DI also are oriented next to each other in HCMV prefusion gB, consistent with the interference of anti-AD-1 antibodies with anti-AD-5 antibody protection from infection.

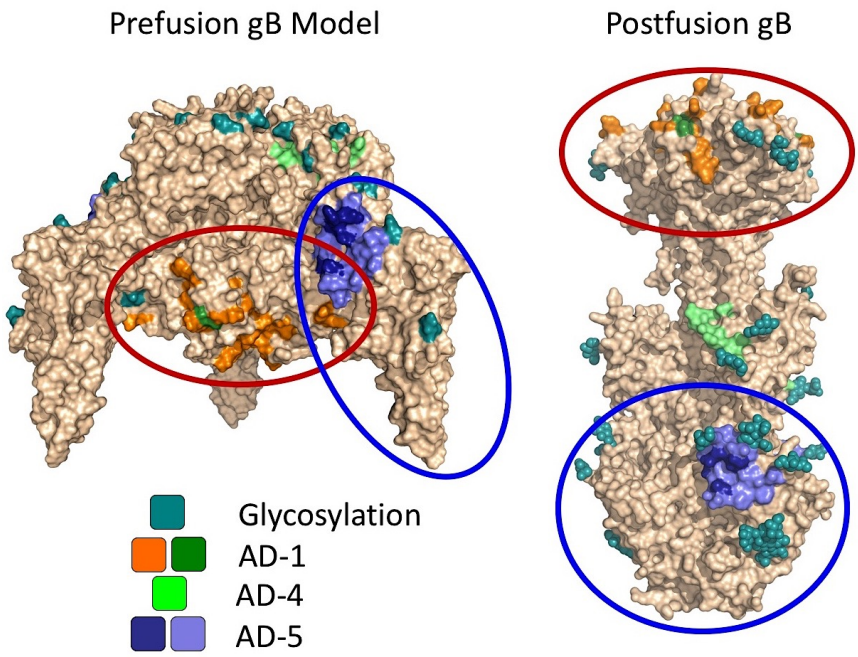

Figure 5.6. The orientation of AD-1 and AD-5 on a Prefusion Model Compared to the Postfusion Structure. A prefusion model (left) was generated based on the prefusion structure of the type III fusogen, VSV G, using the coiled-coiled stem for initial alignment (Stampfer, unpublished results). The postfusion structure (right) for comparison of AD-1 and AD-5 domain rearrangement. Orange circles AD-1 while blue circles AD-5. Residues important for binding are colored as indicated.

5.3 Discussion

Two trends were identified in this study. First, the presence of anti-AD-1 antibodies correlated with infant seroconversion at six months of age and with HCMV disease. Second, anti-AD-5 antibodies correlated with protection from viruria. While both trends were statistically insignificant, it was likely not possible to obtain significance due to low sample size. Furthermore, the outcome of one infant did not follow the positive anti-AD-5 antibodies trend. An antagonistic effect seems to be playing a role in this contradiction. We observed that if both anti-AD-1 and AD-5 antibodies are present, there

is no protection from infection (2/8 infected infants). It is interesting that the infant whom only had seroconversion and no other indication of HCMV disease had stronger blocking of the anti-AD-5 antibody than of the anti-AD-1 antibody which may have led to protection from disease rather than infection. These numbers are far too low to demonstrate this antagonistic effect conclusively, yet the trend is intriguing. It suggests that anti-AD-1 antibodies interfere with anti-AD-5 antibodies. While the two antigenic regions are opposite ends of postfusion gB [210, 211], a prefusion model predicts the antigenic regions are adjacent. This is the case in the prefusion conformation VSV G, another type III viral fusogen [151]. However, DIV (referred to as DI in VSV G) is located on the underside of the prefusion structure and may be obscured by the viral envelope. If prefusion HCMV gB adopts a similar fold, it is unclear how the anti-AD-1 antibodies bind can bind DIV unless they can access the domain from the sides. If binding cannot occur with prefusion gB, the anti-AD-1 antibodies may bind a fusion intermediate, allowing the larger proportion and variety of non-neutralizing anti-AD-1 antibodies displace the anti-AD-5 antibodies at that stage.

Another possible explanation for the infection of infants #418 and #622 is that the mothers may have had high viral loads at the time of the study which overwhelmed the anti-AD-5 antibody protection. While only maternal serum samples and not viral loads were not taken at the time of birth, high antibody titer has been correlated with high viral load indicating replicative infection. Thus, the overall high level of blocking and anti-gB antibodies in the two maternal samples could indicate that the mothers were actively generating many HCMV particles at the time of the study and were more likely to expose their infants to HCMV. This could have counteracted any protection afforded by anti-

AD-5 antibodies, although the low significance level could simply be due to a lack of a correlation.

If the protective trend holds true with a larger sample size, it would have interesting implications in the use of anti-AD-5 antibodies as a therapeutic for those already infected and could explain the modest efficacy of CMVIG. Anti-AD-5 mAbs may not provide protection in seropositive transplant patients due to anti-AD-1 antibodies generated by the patient. The usefulness in preventing congenital infection may also be limited as the mother likely will provide anti-AD-1 antibodies to the fetus as well. It does give valuable information for recombinant vaccine design, however. It speaks to the importance of preventing the development of anti-AD-1 antibodies with gB based vaccine. This could be accomplished by using the viral strategy of blocking immune recognition with glycosylation. A recombinant protein could be engineered with the surface of the DIV crown coated in a thick glycan shield, inhibiting recognition while still maintaining the structure of the protein. The glycans may interfere with the prefusion conformation, but if protective antibodies recognize both pre- and postfusion as neutralizing anti-AD-5 antibodies must, effective immunization would still be possible.

These results provide valuable insights into the determinants of protection of antibodies against gB. The strong antagonistic effect that antibodies have on the immunodominant DIV has major implications when considering using mAbs as therapeutics. While the protective capacity of antibodies against DI are encouraging, particularly for seronegative patients. A larger study is needed to confirm these trends, yet they can be taken into consideration when rationalizing the results of CMVIG prophylaxis studies or establish a plausible hypothesis for additional studies.

Chapter Six: Pentamer Expression

6.1. The pentameric complex

The HCMV pentameric complex formed by gH/gL/UL128/Ul130/UL131 is required for entry into monocytes via micropinocytosis, and endothelial and epithelial cells via endocytosis in a pH-dependent manner [106]. They are selected against in fibroblasts, thus "laboratory" strains that have been passaged extensively in fibroblasts contain one or more loss-of-function mutations in UL128, UL130 or UL131 [81, 106, 224]. "Clinical" strains, such as Merlin and TR, have been minimally passaged in fibroblasts and the genes for the pentamer are intact. The pentamer is thought to be responsible for binding a cell-type-specific receptor, leading to viral entry, but no receptor has been found. Structural information may provide hints to the identity of the receptor through structural homology. While the structure of HSV-2 and EBV gH/gL are available, HCMV gH and gL have low sequence identity with these homologs and UL128, UL130, and UL131 are HCMV specific, thus a homology model cannot be generated. Only limited structural information from biochemical assays were available at the onset of this work. They included the observation that all members of the pentamer must be present and functional for the complex to exit the ER. gH is disulfide bonded to gL and UL130 is disulfide bonded to UL131 [116]. gH, gL, UL130, and UL131 are predicted to have one or more glycosylation site [116, 123].

6.2 Results

6.2.1. Attempts to express gH/gL in insect cells

To generate glycosylated HCMV gH/gL heterodimer in soluble form, the Baculovirus expression system was initially used. A dual Baculovirus construct

(pFastBacDual::TRgH-His_8/gL – pHB1) was engineered to express gH and gL simultaneously in SF9 insect cells. All sequences used in this study were obtained from the "clinical" strain TR to ensure no selection against any of the pentameric proteins. The transmembrane and cytosolic domains of gH were truncated to express the gH ectodomain (residues 1-718), and a C-terminal 8-Histadine tag (His_8) was added to enable affinity purification. gL (residues 1-286) was expressed in its entirety. The endogenous signal sequences were preserved in both gH and gL. Although the heterodimer was expressed and secreted (Fig. 6.1), the overall expression level and the yield of purified protein were too low, ~0.03 mg per 1 L Sf9 cells, and the final preparation had too many impurities for crystallographic studies.

Expression of HSV-2 gH/gL in soluble form in drosophila (S2) cells generates ~10-fold more protein than expression in SF9 cells [225]. Thus, gH (1-718) and gL (1-286) were cloned into plasmids designed for stable S2 cell transfection, this time with a PreScission protease site (PP) (LEVLFQ) before the His_8 tag (pMT/BiP/V5-His::gH-PP-His_8 - pHB12 and pMT/BiP/V5-His::gL – pHB13). Several transfection ratios of gH and gL were tried, but only gL was expressed while no gH expression was detected. gL was found only in the intracellular fraction (Fig. 6.1C). Since both gH and gL are required for proper folding of the other, it is not surprising that gL was not secreted in the absence of gH. The constructs were confirmed by sequencing to be correct. Because the proteins are not encoded on the same plasmid, there is no way to ensure that they are expressed in a molar ratio as is the case with the pFastBacDual plasmid. The same selective pressure is used to keep both plasmids in transfected S2 cells. gL is smaller, thus, cells may simply favor maintaining the gL construct. Additionally, it has been shown recently that gL is

disulfide bonded to gO or UL128 and mutation of the cysteine (C144) involved in this disulfide bond is required to obtain gH/gL alone [117]. It is likely that the additional binding partners (gO or UL128/130/131) are required for proper folding of gH/gL and gH/gL cannot be secreted on their own in sufficient quantities.

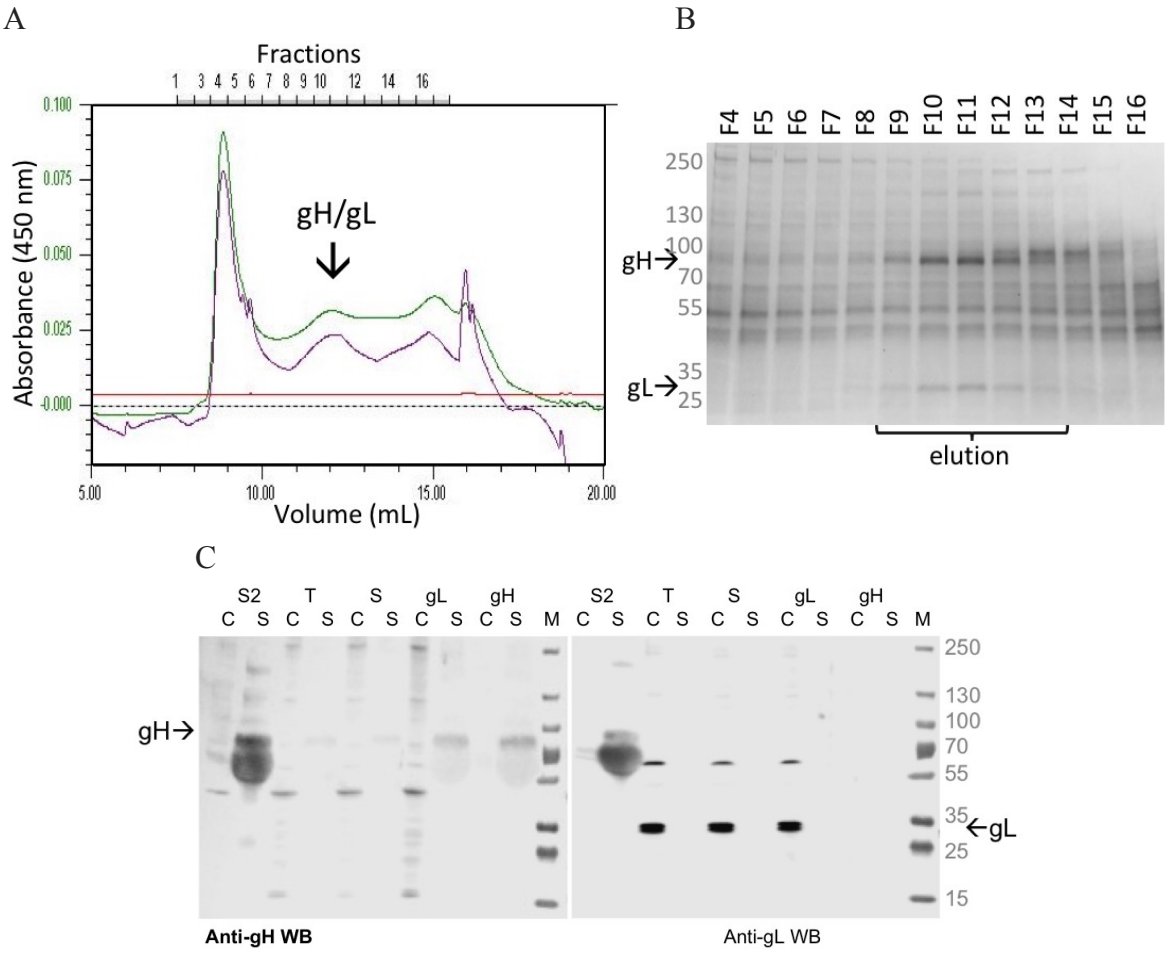

Figure 6.1. Expression and Purification of TR gH/gL. (A) Gel filtration spectrum of TR gH/gL after expression in insect cells. (B) Fractions 4-17 were collected and run on a Coomassie gel under reducing conditions. gH migrates at around 90 kDa and gL migrates at around 30 kDa. (C) gH/gL transient and stable transfection of S2 cells. Anti-gH and anti-gL western blots of stably and transiently transfected S2 cells. C = cells, S = supernatant, M = marker. gH should ~95 kDa with glycosylation and gL is ~33 kDa. gH is not expressed. gL is expressed, but not secreted.

6.2.2. Attempts to express UL128, UL130, and UL131 in E. coli

Plasmids containing UL128, UL130, and UL131 codon optimized for *E. coli.* with N-terminal solubility tags (GST or His_6-SUMO) (pHB3 = pGEX-6P-1::GST-UL130, pHB4 = JP4:: His-SUMO-UL130, pHB5 = pGEX-6P-1::GST-UL128, pHB4 = JP6:: His-SUMO-UL128, pHB7 = pGEX-6P-1::GST-UL131, pHB8 = JP4:: His-SUMO-UL131) were individually transformed into *E. coli* (T7-Express) for expression. Both UL128 and UL130 were present primarily in the insoluble cellular fractions, whereas a small proportion of UL131, containing an N-terminal His_6-SUMO tag, was present in the soluble fraction (Fig. 6.2A-C). This soluble UL131 aggregated, eluting in the void of the size exclusion chromatography (SEC) column S200 (Fig. 6.2D).

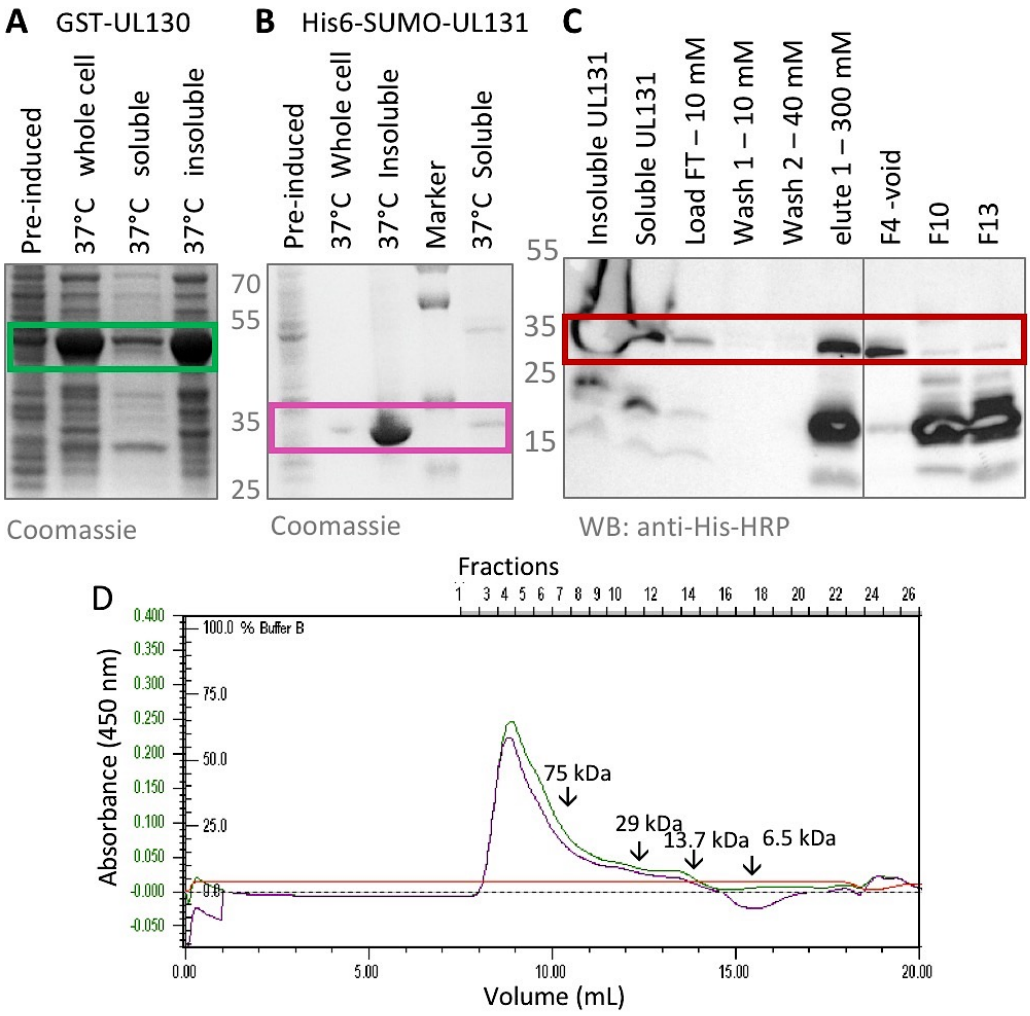

Figure 6.2. Expression and purification of UL130 and UL131. (A) UL130 with a GST tag was expressed in T7-express. The green box indicates the predicted size of GST-UL130 when run on an SDS-PAGE Coomassie gel (48.5 kDa). (B) UL131 with a His6-SUMO tag was expressed in T7-express and samples were run on a Coomassie stained gel. The pink box indicates the predicted size of His6-SUMO-UL131 (31.7 kDa). (C) Samples of His6-SUMO-UL131 were taken at each stage of purification, ran on an SDS-PAGE gel and Western blotting (WB) was performed using an anti-His antibody. The predicted position of His6-SUMO-UL131 is boxed in red (36.6 kDa). Various mM levels indicate imidazole concentrations. The lower band ~16 kDa is likely the His6-SUMO tag. (D) The spectra of His6-SUMO-UL131 run over SEC. Gel filtration

standards for the column are marked.The major peak is the void indicating the protein was aggregated.

The cytosol of *E. coli* is a reducing environment. Since UL128 is a putative CC chemokine, reduction of the two CC disulfide bonds is likely important for proper folding [18]. To favor formation of disulfide bonds during expression and to achieve proper folding, I took advantage of the *E. coli* strain Origami, which has an "oxidizing" cytosolic environment due to knocked out thioredoxin/glutaredoxin reductase pathway. Unfortunately, UL128 expression in Origami *E. coli* resulted mostly in insoluble protein as well (Fig. 6.3).

Many chemokines have been purified by extracting them from the insoluble fraction with guanidine hydrochloride (Gdn-HCl), relying on the disulfide bonds to keep aid in refolding of the protein [21]. This was attempted with the insoluble fraction of UL128 generated by expressing His6-SUMO-UL128 in Origami cells. The insoluble fraction was suspended in 6 M Gdn-HCl, then dialyzed to 2 M Gdn-HCl. The Gdn-HCl was decreased slowly by dialysis to varying Gdn-HCl molarities, yet His6-SUMO-UL128 still precipitated once the Gdn-HCl concentration is lowered below 0.75 M. To rule out the possibility that the His6-SUMO tag was disrupting the folding of UL128, a PreScission Protease site was introduced between the tag and UL128 and refolding experiments were repeated. Unfortunately, PreScission Protease loses activity in 0.75 M Gdn-HCl or above, the point at which His-SUMO-UL128 precipitates (Fig. 6.3). Thus, pure soluble UL128 was also not obtained through re-folding.

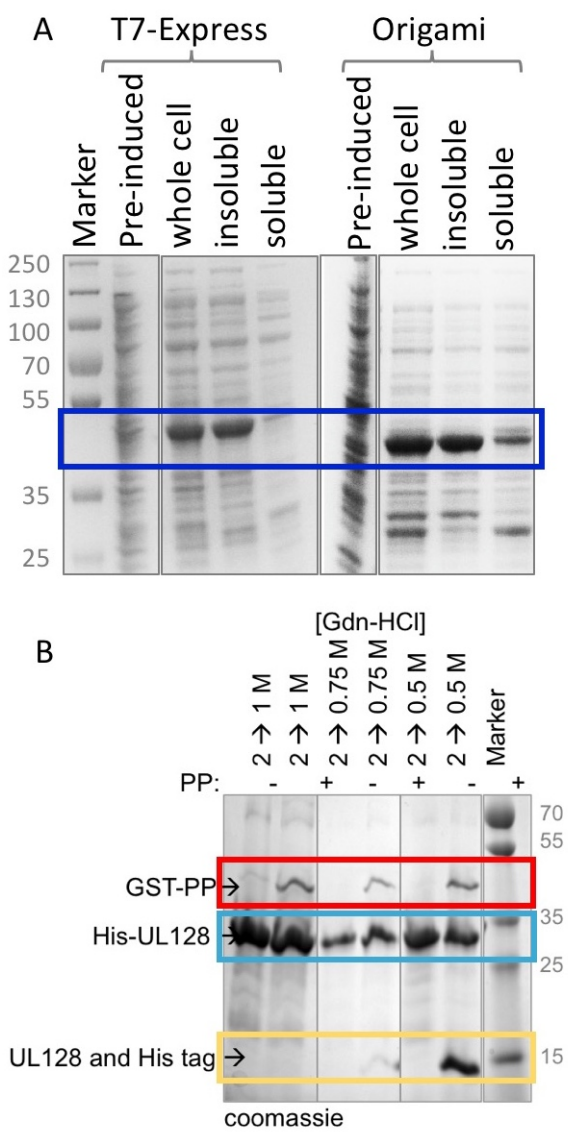

Figure 6.3. UL128 Expression and Refolding. A) UL128 expression in *E. coli*. GST-UL28 were expressed in reducing *E. coli* (T7- express) and oxidizing *E. coli* (Origami) at 18°C overnight. Insoluble and soluble fractions of bacterial lysates were run on a 12% SDS page gel and stained with Coomassie. GST-UL128 runs at 41.1 kDa. (blue box). Numbers to the left indicate the size of protein standards in kDa (B) To refold insoluble UL128, Ni-NTA purified His-SUMO-UL128 in 6 M Gdn-HCl was dialyzed to 2 M Gdn-HCl, then further dialyzed to 1 M, 0.75 M, and 0.5 M Gdn-HCl. The protein began to precipitate at 0.75 M Gdn-HCl with ~3/4 precipitated at 0.5 M Gdn-HCL. Samples were taken, then the tag was cleaved with PreScission Protease (PP) to test the activity of PP under various Gdn-HCl concentrations. Again, samples were run on a 12% gel and stained with Coomassie. GST-PP - 46 kDa (red box), His-SUMO-UL128 - 28 kDa, UL128 (teal box) and His-SUMO - 14 kDa (yellow box). Numbers on right indicate kDa.

6.3 Discussion

The pentamer formed by gH/gL/U128/UL130/UL131 is a large complex with post-translational modifications and several types of interactions holding the complex

together. This complexity may prevent the proper expression and folding of individually expressed proteins or in foreign expression systems such as *E. coli* rather than in mammalian cells. UL130 is predicted to be glycosylated, and this posttranslational modification may be essential for UL130 folding and function [20]. Additionally, UL130 and UL131 have been shown to be disulfide bonded [22]. Expressing these proteins together in insect or mammalian cells may be necessary to provide these post-translational modifications and bonds.

Despite being expressed in the *E. coli* Origami strain, UL128 may not be forming the correct characteristic CC chemokine disulfide bonds, which would cause it to misfold. Given that there are nine cysteines present in the molecule, the probability that incorrect cysteine pairs would form is high. UL128 may also need to be expressed in insect cells or mammalian cells to improve the likelihood of proper disulfide bond formation and increase solubility. Recently, a low-resolution EM reconstruction of the pentamer was published [117]. Using mass spectrometry (MS), the study also revealed that UL128-C162 forms a disulfide bond with gL-C144. Moreover, the authors found that all five proteins had to be expressed together in mammalian cells to obtain the complex [117]. This finding is supported by the observation that all protomers of the pentamer must be expressed and intact, or the remaining proteins are retained in the ER [12]. Additional attempts at determining the crystal structure of the pentamer should build on this information to improve the likelihood of doing so. The presence of UL128/UL130/UL131 or gO may be necessary for proper folding of gH/gL which has recently been shown to rarely be present on the viral envelope alone [114]. This could explain why gL was not secreted from S2 cells despite expression.

An EM reconstruction of gH/gL/gO was presented alongside that of the pentamer which indicated that gO binds gH/gL in the same location as UL128 [117]. Furthermore, MS analysis indicated gO form a disulfide bond with the same gL cysteine (C144), making the two complexes mutually exclusive [117]. A human neutralizing antibody, MSL-109, was used to stabilize gH/gL alone and a negative stain EM reconstruction of the gH/gL/MSL-109 complex was also determined. The gH/gL heterodimer forms a homodimer of gH/gL heterodimers when the binding partners gH/gL are not present. The two heterodimers (with MSL-109 attached) bind each other in the same location as gO and UL128, forming a disulfide bond between the two unpaired C144 in gL. This suggests that bonding of C144 is required for proper folding of gH/gL. The binding of both complexes at the same location explains why a complex with all six proteins is never observed and why altering the amount of one complex, through deletions or expression in the preferred cell type, alters the amount of the other. For example, gH/gL/gO becomes abundant when mutations arise in UL128, UL130, or UL131 [110]. This is reminiscent of the mechanism of cell type receptor specificity achieved with by EBV using the gH/gL binding partner, gp42. gp42 in complex with gH/gL, binds the B-cell receptor HLA-DR [53, 57, 58]. Additionally, gp42 binds the same location at which gH/gL binds integrins for entry into epithelial cells making these interactions mutually exclusive [59]. Replication in B-cells sequesters gp42, priming the virions for epithelial cell entry. A similar mechanism could be occurring with the mutually exclusive HCMV gH/gL complexes. Additional studies are needed to elucidate this mechanism, yet it has already been noted that the cell type HCMV replicates in alters the proportion of gH/gL/gO and pentamer on the viral surface [114]. As gH/gL and the complexes they

form are major neutralizing immunogens and targets for vaccines and mAb therapeutics, obtaining the crystal structure of both complexes is of great value. Given the right resources such as a high-throughput mammalian expression system and complex specific mAb for stabilization, obtaining such a structure is a feasible goal.

Chapter Seven: Discussion

7.1 Significance of Work

7.1.1. gB is the HCMV Fusogen with Species-Specific Functions

The structure of the gB ectodomain confirms gB is the fusogen of HCMV, as suggested by homology with the HSV and EBV gB fusogens, despite low sequence identity. Like the gB homologs, expression and crystallization of the HCMV gB ectodomain generated the stable postfusion structure. The disulfide bonds are conserved between the three homologs as are the individual domains. The domains are orientated differently in relation to one another giving a unique twisted in each of the homologs, suggesting structural plasticity. This plasticity may accommodate species-specific gB functions while still maintaining the ability to interact with gH/gL and perform membrane fusion.

One structural aspect not shared by the three homologs is partial cleavage at a conserved furin cleavage site. This site is present in EBV and HCMV, but not HSV. Proteolytic cleavage of viral fusogens or accompanying proteins is a method of fusion activation in class I and II viral fusogens. The deletion of the furin cleavage site in HCMV gB was not found to be detrimental to infection. However, the site is under positive selective pressure because the sequence varies between HCMV strains while remaining within the allowable variation of furin recognition (RRRK, RTKR, or RAKR). It could be that the lack of cleavage is not detrimental to entry, but that the mixed population of gB provided by partial cleavage affords some advantage. HSV-1 gB may be present in both the pre- and the postfusion forms on the viral surface [216, 226]. It may be that cleavage favors the postfusion form and the heterogeneity of cleavage encourages the heterogeneity of pre- and postfusion gB on the viral surface of HCMV gB as well. Clearly, cleavage is not required for the transition to the postfusion form as the

furin site was mutated in our gB construct, yet still, the structure represents the postfusion conformation. Another possibility is that cleavage of the disordered loop creates an additional, unstable region to interfere with immune recognition. The functional importance of DII, containing the disordered loop is suggested by the fact that the region elicits only neutralizing antibodies and is heavily glycosylated. Furthermore, the disordered loop is predicted to have three unresolved glycans in HCMV gB, two in EBV gB, and one in HSV gB, which also speaks to its functional importance. The heterogeneity of cleavage may produce multiple structural forms, further interfering with the immunogenicity of the domain.

HCMV gB has been suggested to bind cellular β1 integrins through a putative DL motif, aiding in cell surface attachment. This motif is partially buried in the postfusion structure, but two neighboring glycans suggest functional importance of the region as HCMV gB uses glycans to shield recognition of such areas. These glycans are not present on gB of HSV-1 or EBV, which is consistent with the species specificity of the putative function. Therefore, it remains a possibility that the DL motif is exposed in the prefusion conformation, allowing binding of integrins and requiring protection from immune recognition.

7.1.2. A Sugar Shield and Immune Decoy

HCMV gB is densely coated in sugar chains, or glycans, creating a shield that protects important functional regions which limit the ability of immune system to generate antibodies capable of preventing viral entry. Meanwhile, gB exposes regions lacking functional importance to direct antibody recognition to them, generating a

plethora of non-neutralizing antibodies. This tactic appears to be an even more effective with the identification of two opposing trends in gB-Ab protection. Antibodies that recognize the shielded DI or AD-5, which are presumed to be neutralizing, appear to provide protection against HCMV infection in patients. This protection may be overcome by primarily non-neutralizing antibodies against the glycan-bare DI or AD-1 which appears to be inversely correlated with protection from infection. Contrary to this finding, when initially identifying and characterizing AD-5, Poetzsch, et al. did not see a reduction in gB binding in competition experiments with AD-5 antibodies and a non-neutralizing, anti-AD-1 antibody, 1E5 [155]. This is not entirely surprising since they were using gB likely in the postfusion conformation with AD-1 and AD-5 on opposite ends of the protein. The anti-AD-1 antibody interference is more likely to occur on the prefusion or intermediate conformation, which by homology to VSV G, should place the two domains (DI and DIV) in proximity. It is interesting that they also did not observe a decrease in cell culture neutralization assays. There could be two explanations for this. First, cell culture neutralization may not mimic the complex human host immune environments. Second, the human immune system does not generate one type of antibody against an antigenic region. As Poetzsch, et al. also demonstrated, up to 50% of anti-gB antibodies in an individual bind AD-1 suggesting a variety or specificity is possible. Additionally, they showed the maturation of anti-gB antibodies occurs in an individual, which improves binding [155]. Therefore, the AD-1 antibody used in the competition assay may have had lesser affinity allowing AD-5 antibodies to bind unhindered or the variety of antibodies generated by an individual such as the mothers in this study overwhelms the few anti-AD-5 antibodies.

These trends were identified in immune-naive premature infants, therefore in the absence of cellular immunity [222]. This allows us to examine the impact of antibodies without the complications of other immune factors and models the effect of administering mAb therapeutics to a seronegative population. HCMV gH/gL and the complexes it forms are also major immunogens. Given that anti-gB and not anti-pentamer antibodies are capable of protecting placental precursor cells (TBPCs) [167].

7.1.3. Clinical significance

Human cytomegalovirus (HCMV) establishes lifelong infection in the majority of the population worldwide and causes disease in developing fetuses, neonates, and the immunocompromised such as HIV, cancer, and transplant patients. No vaccine is currently available and the standard of treatment, ganciclovir, has associated toxicity and an increasing prevalence of resistance [227-229]. CMV immunoglobulin (CMVIG) has shown some promise as a prophylactic but does not provide the protection level of ganciclovir and has related safety concerns. Thus, the treatment and prevention of HCMV represent a major unmet medical need (reviewed in [230]).

The HCMV fusogen, gB is a historical and ongoing recombinant protein vaccine candidate and target for monoclonal antibody therapeutics. This work informs such efforts by presenting the crystal structure of gB solved to a resolution of 3.6-Å. While the structure is the postfusion conformation, mapping of regions important in immune recognition was still possible, indicating that all antibodies isolated to date bind at least the postfusion state. Such findings have already greatly improved our understanding of the structural determinates of antigenic sites present on gB while providing a structural

framework for future findings. If the opposing anti-AD-1/anti-AD-5 antibody protection trends hold true, they will have drastic implications on the use of mAb therapeutics in current development. They argue for focusing efforts on AD-5, but suggest efficacy could be limited in anti-AD-1 seropositive patients.

7.2 Future Studies

7.2.1. The HCMV gB Structure

The postfusion structure of HCMV gB has proven to be a valuable asset in understanding the immunogenicity of the fusogen. However, to truly understand the mechanism of fusion and neutralization, the prefusion structure is needed. Many approaches for obtaining other prefusion structures have been tried with HSV gB without success [196], with the exception of locking gB in the prefusion conformation with a prefusion-specific antibody. Since all HCMV gB neutralizing antibodies currently known bind the postfusion conformation, this has not been a possibility. The modifications made to our current construct of gB drastically decreased rosette formation which could obscure structural regions shared by both prefusion and postfusion gB, thus improving its use in depletion of postfusion binding Abs. This, the newly produced, high-quality gH/gL/gO and the pentamer complex and gM/gN would allow discarding of neutralizing B-cells specific to these proteins and improve the likelihood of obtaining an anti-prefusion specific gB antibody. The prefusion structure would help understand antibody protection trends identified here and would provide a more protective, pre-action form of gB for use in recombinant vaccines.

Pending questions raised by the postfusion structure of gB include determining which ion is present in gB coiled-coil of the stem, though the relevance of this information is low. Co-IP's could be carried out with this gB construct to see if the postfusion ectodomain expressed can, if fact, bind β1 integrins [104, 159], although the structure suggests this is unlikely. Finally, the importance of furin cleavage of gB could be revisited. The conservation suggests that it has some beneficial role. While having no effect on entry [153], it may represent another mechanism of immune evasion. To test this, one could compare the binding of anti-AD-4 antibodies to completely cleaved gB and gB with the furin site removed to see if cleavage interferes with binding. This would be more conclusive if the binding of various anti-AD-4 antibodies was compared. This would require the isolation of more anti-AD-4 antibodies, as only one set is available, isolated from the same individual with overlapping epitopes [155]. Alternatively, one could repeat this experiment in HSV engineered with a cleavage site in the disordered DII loop to test the mechanism. More antibody epitopes are present on HSV gB, which lacks a cleavage site in the loop. Finally, furin site mutated viruses could be examined in an animal model to test if there is a decrease in the effectiveness of the immune response.

7.2.2. gB/Antibody Structure

To obtain the structure of gB in complex with the anti-AD-2 human neutralizing antibody TRL345 new truncations of gB N-terminus should be made. As suggested in chapter 4, residues V63 or V57 are promising truncation candidates based on sequence conservation. Ideal truncations would balance the need for high expression, crystal formation, and maintenance of the AD-2, site I. The former two were achieved through

truncation at Y78, thus adding 15-21 residues, which is not likely to be detrimental and obtaining the structure is feasible. The initial crystal hit from limited screening with a poor gB construct is encouraging. If additional truncations do not yield diffracting crystals, the structure of TRL345 in complex with the linear peptide could be obtained, though it would not be as informative. The peptide would not be glycosylated and therefore, no information would be gained on how TRL345 interacts with the two glycans in the epitope. It would not provide any information on for the anti-AD-2 site I antibody mechanism of neutralization because it would not have the informative interactions with gB as a whole. Another approach would be to make an N-terminal gB truncation with site II intact as well (residues 50-54). Since site II does not inhibit binding of site I, one could test if a site II antibody could stabilize the remaining part of N terminus. Finally, cry- EM could be used to determine a lower resolution structure which may answer some of these pending questions.

7.2.3. Maternal Antibody Protection

As stated, a larger sample size is needed to confirm the trends identified by this study testing the protective capacity of maternal antibodies. A new clinical study could be initiated to provide this increase. Such as study could be expanded to test gH/gL/UL128/UL130/UL131and gH/gL/gO antibody binding for correlation with protection as well. In the short term, the infants from the globulin cohort who were confirmed to be exposed to blood products positive for HCMV and whose mothers are seronegative could be examined. Information on which sample of CMVIG the infant

received would have to be available, however, so that the repertoire of anti-gB antibodies in the treatment could be examined.

7.2.4. Structure of HCMV pentamer

To obtain the crystal structure of the pentameric complex formed by gH/gL/UL128/UL130/UL131, the methods presented by Ciferri, et al. to obtain the low-resolution, negative-stain EM image should be followed. This includes expression in mammalian cells and stabilization with an antibody. In addition to gB, the pentamer is a major immunogen and any vaccine or mAb-based therapeutic cocktail should target it along with gB for the broadest protection. Thus, a high-resolution structure is worth pursuing to aid in such design efforts.

Bibliography

1. Davison, A.J., *Herpesvirus systematics.* Vet Microbiol, 2010. **143**(1): p. 52-69.
2. Fatahzadeh, M. and R.A. Schwartz, *Human herpes simplex virus infections: epidemiology, pathogenesis, symptomatology, diagnosis, and management.* J Am Acad Dermatol, 2007. **57**(5): p. 737-63; quiz 764-6.
3. GERALD NIEDOBITEK, N.M.A.H.-J.D., *Epstein-Barr virus infection and human malignancies.* Viruses and cancer, 2001. **82**: p. 149-170.
4. Manicklal, S., et al., *The "silent" global burden of congenital cytomegalovirus.* Clin Microbiol Rev, 2013. **26**(1): p. 86-102.
5. Thomas Catron, M., H. Gene Hern, MD, MS, *Herpes Zoster Ophthalmicus.* Western Journal of Emergency Medicine 2008. **IX**(3): p. 174-176.
6. Tsatsos, M., et al., *Herpes simplex virus keratitis: an update of the pathogenesis and current treatment with oral and topical antiviral agents.* Clin Experiment Ophthalmol, 2016.
7. Jouan, Y., et al., *Long-term outcome of severe herpes simplex encephalitis: a population-based observational study.* Crit Care, 2015. **19**: p. 345.
8. De Cauwer, H., et al., *Neurological deterioration in the treatment of Herpes zoster: encephalitis or neurotoxic effect of acyclovir?* Acta Neurol Belg, 2016.
9. Elisabetta Caselli, D.D.L., *Molecular biology and clinical associations of Roseoloviruses human herpesvirus 6 and human herpesvirus 7.* NEW MICROBIOLOGICA, 2007. **30**: p. 173-187.
10. Papageorgiou, E., et al., *Fourth cranial nerve palsy and bilateral acute retinal necrosis following human herpesvirus 6 infection of the central nervous system.* Ocul Immunol Inflamm, 2014. **22**(3): p. 228-32.
11. Marci, R., et al., *Presence of HHV-6A in Endometrial Epithelial Cells from Women with Primary Unexplained Infertility.* PLoS One, 2016. **11**(7): p. e0158304.
12. Theodore, W.H., et al., *Human herpes virus 6B: a possible role in epilepsy?* Epilepsia, 2008. **49**(11): p. 1828-37.
13. Soorebettu R. Prabhu, D.F.W., *Evidence of Epstein–Barr Virus Association with Head and Neck Cancers: A Review.* J Can Dent Assoc, 2016. **82**(g2): p. 1-11.
14. Cohen, J.I., *Optimal treatment for chronic active Epstein-Barr virus disease.* Pediatr Transplant, 2009. **13**(4): p. 393-6.
15. MacGill, M., *Kaposi Sarcoma: Causes, Symptoms and Treatment.* Medical News Today, 2016.
16. Bate, S.L., S.C. Dollard, and M.J. Cannon, *Cytomegalovirus seroprevalence in the United States: the national health and nutrition examination surveys, 1988-2004.* Clin Infect Dis, 2010. **50**(11): p. 1439-47.
17. Crumpacker CS II, Z.J., *Cytomegalovirus. .* Principles and Practice of Infectious Diseases. , 2009. **7th ed.**: p. Chapter 138.
18. WL., D., *Cytomegalovirus.* Goldman's Cecil Medicine. , 2011. **24th ed.**: p. Chapter 384.
19. Dupont, L. and M.B. Reeves, *Cytomegalovirus latency and reactivation: recent insights into an age old problem.* Rev Med Virol, 2016. **26**(2): p. 75-89.

20. Jackson, S.E., G.M. Mason, and M.R. Wills, *Human cytomegalovirus immunity and immune evasion.* Virus Res, 2011. **157**(2): p. 151-60.
21. Sinclair, J. and P. Sissons, *Latency and reactivation of human cytomegalovirus.* J Gen Virol, 2006. **87**(Pt 7): p. 1763-79.
22. MacGregor RR, P.S., Graziani AL, Montzka DP, Hodinka RL, Nichols CW, Friedman HM., *Evidence of active cytomegalovirus infection in clinically stable HIV-infected individuals with CD4+ lymphocyte counts below 100/microliters of blood: features and relation to risk of subsequent CMV retinitis.* J Acquir Immune Defic Syndr Hum Retrovirol. , 1995. **10**(3): p. 324-30.
23. Hoover DR, S.A., Bacellar H, Phair J, Detels R, Anderson R, Kaslow RA., *Clinical manifestations of AIDS in the era of pneumocystis prophylaxis. Multicenter AIDS Cohort Study.* N Engl J Med. , 1993. **329**(26): p. 1922-6.
24. Lerner CW, T.M., ***Opportunistic infection complicating acquired immune deficiency syndrome. Clinical features of 25 cases.*** Medicine (Baltimore), 1984. **63**(3): p. 155-64.
25. Sugar, E.A., et al., *Incidence of cytomegalovirus retinitis in the era of highly active antiretroviral therapy.* Am J Ophthalmol, 2012. **153**(6): p. 1016-24 e5.
26. Baryawno, N., et al., *Detection of human cytomegalovirus in medulloblastomas reveals a potential therapeutic target.* J Clin Invest, 2011. **121**(10): p. 4043-55.
27. Cobbs CS, H.L., Samanta M, Gillespie GY, Bharara S, King PH, Nabors LB, Cobbs CG, Britt WJ., *Human cytomegalovirus infection and expression in human malignant glioma.* Cancer Res. , 2002. **62**(12): p. 3347-50.
28. Rahbar, A., et al., *Human cytomegalovirus infection levels in glioblastoma multiforme are of prognostic value for survival.* J Clin Virol, 2013. **57**(1): p. 36-42.
29. Samanta, M., et al., *High prevalence of human cytomegalovirus in prostatic intraepithelial neoplasia and prostatic carcinoma.* J Urol, 2003. **170**(3): p. 998-1002.
30. Wolmer-Solberg, N., et al., *Frequent detection of human cytomegalovirus in neuroblastoma: a novel therapeutic target?* Int J Cancer, 2013. **133**(10): p. 2351-61.
31. Hadaczek, P., et al., *Cidofovir: a novel antitumor agent for glioblastoma.* Clin Cancer Res, 2013. **19**(23): p. 6473-83.
32. Söderberg-Nauclér C, R.A., Stragliotto G., *Survival in Patients with Glioblastoma Receiving Valganciclovir.* N Engl J Med, 2013. **369**(10): p. 984-5.
33. M. B. Reeves, P.A.M., P. J. Lehner, J. G. P. Sissons, and J. H. Sinclair, *Latency, chromatin remodeling, and reactivation of human cytomegalovirus in the dendritic cells of healthy carriers.* PNAS, 2005. **102**(11): p. 4140-4145.
34. Soderberg-Naucler, C., et al., *Reactivation of Latent Human Cytomegalovirus in CD14+ Monocytes Is Differentiation Dependent.* Journal of Virology, 2001. **75**(16): p. 7543-7554.
35. Ruell, J., et al., *Active CMV disease does not always correlate with viral load detection.* Bone Marrow Transplant, 2007. **40**(1): p. 55-61.
36. Azevedo, L.S., et al., *Cytomegalovirus infection in transplant recipients.* Clinics, 2015. **70**(7): p. 515-523.

37. Humar, A., D. Snydman, and A.S.T.I.D.C.o. Practice, *Cytomegalovirus in solid organ transplant recipients.* Am J Transplant, 2009. **9 Suppl 4**: p. S78-86.
38. Cheeran, M.C., J.R. Lokensgard, and M.R. Schleiss, *Neuropathogenesis of congenital cytomegalovirus infection: disease mechanisms and prospects for intervention.* Clin Microbiol Rev, 2009. **22**(1): p. 99-126, Table of Contents.
39. Revello, M.G., et al., *A randomized trial of hyperimmune globulin to prevent congenital cytomegalovirus.* N Engl J Med, 2014. **370**(14): p. 1316-26.
40. Cannon, M.J. and K.F. Davis, *Washing our hands of the congenital cytomegalovirus disease epidemic.* BMC Public Health, 2005. **5**: p. 70.
41. Colugnati, F.A., et al., *Incidence of cytomegalovirus infection among the general population and pregnant women in the United States.* BMC Infect Dis, 2007. **7**: p. 71.
42. Kenneson, A. and M.J. Cannon, *Review and meta-analysis of the epidemiology of congenital cytomegalovirus (CMV) infection.* Rev Med Virol, 2007. **17**(4): p. 253-76.
43. Kimon C Zachary, M., *Ganciclovir and valganciclovir: An overview.* UpToDate, 2016: p. 1.
44. Matthews T, B.R., *Antiviral activity and mechanism of action of ganciclovir.* Rev Infect Dis., 1988. **3**: p. S490-4.
45. V. FOULONGNE, C.T.R., F. DIAFOUKA, B. ABRAHAM1, S. LASTERE, M. SEGONDY, *Ganciclovir resistance mutations in UL97 and UL54 genes of Human cytomegalovirus isolates resistant to ganciclovir.* Acta virologica 2004. **48**(51-55).
46. Palestine AG, P.M., De Smet MD, Baird BF, Falloon J, Kovacs JA, Davey RT, Zurlo JJ, Zunich KM, Davis M, et al., *A randomized, controlled trial of foscarnet in the treatment of cytomegalovirus retinitis in patients with AIDS.* Ann Intern Med., 1991. **115**(9): p. 665-73.
47. Battiwalla, M., et al., *Leflunomide failure to control recurrent cytomegalovirus infection in the setting of renal failure after allogeneic stem cell transplantation.* Transpl Infect Dis, 2007. **9**(1): p. 28-32.
48. Wolf, D.G., et al., *Human cytomegalovirus kinetics following institution of artesunate after hematopoietic stem cell transplantation.* Antiviral Res, 2011. **90**(3): p. 183-6.
49. Shapira, M.Y., et al., *Artesunate as a potent antiviral agent in a patient with late drug-resistant cytomegalovirus infection after hematopoietic stem cell transplantation.* Clin Infect Dis, 2008. **46**(9): p. 1455-7.
50. Avery, R.K., et al., *Oral maribavir for treatment of refractory or resistant cytomegalovirus infections in transplant recipients.* Transpl Infect Dis, 2010. **12**(6): p. 489-96.
51. Marty, F.M., et al., *Maribavir prophylaxis for prevention of cytomegalovirus disease in recipients of allogeneic stem-cell transplants: a phase 3, double-blind, placebo-controlled, randomised trial.* The Lancet Infectious Diseases, 2011. **11**(4): p. 284-292.
52. Price, N.B. and M.N. Prichard, *Progress in the development of new therapies for herpesvirus infections.* Curr Opin Virol, 2011. **1**(6): p. 548-54.

53. Kaul, D.R., et al., *First report of successful treatment of multidrug-resistant cytomegalovirus disease with the novel anti-CMV compound AIC246.* Am J Transplant, 2011. **11**(5): p. 1079-84.
54. Snydman DR, W.B., Dougherty NN, Griffith J, Rubin RH, Dienstag JL, Rohrer RH, Freeman R, Jenkins R, Lewis WD, Hammer S, O'Rourke E, Grady GF, Fawaz K, Kaplan MM, Hoffman MA, Katz AT, Doran M, *Cytomegalovirus immune globulin prophylaxis in liver transplantation. A randomized, double-blind, placebo-controlled trial.* Ann Intern Med., 1993. **119**(10): p. 984-91.
55. DesJardin JA, S.D., *Antiviral immunotherapy: a review of current status.* BioDrugs, 1998. **9**(6): p. 487-507.
56. Raanani, P., et al., *Immunoglobulin prophylaxis in hematopoietic stem cell transplantation: systematic review and meta-analysis.* J Clin Oncol, 2009. **27**(5): p. 770-81.
57. David R Snydman, M., Barbara G. Werner, PhD, H. Cody Meissner, MD, Sarah H. Cheeseman, MD, Johnathan Schwab, MD, Francis Bednarek, MD, Joseph L. Kennedy, JR., MD, Marguerite Herschel, MD, Andrea Magno MD, Myron J. Levin, MD, Timos Valaes, MD, Eugene Berkman, MD, James McIver, PhD, Jeanne Leszczynski, DRPH, John Griffith, PhD, and George F. Grady, MD, *Use of cytomegalovirus immunoglobulin in multiply transfused permature neonates.* Pediatric Infectious Disease, 1995. **14**(1): p. 34-40.
58. Kauvar, L.M., et al., *A high-affinity native human antibody neutralizes human cytomegalovirus infection of diverse cell types.* Antimicrob Agents Chemother, 2015. **59**(3): p. 1558-68.
59. Ishida, J.H., et al., *Phase 1 Randomized, Double-Blind, Placebo-Controlled Study of RG7667, an Anticytomegalovirus Combination Monoclonal Antibody Therapy, in Healthy Adults.* Antimicrob Agents Chemother, 2015. **59**(8): p. 4919-29.
60. Ann M. Arvin, P.F., Martin Myers, Stanley Plotkin, and Regina Rabinovich, *Vaccine Development to Prevent Cytomegalovirus Disease: Report from the National Vaccine Advisory Committee.* Clinical Infectious Diseases, 2004. **39**: p. 233-9.
61. Griffiths, P.D., et al., *Cytomegalovirus glycoprotein-B vaccine with MF59 adjuvant in transplant recipients: a phase 2 randomised placebo-controlled trial.* The Lancet, 2011. **377**(9773): p. 1256-1263.
62. Robert F. Pass, M.D., Changpin Zhang, M.D., Ashley Evans, M.D.,, et al., *Vaccine Prevention of Maternal Cytomegalovirus Infection.* The new england journal o f medicine, 2009. **360**: p. 1191-9.
63. Dominguez G, B.J., Stamey FR, Inoue N, Pellett PE, *Physical and genetic maps of the human herpesvirus 7 strain SB genome.* Arch Virol., 1996. **141**(12): p. 2387-2408.
64. GERALDINA DOMINGUEZ, T.R.D., FELICIA R. STAMEY, and N.I. STEPHEN DEWHURST, AND PHILIP E. PELLETT, *Human Herpesvirus 6B Genome Sequence: Coding Content and Comparison with Human Herpesvirus 6A.* JOURNAL OF VIROLOGY, 1999. **73**(10): p. 8040–8052.

65. LISE J. PERRY, A.D.J.M., *The DNA Sequences of the Long Repeat Region and Adjoining Parts of the Long Unique Region in the Genome of Herpes Simplex Virus Type 1.* J. gen. Virol, 1988. **69**: p. 2831-2846.
66. AIDAN DOLAN, F.E.J., CHARLES CUNNINGHAM, and A.D.J.M. BARBARA C. BARNETT, *The Genome Sequence of Herpes Simplex Virus Type 2.* JOURNAL OF VIROLOGY, 1998. **72**(3): p. 2010–2021.
67. Santpere, G., et al., *Genome-wide analysis of wild-type Epstein-Barr virus genomes derived from healthy individuals of the 1,000 Genomes Project.* Genome Biol Evol, 2014. **6**(4): p. 846-60.
68. Knowles, E.C.a.D.M., *The role of Kaposi's sarcoma-associated herpesvirus (KSHVrHHV-8 in lymphoproliferative diseases.* 1999. **9**: p. 165-174.
69. SCOTT, A.J.D.A.J.E., *The Complete DNA Sequence of Varicella-Zoster Virus* J. gen. Virol, 1986. **67**: p. 1759-1816.
70. Eain Murphy, I.R., Tetsuo Shibuya, and Thomas E. Shenk, *Reevaluation of human cytomegalovirus coding potential.* PNAS, 2003. **100**(23): p. 13585-13590.
71. Chee MS, B.A., Beck S, Bohni R, Brown CM, Cerny R, Horsnell T, Hutchison CA 3rd, Kouzarides T, Martignetti JA, et al., *Analysis of the protein-coding content of the sequence of human cytomegalovirus strain AD169.* Curr Top Microbiol Immunol., 1990. **154**: p. 125-169.
72. Chee M, R.S., Plachter B, Barrell B, Jahn G., *Identification of the Major Capsid Protein Gene of Human Cytomegalovirus.* J Virol., 1989. **63**(3): p. 1345-53.
73. Gibson W, B.M., Clopper KS., *Cytomegalovirus "missing" capsid protein identified as heat-aggregable product of human cytomegalovirus UL46.* j Virol., 1996. **70**(11): p. 7454-61.
74. Gibson W, C.K., Britt WJ, Baxter MK., *Human Cytomegalovirus (HCMV) Smallest Capsid Protein Identified as Product of Short Open Reading Frame Located between HCMV UL48 and UL49.* J Virol., 1996. **70**(8): p. 5680-3.
75. Homman-Loudiyi, M., et al., *Envelopment of Human Cytomegalovirus Occurs by Budding into Golgi-Derived Vacuole Compartments Positive for gB, Rab 3, Trans-Golgi Network 46, and Mannosidase II.* Journal of Virology, 2003. **77**(5): p. 3191-3203.
76. Vanarsdall, A.L. and D.C. Johnson, *Human cytomegalovirus entry into cells.* Curr Opin Virol, 2012. **2**(1): p. 37-42.
77. Haspot, F., et al., *Human cytomegalovirus entry into dendritic cells occurs via a macropinocytosis-like pathway in a pH-independent and cholesterol-dependent manner.* PLoS One, 2012. **7**(4): p. e34795.
78. Bissinger, A.L., et al., *Human cytomegalovirus as a direct pathogen: correlation of multiorgan involvement and cell distribution with clinical and pathological findings in a case of congenital inclusion disease.* J Med Virol, 2002. **67**(2): p. 200-6.
79. Christian Sinzger, A.G., Bodo Plachter, Annette S. H. Gouw, T. Hauw, and Gerhard Jahn *Fibroblasts, epithelial cells, endothelial cells and smooth muscle cells are major targets of human cytomegalovirus infection in lung and gastrointestinal tissues* Journal of General Virology, 1995. **76**: p. 741-750.

80. Soderberg-Naucler, C., Fish, K.N., Nelson, J.A.,, *Reactivation of latent human cytomegalovirus by allogeneic stimulation of blood cells from healthy donors.* Cell 1997. **91**: p. 119-126.
81. Dai Wang, a.T.S., *Human Cytomegalovirus UL131 Open Reading Frame Is Required for Epithelial Cell Tropism.* Journal of Virology, 2005. **79**: p. 10330-10338.
82. Jean Beltran, P.M. and I.M. Cristea, *The life cycle and pathogenesis of human cytomegalovirus infection: lessons from proteomics.* Expert Rev Proteomics, 2014. **11**(6): p. 697-711.
83. Webel, R., et al., *Differential properties of cytomegalovirus pUL97 kinase isoforms affect viral replication and maribavir susceptibility.* J Virol, 2014. **88**(9): p. 4776-85.
84. Kalejta, R.F., *Tegument proteins of human cytomegalovirus.* Microbiol Mol Biol Rev, 2008. **72**(2): p. 249-65, table of contents.
85. Bigalke, J.M. and E.E. Heldwein, *Nuclear Exodus: Herpesviruses Lead the Way.* Annu Rev Virol, 2016: p. 14-24.
86. Das, S., A. Vasanji, and P.E. Pellett, *Three-dimensional structure of the human cytomegalovirus cytoplasmic virion assembly complex includes a reoriented secretory apparatus.* J Virol, 2007. **81**(21): p. 11861-9.
87. Sean T. H. Liu, R.S.-F., Pavlina Ivanova, Stephen B. Milne, David S. Myers, Joshua D. Rabinowitz, H. Alex Brown, and Thomas Shenk, *Synaptic vesicle-like lipidome of human cytomegalovirus virions reveals a role for SNARE machinery in virion egress.* PNAS, 2011. **108**(31): p. 12869-12874.
88. Wills, M.R., et al., *The immunology of human cytomegalovirus latency: could latent infection be cleared by novel immunotherapeutic strategies?* Cell Mol Immunol, 2015. **12**(2): p. 128-38.
89. Kenneth Kaushansky, M.L., E. Beutler, Thomas Kipps, Josef Prchal, Uri Seligsohn, *Williams Hematology*. Eighth Edition ed. 2010: McGraw-Hill Education.
90. Tal-Singer R, P.C., Ponce De Leon M, Abrams WR, Banfield BW, Tufaro F, Cohen GH, Eisenberg RJ., *Interaction of Herpes Simplex Virus Glycoprotein gC with Mammalian Cell Surface Molecules.* J Virol., 1995. **69**(7): p. 4471-4483.
91. Sylvie Laquerre, R.A., Dina B. Anderson, Silvia Zucchini, Roberto Manservigi, and Joseph C. Glorioso, *Heparan Sulfate Proteoglycan Binding by Herpes Simplex Virus Type 1 Glycoproteins B and C, Which Differ in Their Contributions to Virus Attachment, Penetration, and Cell-to-Cell Spread.* Journal of Virology, 1998. **72**(7): p. 6119-6130.
92. J C Whitbeck, C.P., H Lou, R Xu, S H Willis, M Ponce de Leon, T Peng, A V Nicola, R I Montgomery, M S Warner, A M Soulika, L A Spruce, W T Moore, J D Lambris, P G Spear, G H Cohen, and R J Eisenberg, *Glycoprotein D of Herpes Simplex Virus (HSV) Binds Directly to HVEM, a Member of the Tumor Necrosis Factor Receptor Superfamily and a Mediator of HSV Entry.* J Virol. , 1997. **71**(8): p. 6083-6093.
93. Deepak Shukla, J.L., Peter Blaiklock, Nicholas W. Shworak, Xiaomei Bai, Jeffrey D. Esko, Gary H. Cohen, Roselyn J. Eisenberg, Robert D. Rosenberg,

Patricia G. Spear, *A Novel Role for 3-O-Sulfated Heparan Sulfate in Herpes Simplex Virus 1 Entry.* Cell Host Microbe, 1999. **99**(13-22).
94. Pertel, P.E., et al., *Cell fusion induced by herpes simplex virus glycoproteins gB, gD, and gH-gL requires a gD receptor but not necessarily heparan sulfate.* Virology, 2001. **279**(1): p. 313-24.
95. Chowdary, T.K., et al., *Crystal structure of the conserved herpesvirus fusion regulator complex gH-gL.* Nat Struct Mol Biol, 2010. **17**(7): p. 882-8.
96. Cairns, T.M., et al., *N-terminal mutants of herpes simplex virus type 2 gH are transported without gL but require gL for function.* J Virol, 2007. **81**(10): p. 5102-11.
97. C Roop, L.H., and D C Johnson, *A mutant herpes simplex virus type 1 unable to express glycoprotein L cannot enter cells, and its particles lack glycoprotein H.* journal of Virology, 1993. **67**(4): p. 2285–2297.
98. Rogalin, H.B. and E.E. Heldwein, *Interplay between the Herpes Simplex Virus 1 gB Cytodomain and the gH Cytotail during Cell-Cell Fusion.* J Virol, 2015. **89**(24): p. 12262-72.
99. Foster, T.P., J.M. Melancon, and K.G. Kousoulas, *An alpha-helical domain within the carboxyl terminus of herpes simplex virus type 1 (HSV-1) glycoprotein B (gB) is associated with cell fusion and resistance to heparin inhibition of cell fusion.* Virology, 2001. **287**(1): p. 18-29.
100. Silverman, J.L., et al., *Membrane requirement for folding of the herpes simplex virus 1 gB cytodomain suggests a unique mechanism of fusion regulation.* J Virol, 2012. **86**(15): p. 8171-84.
101. Ravi P. Subramanian, a.R.J.G., *Herpes simplex virus type 1 mediates fusion through a hemifusion intermediate by sequential activity of glycoproteins D, H, L, and B.* PNAS, 2007. **104**(8): p. 2903-2908.
102. Heldwein, E.E., et al., *Crystal structure of glycoprotein B from herpes simplex virus 1.* Science, 2006. **313**(5784): p. 217-20.
103. Hannah, B.P., et al., *Herpes simplex virus glycoprotein B associates with target membranes via its fusion loops.* J Virol, 2009. **83**(13): p. 6825-36.
104. Feire, A.L., H. Koss, and T. Compton, *Cellular integrins function as entry receptors for human cytomegalovirus via a highly conserved disintegrin-like domain.* Proceedings of the National Academy of Sciences of the United States of America, 2004. **101**(43): p. 15470-5.
105. Soroceanu, L., A. Akhavan, and C.S. Cobbs, *Platelet-derived growth factor-alpha receptor activation is required for human cytomegalovirus infection.* Nature, 2008. **455**(7211): p. 391-5.
106. Ryckman, B.J., et al., *Human cytomegalovirus entry into epithelial and endothelial cells depends on genes UL128 to UL150 and occurs by endocytosis and low-pH fusion.* J Virol, 2006. **80**(2): p. 710-22.
107. Vanarsdall, A.L., et al., *Human cytomegalovirus glycoproteins gB and gH/gL mediate epithelial cell-cell fusion when expressed either in cis or in trans.* J Virol, 2008. **82**(23): p. 11837-50.
108. Wille, P.T., et al., *Human cytomegalovirus (HCMV) glycoprotein gB promotes virus entry in trans acting as the viral fusion protein rather than as a receptor-binding protein.* MBio, 2013. **4**(3): p. e00332-13.

109. Brent J. Ryckman, M.C.C., and David C. Johnson, *HCMV gH/gL/UL128–131 interferes with virus entry into epithelial cells: Evidence for cell type-specific receptors.* PNAS, 2008. **105**(37): p. 14118-14123.
110. Akter, P., et al., *Two novel spliced genes in human cytomegalovirus.* J Gen Virol, 2003. **84**(Pt 5): p. 1117-22.
111. Kabanova A, M.J., Zhou T, Bianchi S, Baxa U, Tsybovsky Y, Lilleri D, Silacci-Fregni C, Foglierini M, Fernandez-Rodriguez BM, Druz A, Zhang B, Geiger R, Pagani M, Sallusto F, Kwong PD, Corti D, Lanzavecchia A, Perez L., *Platelet-derived growth factor-α receptor is the cellular receptor for human cytomegalovirus gHgLgO trimer.* Nat Microbiol., 2016. **1**(8).
112. Hisae Matsuuraa, A.N.K., Richard Longneckerc, and Theodore S. Jardetzky, *Crystal structure of the Epstein-Barr virus (EBV) glycoprotein H/glycoprotein L (gH/gL) complex.* PNAS, 2010. **107**(52): p. 22641-22646.
113. Backovic, M., R. Longnecker, and T.S. Jardetzky, *Structure of a trimeric variant of the Epstein-Barr virus glycoprotein B.* Proc Natl Acad Sci U S A, 2009. **106**(8): p. 2880-5.
114. Zhou, M., et al., *Comparative analysis of gO isoforms reveals that strains of human cytomegalovirus differ in the ratio of gH/gL/gO and gH/gL/UL128-131 in the virion envelope.* J Virol, 2013. **87**(17): p. 9680-90.
115. Wyrwicz, L.S. and L. Rychlewski, *Herpes glycoprotein gL is distantly related to chemokine receptor ligands.* Antiviral Res, 2007. **75**(1): p. 83-6.
116. Ryckman, B.J., et al., *Characterization of the human cytomegalovirus gH/gL/UL128-131 complex that mediates entry into epithelial and endothelial cells.* J Virol, 2008. **82**(1): p. 60-70.
117. Ciferri, C., et al., *Structural and biochemical studies of HCMV gH/gL/gO and Pentamer reveal mutually exclusive cell entry complexes.* Proc Natl Acad Sci U S A, 2015. **112**(6): p. 1767-72.
118. Stampfer, S.D. and E.E. Heldwein, *Stuck in the middle: structural insights into the role of the gH/gL heterodimer in herpesvirus entry.* Curr Opin Virol, 2013. **3**(1): p. 13-9.
119. Ryckman, B.J., M.C. Chase, and D.C. Johnson, *Human cytomegalovirus TR strain glycoprotein O acts as a chaperone promoting gH/gL incorporation into virions but is not present in virions.* J Virol, 2010. **84**(5): p. 2597-609.
120. Scrivano, L., et al., *HCMV spread and cell tropism are determined by distinct virus populations.* PLoS Pathog, 2011. **7**(1): p. e1001256.
121. Eric R Kinzler, R.N.T., Teresa Compton, *Expression and reconstitution of the gH/gL/gO complex of human cytomegalovirus.* Journal of Clincal Virology 2002. **25**(2): p. 87-95.
122. Zheng, Q., et al., *HCMV-encoded UL128 enhances TNF-alpha and IL-6 expression and promotes PBMC proliferation through the MAPK/ERK pathway in vitro.* Viral Immunol, 2012. **25**(2): p. 98-105.
123. Patrone, M., et al., *Human cytomegalovirus UL130 protein promotes endothelial cell infection through a producer cell modification of the virion.* J Virol, 2005. **79**(13): p. 8361-73.
124. Sun, Z., et al., *Transcription pattern of UL131A-128 mRNA in clinical strains of human cytomegalovirus.* Journal of Biosciences, 2010. **35**(3): p. 365-370.

125. Harrison, S.C., *Viral membrane fusion.* Virology, 2015. **479-480C**: p. 498-507.
126. Kim, Y.H., et al., *Capture and imaging of a prehairpin fusion intermediate of the paramyxovirus PIV5.* Proc Natl Acad Sci U S A, 2011. **108**(52): p. 20992-7.
127. Harrison, S.C., *Viral membrane fusion.* Nat Struct Mol Biol, 2008. **15**(7): p. 690-8.
128. Connolly, S.A., et al., *Fusing structure and function: a structural view of the herpesvirus entry machinery.* Nature reviews. Microbiology, 2011. **9**(5): p. 369-81.
129. Cooper, R.S. and E.E. Heldwein, *Herpesvirus gB: A Finely Tuned Fusion Machine.* Viruses, 2015. **7**(12): p. 6552-69.
130. Yin, H.S., et al., *Structure of the uncleaved ectodomain of the paramyxovirus (hPIV3) fusion protein.* Proc Natl Acad Sci U S A, 2005. **102**(26): p. 9288-93.
131. Yin, H.S., et al., *Structure of the parainfluenza virus 5 F protein in its metastable, prefusion conformation.* Nature, 2006. **439**(7072): p. 38-44.
132. Bullough, P.A., et al., *Structure of influenza haemagglutinin at the pH of membrane fusion.* Nature, 1994. **371**(6492): p. 37-43.
133. Wilson, I.A., J.J. Skehel, and D.C. Wiley, *Structure of the haemagglutinin membrane glycoprotein of influenza virus at 3 A resolution.* Nature, 1981. **289**(5796): p. 366-73.
134. White, J.M., et al., *Structures and mechanisms of viral membrane fusion proteins: multiple variations on a common theme.* Crit Rev Biochem Mol Biol, 2008. **43**(3): p. 189-219.
135. Melikyan, G.B., et al., *Evidence that the transition of HIV-1 gp41 into a six-helix bundle, not the bundle configuration, induces membrane fusion.* J Cell Biol, 2000. **151**(2): p. 413-23.
136. Brasseur, R., et al., *Mode of insertion into a lipid membrane of the N-terminal HIV gp41 peptide segment.* AIDS Res Hum Retroviruses, 1988. **4**(2): p. 83-90.
137. McCune, J.M., et al., *Endoproteolytic cleavage of gp160 is required for the activation of human immunodeficiency virus.* Cell, 1988. **53**(1): p. 55-67.
138. Stein, B.S. and E.G. Engleman, *Intracellular processing of the gp160 HIV-1 envelope precursor. Endoproteolytic cleavage occurs in a cis or medial compartment of the Golgi complex.* J Biol Chem, 1990. **265**(5): p. 2640-9.
139. Lazarowitz, S.G. and P.W. Choppin, *Enhancement of the infectivity of influenza A and B viruses by proteolytic cleavage of the hemagglutinin polypeptide.* Virology, 1975. **68**(2): p. 440-54.
140. White, J., J. Kartenbeck, and A. Helenius, *Membrane fusion activity of influenza virus.* EMBO J, 1982. **1**(2): p. 217-22.
141. Buzon, V., et al., *Crystal structure of HIV-1 gp41 including both fusion peptide and membrane proximal external regions.* PLoS Pathog, 2010. **6**(5): p. e1000880.
142. Modis, Y., et al., *A ligand-binding pocket in the dengue virus envelope glycoprotein.* Proc Natl Acad Sci U S A, 2003. **100**(12): p. 6986-91.
143. Modis, Y., et al., *Structure of the dengue virus envelope protein after membrane fusion.* Nature, 2004. **427**(6972): p. 313-9.
144. Bressanelli, S., et al., *Structure of a flavivirus envelope glycoprotein in its low-pH-induced membrane fusion conformation.* EMBO J, 2004. **23**(4): p. 728-38.

145. Kielian, M., C. Chanel-Vos, and M. Liao, *Alphavirus Entry and Membrane Fusion.* Viruses, 2010. **2**(4): p. 796-825.
146. Heinz, F.X., et al., *Structural changes and functional control of the tick-borne encephalitis virus glycoprotein E by the heterodimeric association with protein prM.* Virology, 1994. **198**(1): p. 109-17.
147. Fields, W. and M. Kielian, *A key interaction between the alphavirus envelope proteins responsible for initial dimer dissociation during fusion.* J Virol, 2013. **87**(7): p. 3774-81.
148. Roussel, A., et al., *Structure and interactions at the viral surface of the envelope protein E1 of Semliki Forest virus.* Structure, 2006. **14**(1): p. 75-86.
149. Steven AC, S.P., *Biochemistry. Viral glycoproteins and an evolutionary conundrum.* Science, 2006. **313**(5784): p. 177-8.
150. Roche, S., et al., *Structure of the prefusion form of the vesicular stomatitis virus glycoprotein G.* Science, 2007. **315**(5813): p. 843-8.
151. Stéphane Roche, F.A.R., Yves Gaudin, Stéphane Bressanell, *Structure of the Prefusion Form of the Vesicular Stomatitis Virus Glycoprotein G.* Science, 2007. **315**(843-848).
152. Roche, S., et al., *Crystal structure of the low-pH form of the vesicular stomatitis virus glycoprotein G.* Science, 2006. **313**(5784): p. 187-191.
153. Strive, T., et al., *Proteolytic Processing of Human Cytomegalovirus Glycoprotein B Is Dispensable for Viral Growth in Culture.* Journal of Virology, 2002. **76**(3): p. 1252-1264.
154. Kadlec, J., et al., *The postfusion structure of baculovirus gp64 supports a unified view of viral fusion machines.* Nat Struct Mol Biol, 2008. **15**(10): p. 1024-30.
155. Potzsch, S., et al., *B cell repertoire analysis identifies new antigenic domains on glycoprotein B of human cytomegalovirus which are target of neutralizing antibodies.* PLoS Pathog, 2011. **7**(8): p. e1002172.
156. Sharma, S., et al., *HCMV gB shares structural and functional properties with gB proteins from other herpesviruses.* Virology, 2013. **435**(2): p. 239-49.
157. Eto, K., et al., *Functional classification of ADAMs based on a conserved motif for binding to integrin alpha 9beta 1: implications for sperm-egg binding and other cell interactions.* J Biol Chem, 2002. **277**(20): p. 17804-10.
158. Takeda, S., *ADAM and ADAMTS Family Proteins and Snake Venom Metalloproteinases: A Structural Overview.* Toxins (Basel), 2016. **8**(5).
159. Feire, A.L., et al., *The glycoprotein B disintegrin-like domain binds beta 1 integrin to mediate cytomegalovirus entry.* Journal of virology, 2010. **84**(19): p. 10026-37.
160. Tina M. Cairns, Z.-Y.H., J. Charles Whitbeck, Manuel Ponce de Leon, Huan Lou, Anna Wald, Claude Krummenacher, Roselyn J. Eisenberg and Gary H. Cohen, *Dissection of the Antibody Response against Herpes Simplex Virus Glycoproteins in Naturally Infected Humans.* J Virol, 2014. **88**(21): p. 12612-12622.
161. Cairns, T.M., et al., *Mechanism of neutralization of herpes simplex virus by antibodies directed at the fusion domain of glycoprotein B.* J Virol, 2014. **88**(5): p. 2677-89.

162. Stampfer, S.D., et al., *Structural basis of local, pH-dependent conformational changes in glycoprotein B from herpes simplex virus type 1.* J Virol, 2010. **84**(24): p. 12924-33.
163. Wiegers, A.K., et al., *Identification of a neutralizing epitope within antigenic domain 5 of glycoprotein B of human cytomegalovirus.* J Virol, 2015. **89**(1): p. 361-72.
164. W J Britt, L.V., E J Butfiloski, and E B Stephens, *Cell surface expression of human cytomegalovirus (HCMV) gp55-116 (gB): use of HCMV-recombinant vaccinia virus-infected cells in analysis of the human neutralizing antibody response.* J Virol, 1990. **64**(3): p. 1079-1085.
165. Eva Gönczöl, C.d.T., Gabor Hirka, Klara Berencsi, Weichi Lin, Enzo Paoletti, Stanley Plotkin, *High expression of human cytomegalovirus (HCMV)-gB protein in cells infected with a vaccinia-gB recombinant: the importance of the gB protein in HCMV immunity.* Vaccine, 1991. **9**(9): p. 631-637.
166. Fouts, A.E., et al., *Antibodies against the gH/gL/UL128/UL130/UL131 complex comprise the majority of the anti-cytomegalovirus (anti-CMV) neutralizing antibody response in CMV hyperimmune globulin.* J Virol, 2012. **86**(13): p. 7444-7.
167. Zydek, M., et al., *HCMV infection of human trophoblast progenitor cells of the placenta is neutralized by a human monoclonal antibody to glycoprotein B and not by antibodies to the pentamer complex.* Viruses, 2014. **6**(3): p. 1346-64.
168. Michel Silvestri, V.-A.S., Ulla Rudén, Britta Wahren, *Characterization of a Major Antigenic Region on gp55 of Human Cytomegalovirus.* 1991. **J. Gen. Virol.**(72): p. 3017-3023.
169. Kniess, N., et al., *Distribution of linear antigenic sites on glycoprotein gp55 of human cytomegalovirus.* Journal of virology, 1991. **65**(1): p. 138-46.
170. Potzsch, S., et al., *B cell repertoire analysis identifies new antigenic domains on glycoprotein B of human cytomegalovirus which are target of neutralizing antibodies.* PLoS pathogens, 2011. **7**(8): p. e1002172.
171. Ohlin, M., et al., *Fine specificity of the human immune response to the major neutralization epitopes expressed on cytomegalovirus gp58/116 (gB), as determined with human monoclonal antibodies.* J Virol, 1993. **67**(2): p. 703-10.
172. Wagner, B., et al., *A continuous sequence of more than 70 amino acids is essential for antibody binding to the dominant antigenic site of glycoprotein gp58 of human cytomegalovirus.* J Virol, 1992. **66**(9): p. 5290-7.
173. Schoppel, K., et al., *Antibodies specific for the antigenic domain 1 of glycoprotein B (gpUL55) of human cytomegalovirus bind to different substructures.* Virology, 1996. **216**(1): p. 133-45.
174. Norbert Kniess, M.M., Jaydie Fay, And William J. Britt, *Distribution of Linear Antigenic Sites on Glycoprotein gp55 of Human Cytomegalovirus.* Journal of Virology, 1991. **65**(1): p. 138-146.
175. Utz U, B.W., Vugler L, Mach M., *Identification of a neutralizing epitope on glycoprotein gp58 of human cytomegalovirus.* J Virol, 1989. **63**(5): p. 1995-2001.

176. Andrea Speckner, D.G., Mats Ohlin and Michael Mach, *Antigenic domain 1 of human cytomegalovirus glycoprotein B induces a multitude of different antibodies which, when combined, results in incomplete virus neutralization.* 1999. **Journal of Genral Virology** (80).
177. Speckner, A., et al., *Antigenic domain 1 of human cytomegalovirus glycoprotein B induces a multitude of different antibodies which, when combined, results in incomplete virus neutralization.* J Gen Virol, 1999. **80 (Pt 8)**: p. 2183-91.
178. H. Meyer, V.-A.S., L. Pereira and M. Mach, *Glycoprotein gpll6 of human cytomegalovirus contains epitopes for strain-common and strain-specific antibodies.* Journal of General Virology, 1992. **73**: p. 2375-2383.
179. Heidi Meyer, Y.M., and Michael Mach, *The gpll6 of the gp58/116 complex of human cytomegalovirus represents the amino-terminal part of the precursor molecule and contains a neutralizing epitope* Journal of General Virology, 1990. **71**(2443-2450).
180. Konrad Schoppel, B.K., Christian Schmidt, and a.M.M. Rolf Vornhagen, *The Humoral Immune Response against Human Cytomegalovirus Is Characterized by a Delayed Synthesis of Glycoprotein-Specific Antibodies.* The Journal of Infectious Diseases, 1997. **175**: p. 533-44.
181. MATS OHLIN, V.-A.S., MICHAEL MACH, BRITTA WAHREN, and A.C.A.K. BORREBAECK, *Fine Specificity of the Human Immune Response to the Major Neutralization Epitopes Expressed on Cytomegalovirus gp58/116 (gB), as Determined with Human Monoclonal Antibodies.* JOURNAL OF VIROLOGY, 1993: p. 703-710.
182. Spindler, N., et al., *Structural basis for the recognition of human cytomegalovirus glycoprotein B by a neutralizing human antibody.* PLoS Pathog, 2014. **10**(10): p. e1004377.
183. *<anti-gB 27-156 - SPAETE 1988.pdf>.*
184. Britt, W.J. and L.G. Vugler, *Oligomerization of the human cytomegalovirus major envelope glycoprotein complex gB (gp55-116).* J Virol, 1992. **66**(11): p. 6747-54.
185. M. Urban, W.B., AND M. Mach, *The Dominant Linear Neutralizing Antibody-Binding Site of Glycoprotein gp86 of Human Cytomegalovirus Is Strain Specific.* JOURNAL OF VIROLOGY, 1992. **66**(3): p. 1303-1311.
186. Kabsch, W., *Xds.* Acta Crystallogr D Biol Crystallogr, 2010. **66**(Pt 2): p. 125-32.
187. Adams, P.D., et al., *PHENIX: a comprehensive Python-based system for macromolecular structure solution.* Acta Crystallogr D Biol Crystallogr, 2010. **66**(Pt 2): p. 213-21.
188. Emsley, P., et al., *Features and development of Coot.* Acta crystallographica. Section D, Biological crystallography, 2010. **66**(Pt 4): p. 486-501.
189. Vey, M., et al., *Proteolytic processing of human cytomegalovirus glycoprotein B (gpUL55) is mediated by the human endoprotease furin.* Virology, 1995. **206**(1): p. 746-9.
190. Britt, W.J. and L.G. Vugler, *Processing of the gp55-116 envelope glycoprotein complex (gB) of human cytomegalovirus.* J Virol, 1989. **63**(1): p. 403-10.

191. Cieplik, M., H.D. Klenk, and W. Garten, *Identification and characterization of spodoptera frugiperda furin: a thermostable subtilisin-like endopeptidase.* Biological chemistry, 1998. **379**(12): p. 1433-40.
192. Lopper, M. and T. Compton, *Disulfide bond configuration of human cytomegalovirus glycoprotein B.* J Virol, 2002. **76**(12): p. 6073-6082.
193. Davis, I.W., et al., *MolProbity: all-atom contacts and structure validation for proteins and nucleic acids.* Nucleic Acids Res, 2007. **35**(Web Server issue): p. W375-83.
194. Larkin, M.A., et al., *Clustal W and Clustal X version 2.0.* Bioinformatics, 2007. **23**(21): p. 2947-8.
195. Robert, X. and P. Gouet, *Deciphering key features in protein structures with the new ENDscript server.* Nucleic Acids Res, 2014. **42**(Web Server issue): p. W320-4.
196. Vitu, E., et al., *Extensive mutagenesis of the HSV-1 gB ectodomain reveals remarkable stability of its postfusion form.* Journal of molecular biology, 2013. **425**(11): p. 2056-71.
197. Roche, S., et al., *Structure of the prefusion form of the vesicular stomatitis virus glycoprotein G.* Science, 2007. **315**(5813): p. 843-848.
198. Renzette, N., et al., *Extensive genome-wide variability of human cytomegalovirus in congenitally infected infants.* PLoS Pathog, 2011. **7**(5): p. e1001344.
199. Sijmons, S., et al., *High-throughput analysis of human cytomegalovirus genome diversity highlights the widespread occurrence of gene-disrupting mutations and pervasive recombination.* J Virol, 2015.
200. Strive, T., et al., *Proteolytic processing of human cytomegalovirus glycoprotein B is dispensable for viral growth in culture.* J Virol, 2002. **76**(3): p. 1252-64.
201. Lopper, M. and T. Compton, *Coiled-coil domains in glycoproteins B and H are involved in human cytomegalovirus membrane fusion.* J Virol, 2004. **78**(15): p. 8333-8341.
202. Russell, C.J., T.S. Jardetzky, and R.A. Lamb, *Membrane fusion machines of paramyxoviruses: capture of intermediates of fusion.* EMBO J, 2001. **20**(15): p. 4024-34.
203. Chan, D.C. and P.S. Kim, *HIV entry and its inhibition.* Cell, 1998. **93**(5): p. 681-4.
204. Eto, K., et al., *RGD-independent binding of integrin alpha9beta1 to the ADAM-12 and -15 disintegrin domains mediates cell-cell interaction.* J Biol Chem, 2000. **275**(45): p. 34922-30.
205. Jarvis, D.L., *Developing baculovirus-insect cell expression systems for humanized recombinant glycoprotein production.* Virology, 2003. **310**(1): p. 1-7.
206. Chen, B., et al., *Structure of an unliganded simian immunodeficiency virus gp120 core.* Nature, 2005. **433**(7028): p. 834-41.
207. Lee, J.E., et al., *Structure of the Ebola virus glycoprotein bound to an antibody from a human survivor.* Nature, 2008. **454**(7201): p. 177-82.
208. Szakonyi, G., et al., *Structure of the Epstein-Barr virus major envelope glycoprotein.* Nat Struct Mol Biol, 2006. **13**(11): p. 996-1001.

209. Meyer, H., et al., *Glycoprotein gp116 of human cytomegalovirus contains epitopes for strain-common and strain-specific antibodies.* J Gen Virol, 1992. **73 (Pt 9)**: p. 2375-83.
210. Burke, H.G. and E.E. Heldwein, *Crystal Structure of the Human Cytomegalovirus Glycoprotein B.* PLoS Pathog, 2015. **11**(10): p. e1005227.
211. Sumana Chandramouli, C.C., w, Pavel A. Nikitin, Stefano Calo´, Rachel Gerrein, Kara Balabanis, and C.H. James Monroe, Anders E. Lilja,w, Ethan C. Settembre, & Andrea Carfi, *Structure of HCMV glycoprotein B in the postfusion conformation bound to a neutralizing human antibody.* NATURE COMMUNICATIONS, 2015. **6**(8176): p. 1-12.
212. Baquero, E., et al., *Structure of the low pH conformation of Chandipura virus G reveals important features in the evolution of the vesiculovirus glycoprotein.* PLoS Pathog, 2015. **11**(3): p. e1004756.
213. Vigerust, D.J. and V.L. Shepherd, *Virus glycosylation: role in virulence and immune interactions.* Trends Microbiol, 2007. **15**(5): p. 211-8.
214. Wei, X., et al., *Antibody neutralization and escape by HIV-1.* Nature, 2003. **422**(6929): p. 307-12.
215. Atanasiu, D., et al., *Bimolecular complementation defines functional regions of Herpes simplex virus gB that are involved with gH/gL as a necessary step leading to cell fusion.* J Virol, 2010. **84**(8): p. 3825-34.
216. Maurer, U.E., et al., *The structure of herpesvirus fusion glycoprotein B-bilayer complex reveals the protein-membrane and lateral protein-protein interaction.* Structure, 2013. **21**(8): p. 1396-405.
217. Stannard, L.M., A.O. Fuller, and P.G. Spear, *Herpes simplex virus glycoproteins associated with different morphological entities projecting from the virion envelope.* J Gen Virol, 1987. **68 (Pt 3)**: p. 715-725.
218. Borucki, M.J., et al., *A phase II, double-masked, randomized, placebo-controlled evaluation of a human monoclonal anti-Cytomegalovirus antibody (MSL-109) in combination with standard therapy versus standard therapy alone in the treatment of AIDS patients with Cytomegalovirus retinitis.* Antiviral Res, 2004. **64**(2): p. 103-11.
219. Funaro, A., et al., *Generation of potent neutralizing human monoclonal antibodies against cytomegalovirus infection from immune B cells.* BMC Biotechnol, 2008. **8**: p. 85.
220. Pandey, J.P., et al., *Immunoglobulin genes influence the magnitude of humoral immunity to cytomegalovirus glycoprotein B.* J Infect Dis, 2014. **210**(11): p. 1823-6.
221. Belshe, R.B., et al., *Efficacy results of a trial of a herpes simplex vaccine.* N Engl J Med, 2012. **366**(1): p. 34-43.
222. Melville, J.M. and T.J. Moss, *The immune consequences of preterm birth.* Front Neurosci, 2013. **7**: p. 79.
223. RICHARD R. SPAETE, R.M.T., WILLIAM S. PROBERT, FRANK R. MASIARZ, and L.R. SCOn H. CHAMBERLAIN, THOMAS C. MERIGAN,tAND CAROL PACHL, *Human Cytomegalovirus Strain Towne Glycoprotein B Is Processed by Proteolytic Cleavage* Virology, 1988. **167**: p. 207-225.

224. Adler, B., et al., *Role of human cytomegalovirus UL131A in cell type-specific virus entry and release.* J Gen Virol, 2006. **87**(Pt 9): p. 2451-60.
225. Rogalin, H.B., *Molecular mechanisms of HSV-1 entry and membrane fusion* Tufts Doctoral Dissertation, 2016.
226. Linda M. Stannard, A.O.F., Patricia G. Spear, *Herpes Simplex Virus Glycoproteins Associated with Different Morphological Entities Projecting from the Virion Envelope.* Journal of General Virology, 1987. **68**: p. 715-725.
227. Snydman, D.R., et al., *Use of cytomegalovirus immune globulin to prevent cytomegalovirus disease in renal-transplant recipients.* N Engl J Med, 1987. **317**(17): p. 1049-54.
228. Hanson, M.N., et al., *Novel mutation in the UL97 gene of a clinical cytomegalovirus strain conferring resistance to ganciclovir.* Antimicrob Agents Chemother, 1995. **39**(5): p. 1204-5.
229. Minces, L.R., et al., *Ganciclovir-resistant cytomegalovirus infections among lung transplant recipients are associated with poor outcomes despite treatment with foscarnet-containing regimens.* Antimicrob Agents Chemother, 2014. **58**(1): p. 128-35.
230. Ohlin, M. and C. Soderberg-Naucler, *Human antibody technology and the development of antibodies against cytomegalovirus.* Mol Immunol, 2015. **67**(2 Pt A): p. 153-70.

-